

**Investigating Myocardial PI3K α Signaling in Models of Ischemia Reperfusion and
Cardiotoxic Cancer Therapies**

by

Brent Andrew McLean

A thesis submitted in partial fulfillment of the requirements for the degree of

Doctor of Philosophy

Department of Physiology
University of Alberta

© Brent Andrew McLean, 2016

Abstract

Background. Phosphoinositide 3-kinase (PI3K) is a lipid kinase that functions as a central intracellular signaling transduction node, receiving input from cell receptors and initiating a cascade of cellular signaling that regulates and integrates central cellular processes such as glucose uptake, growth and survival. This PhD thesis is primarily concerned with the PI3K α isoform and its role in normal and pathological heart physiology.

Background—Ischemia/reperfusion injury. PI3K signaling, including downstream activation of Akt, is regularly cited as causing cellular protective effects in experimental ischemia/reperfusion (IR) injury; however, a transgenic mouse with reduced PI3K α activity is dramatically protected from IR injury.

Objective. Elucidation of the mechanism(s) underlying this phenomenon could lead to an improved understanding of both IR injury and PI3K α functions. Two chapters of this thesis show experiments aimed at understanding why reduced PI3K α is protective.

Methods and Results. In chapter 3 I test the contribution of the PI3K γ isoform by using PI3K γ knockout mice in Langendorff perfusions, metabolic substrate utilization through working heart perfusions, and downstream signaling. IR protection was not dependent on PI3K γ or glucose oxidation but ERK activation was increased. In chapter 4 I test the importance of downstream signaling through Langendorff perfusions with selective inhibitors of the Akt and ERK pathways, and test an inducible, cardiomyocyte specific PI3K α knockout model. Then, I investigate mechanisms of cellular injury, apoptosis and necrosis, which lead me to consider known regulators of necrotic cellular injury as possibly altered in PI3K α deletion hearts. IR protection was not dependent on acute Akt or ERK activation. Reduced PI3K α prevented necrotic cell death upon IR and preserved mitochondrial membrane potential, investigated with live tissue imaging. I investigated reported regulators of necrotic cell death, RIP1/3, CaMKII, Bax Bak,

Cyp-D through Western blot, Co-IP cell fractionation, but did not find a correlation with the PI3K α phenotype.

Conclusions. PI3K α deletion causes robust IR protection and maintained mitochondrial function, but not through commonly recognized mechanisms of IR protection.

Background—Heart function, cardiotoxicity of PI3K α inhibition. The role of PI3K α in maintaining normal heart function and morphology is an ongoing question, and is topical due to the numerous PI3K inhibitors currently under development as cancer treatments.

Objective. Assess heart function under both genetic and pharmacological PI3K α inhibition in otherwise healthy adult mice, and in the context of the cytotoxic cancer therapy doxorubicin.

Methods and Results. In chapter 5 I use multiple methods to delete or inhibit PI3K α and assess heart and cardiomyocyte function. I found that PI3K α does not directly control heart function, but it does increase the vulnerability of the heart to the cytotoxicity of Cre recombinase with tamoxifen administration. In chapter 6 I look at adverse effects of PI3K α inhibition/deletion in the context of a commonly used cytotoxic cancer therapy doxorubicin. In the context of doxorubicin chemotherapy, PI3K α inhibition caused severe weight loss, heart atrophy and distinct right ventricular dilation. Upon examination of underlying molecular changes, I found increased redox stress and p38 MAPK activation in combination treated hearts. Therapeutic inhibition of p38 MAPK partially ameliorated heart atrophy and dysfunction.

Conclusions. PI3K α inhibition is well tolerated by the heart, except when combined with the additional stress of cytotoxic Cre-tamoxifen or doxorubicin. PI3K α inhibition can cause body weight and muscle loss, as well as heart atrophy, which are already common and serious morbidities present in cancer patients. The right ventricle may be particularly vulnerable to atrophy and redox stress.

Preface

This thesis includes writing and data from both published and unpublished work. Numerous individuals assisted and contributed to this work as outlined below.

Published review article adapted for portions of chapter 1

McLean BA, Zhabyeyev P, Pituskin E, Paterson I, Haykowsky MJ, Oudit GY. PI3K inhibitors as novel cancer therapies: Implications for cardiovascular medicine. *Journal of Cardiac Failure*. 2013;19:268-282. **Role of B.A.M.:** Researched and wrote manuscript and then integrated contributions and comments from co-authors.

Published manuscript adapted for chapter 3

McLean BA, Kienesberger PC, Wang W, Masson G, Zhabyeyev P, Dyck JR, Oudit GY. Enhanced recovery from ischemia-reperfusion injury in pi3k alpha dominant negative hearts: Investigating the role of alternate PI3K isoforms, increased glucose oxidation and mapk signaling. *J Mol Cell Cardiol*. 2013;54:9-18. **Role of B.A.M.:** Responsible for mouse management, tissue collection and processing, biochemical assays, Western blots, figure and manuscript preparation and revision.

Unpublished data and writing for chapter 4

I received assistance from Alois Haromy (Michelakis Lab) with confocal microscopy imaging of live tissue, and Faqi Wang (Oudit Lab) with Co-IP experiments. All other experiments in this section I performed on my own.

Published manuscript adapted for chapter 5

McLean BA, Zhabyeyev P, Patel VB, Basu R, Parajuli N, DesAulniers J, Murray AG, Kassiri Z, Vanhaesebroeck B, Oudit GY. Pi3kalpha is essential for the recovery from cre/tamoxifen cardiotoxicity and in myocardial insulin signaling but is not required for normal myocardial contractility in the adult heart. *Cardiovasc Res.* 2015;105:292-303. **Role of B.A.M.:** Study design, animal treatment and tissue collection, echocardiography analysis and invasive pressure-volume catheterization to assess heart function, cardiomyocyte isolation and culture, molecular investigation including Western blots and mRNA, data analysis, creation of figures and writing of manuscript.

Unpublished manuscript adapted for chapter 6

McLean BA, Patel VB, Zhabyeyev P, Chen X, Basu R, Wang F, Shah S, Vanhaesebroeck B, Oudit GY. Inhibition of PI3K α in a Female Murine Cardiotoxicity Model Causes Heart Atrophy and Distinct Biventricular Remodeling with Pathological p38 MAPK Activation. **Role of B.A.M.:** Study design, daily animal treatment (oral and injected drug administration for 4 weeks), echocardiography analysis, tissue collection, histology and molecular characterization including mRNA and protein with nuclear fractionation, manuscript and figure preparation.

Animal experiments were conducted in accordance with the Canadian Council on Animal Care (CCAC) with approval from a University of Alberta Animal Care and Use Committee (ACUC).

Animal husbandry was performed with the services and oversight of Health Sciences Laboratory Services (HSLAS).

Acknowledgements

I would like to acknowledge and thank the following organizations and individuals for their help and support with this work.

Personal: Thanks to my wife Lianne McLean for all her support during my time as a graduate student.

Personal funding: Thanks to Alberta Innovates-Health Solutions for providing me with studentship funding.

Project funding: Thanks to Alberta Innovates-Health Solutions and Canadian Institutes of Health Research for project funding.

Supervision: Thanks to Dr. Gavin Oudit for his supervision, mentoring and support throughout my graduate student work.

Lab members: Thanks to all Oudit lab members for their support and friendship. Special thanks to Jessica DesAulniers for all her work with animal breeding and genotyping.

Core facility staff: Thanks to Donna Beker for her work doing mouse echocardiography imaging for these projects, Amy Barr who trained me to use core facility equipment and HSLAS staff for animal husbandry.

Collaborators: Thanks to collaborators for their contributions to these projects: Dr. Zam Kassiri, Dr. Jason Dyck, Dr. Petra Kienesberger, Grant Masson, Dr. Edith Pituskin, Dr. Ian Paterson, Dr. Mark Haykowsky, Dr. Alan Murray, Dr. Bart Vanhaesebroeck, Dr. Evangelos Michelakis, Alois Haromy, Dr. Liyan Zhang and Dr. Gary Lopaschuk.

Committee members: Thanks to my committee members for their input and guidance over the course of my graduate studies: Dr. David Brindley, Dr. Mark Haykowsky and Dr. Gary Lopaschuk.

Table of Contents

Abstract.....	ii
Preface	iv
Acknowledgements.....	vi
List of tables, figures and illustrations.....	xi
List of abbreviations and acronyms	xiii
1. Introduction	1
1.1. Introduction to PI3K signaling	1
1.2. PI3K in metabolic signaling.....	2
1.3. PI3K inhibition a target in cancer therapy.....	3
1.4. Development of PI3K Inhibitors	4
1.5. PI3K signaling in heart hypertrophy	5
1.6. PI3K signaling in heart failure	6
1.7. Negative regulation of PI3K through PTEN.....	7
1.8. Ischemia Reperfusion (IR) injury and PI3K α signaling	8
1.9. PI3K α signaling and heart function	10
1.10. Potential for heart toxicity of PI3K α inhibition in cancer patients	11
2. General Methods	14
2.1 Experimental animal use	14
2.1.1. Chapter 3 animal use	14
2.1.2. Chapter 4 animal use	14
2.1.3. Chapter 5 animal use	15
2.1.4 Chapter 6 animal use	15
2.2. Heart functional assessment.....	16
2.2.1. Echocardiography	16
2.2.2 Invasive hemodynamic assessment.....	16
2.3. Blood glucose measurements.....	17
2.4. Body weight, composition and food consumption	17
2.5. Electrocardiogram (ECG)	17
2.6. <i>Ex vivo</i> heart perfusions	17
2.6.1. Isolated Langendorff heart perfusion and ischemia–reperfusion protocol	17
2.6.2. Working heart perfusion and ischemia–reperfusion protocol	18
2.7. Adult mouse and human cardiomyocyte isolation, function and culture	19

2.7.1. Adult mouse cardiomyocyte isolation	19
2.7.2. Adult human cardiomyocyte isolation	19
2.7.3. Measurement of cardiomyocyte contractility	20
2.8. cAMP measurements	20
2.9. Histology.....	21
2.9.1. PSR	21
2.9.2. WGA staining	21
2.9.3. TUNEL staining	21
2.9.4. DHE staining	22
2.10. Quantitative PCR for gene expression	22
2.11. Tissue homogenization and Protein analysis	23
2.11.1. Tissue homogenization	23
2.11.2. Western blot.....	23
2.11.3. Subcellular fractionation	25
2.11.4. Co-immunoprecipitation	25
2.12. Statistics and graphing	25
3. PI3K α in Ischemia Reperfusion Injury Part I: Published Work	27
3.1 Introduction.....	27
3.2 Results and discussion	27
3.2.1. Independent basal effects of PI3K α and PI3K γ	27
3.2.2. Loss of PI3K γ does not reverse protection in PI3K α DN hearts	28
3.2.3. Signaling through Akt and GSK3 β is reduced in PI3KDM hearts	30
3.2.4. PI3K α DN hearts are resistant to myocardial I/R injury in the ex vivo working heart perfusion model	30
3.2.5. Akt and GSK3 β in PI3K α DN and PI3KDM from the working heart perfusion	32
3.2.6 Altered metabolic substrate utilization in PI3K α DN and PI3KDM hearts	33
3.2.7. Increased MAPK signaling in PI3K α DN hearts	37
3.3 Conclusions.....	38
4. PI3K α in Ischemia Reperfusion Injury Part II: Unpublished Work	40
4.1. Introduction.....	40
4.2. Challenge of PI3K α DN hearts with inhibitors against MEK and AKT in IR model.....	40
4.2.1. Background and rational for experiments	40
4.1.2. Results: Akt and ERK inhibition in PI3K α DN and Ctr hearts	41

4.2 IR recovery in an adult, inducible PI3K α deletion model	41
4.2.1 Background and rational for experiments	41
4.2.2 Results: PI3K α Mer, 60min ischemia, p110 α inhibition with BYL719	43
4.3 Assessment of mitochondrial membrane potential and cell injury after IR injury	44
4.3.1 Background and rational for experiments	44
4.3.2 Results: reduced PI3K α models have higher MMP and reduced cell death after IR ..	44
4.4 Investigation of cellular injury processes: apoptosis or necrosis	46
4.4.1 Background and rational for experiments	46
4.4.2 Results: Apoptosis not detected, evidence for necrosis.....	46
4.5 Investigation of molecular mechanisms of IR necrosis and protection in PI3K α DN	46
4.5.1 Justification of experiments	48
4.5.2 Results: RIP protein; Bak protein levels, localization; Cyp-D modifications and interactions	49
4.6 Discussion and conclusions regarding PI3K α in IR injury.....	52
5. PI3K α and Heart Function	53
5.1. Introduction.....	53
5.2. Results	54
5.3. Discussion	62
6. PI3K α and Doxorubicin Toxicity	68
6.1. Introduction.....	68
6.1. Results	68
6.2.1 Co-treatment with PI3K α inhibitor and doxorubicin results in heart atrophy and increased mortality.....	70
6.2.2 Biventricular remodeling is characterized by reduced stroke volume and RV dilation in the setting of weight loss.....	70
6.2.2. Cardiomyocyte-specific loss of PI3K α potentiates the susceptibility to Dox toxicity ..	75
6.2.3. Molecular Basis for the Biventricular Cardiomyopathy.....	76
6.2.4. Inhibition of p38 signaling partially reversed the biventricular cardiomyopathy	80
6.3. Discussion	81
7. Final discussion, research impact and future directions	87
7.1 General comments	87
7.2 Discussion and impact: ischemia/reperfusion project.....	87
7.3 Suggestions for future work	88
7.4 Discussion and impact: heart function project.....	90

7.5 Suggestions for future work	91
References	93

List of tables, figures and illustrations

Figure 1.1 Schematic of PI3K signaling pathway	2
Figure 2.1 Protocol for live tissue imaging	18
Figure 3.1 PI3KDM IR in Langendorff	29
Figure 3.2 Signaling in PI3KDM	31
Figure 3.3 IR recovery in Working Heart model	32
Figure 3.4 Signaling in Working Heart model	34
Figure 3.5 Metabolic changes in IR PI3K models	36
Figure 3.6 MAPK and insulin signaling	38
Figure 4.1 IR with Akt or ERK inhibition	42
Figure 4.2 IR recovery in conditional PI3K α knockout	44
Figure 4.3 Live tissue imaging of mitochondria, cell death	45
Figure 4.4 Markers of apoptosis and necrosis	47
Figure 4.5 Regulators of mitochondrial function	50
Figure 4.6 Regulators of necrotic cell death	51
Figure 5.1 Heart function with inducible PI3K gene deletion	55
Figure 5.2 Heart function with low dose tamoxifen	57
Figure 5.3 Disease markers and altered signaling	58
Figure 5.4 PI3K α knockout heart function, insulin signaling	61
Figure 5.5 PI3K α inhibitor heart function, insulin signaling	64
Figure 6.1 BYL and Dox cause mortality, weight loss, heart atrophy	69
Figure 6.2 Characterization of Dox, BYL treated mice	71
Figure 6.3 Dox, BYL biventricular effects on heart function	74
Figure 6.4 Electrocardiogram	75
Figure 6.5 Dox and PI3K α knockout heart function	77
Figure 6.6 Molecular signaling in Dox, BYL treated hearts	79

Figure 6.7 Markers of inflammation	80
Figure 6.8 Activation of p38 MAPK and redox stress	82
Figure 6.9 Inhibition of p38 MAPK	83
Figure 6.10 Illustration of heart remodeling with Dox, BYL	86
Table 3.1 Hemodynamics and morphometrics	28
Table 5.1 Echocardiography high dose tamoxifen	53
Table 5.2 Echocardiography low dose tamoxifen	56
Table 5.3 Echocardiography PI3K α knockout or inhibition	60
Table 6.1 Left ventricle hemodynamics	72

List of abbreviations and acronyms

4E-BP1	eIF4E-binding protein
AMPK	AMP activated protein Kinase
BSA	Bovine serum albumin
BYL	BYL719 (trade name: Alpelisib)
CABG	Coronary Artery Bypass Graft
cAMP	cyclic adenosine monophosphate
Cre	α MHC-Cre recombinase
Ctr	Control; wildtype or non-transgenic knockout littermate
Cyp-D	Cyclophilin-D or F
DCM	dilated cardiomyopathy
DHE	Dihydroethidium
Dox	Doxorubicin
EGF	Epidermal derived growth factor
ERK	Extracellular signal-Regulated Kinase
Flx	Lox P site inserted flanking target gene, excised by Cre recombinase
GIK	glucose insulin potassium
GLUT4	Glucose transporter 4
GPCR	G-protein coupled receptor
GSK3 β	Glycogen Synthesis Kinase 3 beta
HD	High Dose tamoxifen: 60mg/Kg/day for 4 days
HER2	Human epidermal growth factor 2
HER2	Human epidermal growth factor receptor 2
IGF-1	Insulin like growth factor-1
IPC	Ischemia preconditioning
IR	Ischemia-Reperfusion
IRS	Insulin receptor substrate
IRS-1	Insulin Receptor Substrate 1
LD	Low Dose tamoxifen: 40mg/Kg/day for 4 days
LVAD	Left ventricular assistant device
MCM	Mutated estrogen receptor-Cre recombinase chimeric protein, requires tamoxifen for activation
MI	myocardial infarction

MMP	Matrix metalloproteinase
mPTP	mitochondrial permeability transition pore
NFAT	Nuclear factor of activated T-cells
p38 MAPK	p38 Mitogen Activated Protein Kinase
PCI	percutaneous coronary intervention
PCI	Percutaneous coronary intervention
PCR	polymerase chain reaction
PDGF	Platelet derived growth factor
PDK1	Phosphoinositide-dependent kinase-1
PH domain	Pleckstrin homology domain
PI3K γ	Phosphoinositide Kinase gamma
PI3K α Cre	Cre ^{+/-} /p110 α ^{fix/fix}
PI3K α MCM	MCM ^{+/-} /p110 α ^{fix/fix}
PI3K α	Phosphoinositide 3-kinase catalytic subunit p110 α
PI3K α DN	p110 α dominant negative; transgenic p110 α with mutated catalytic domain expressed under the α MHC promoter
PI3K β Cre	Cre ^{+/-} /p110 β ^{fix/fix}
PIP	Phosphatidylinositol
PKA	Protein kinase A
PDE4	Phosphodiesterase 4
PLN	Phospholamban
PSR	picro-sirius red
PTEN	Phosphatase and tensin homologue
RBD	RAS binding domain
RISK	Reperfusion Injury Salvage Kinase
S6K	Ribosomal protein S6 kinase
SDS-PAGE	sodium dodecyl sulfate polyacrylamide gel electrophoresis
SERCA2a	Sarco/endoplasmic Reticulum Calcium ATPase 2a
SGK-1	Serum and glucocorticoid-regulated kinase 1
STEMI	ST elevated myocardial infarction
TAM	Tamoxifen
TRK or RTK	Tyrosine receptor kinase
TUNEL	Terminal deoxynucleotidyl transferase dUTP nick end labeling
VEGF	Vascular Endothelial growth factor

VEGF	Vascular endothelial growth factor
WGA	wheat germ agglutinin
α MHC or α MyHC	α -Myosin Heavy Chain promoter

1. Introduction

Includes excerpts from published manuscripts listed in the preface

1.1. Introduction to PI3K signaling

Phosphoinositide 3-kinase (PI3K), also known as phosphatidylinositol-4,5-bisphosphate 3-kinase, and here referred to as PI3K, is a protein family that mediates the addition of a phosphate group to phosphatidylinositol (4,5)-bisphosphate (PIP₂) to produce phosphatidylinositol (3,4,5)-trisphosphate (PIP₃). PIP₃ binds signaling proteins at lipid membranes through conserved binding domains such as pleckstrin homology (PH) domains, causing their activation and co-localization with other signaling proteins.¹ As such, PI3K acts as an essential mediator for the activation of numerous intercellular signaling molecules with >250 proteins having potential PH domains.² PI3K signaling is a key downstream mediator of growth and survival signaling from numerous ligands, such as neuregulin, platelet derived growth factor (PDGF), insulin, insulin like growth factor 1 (IGF-1) and epidermal growth factor (EGF) (Figure 1.1). The PI3K family includes multiple classes, but this thesis will only consider members of Class I, which is comprised of catalytic subunits p110 α , β , γ and δ ; and multiple regulatory subunits including p85 and p55 isoforms.³ Catalytic subunits p110 α , β and γ are expressed in the heart.⁴⁻⁶

PI3K enzymes are recruited to activated cell membrane receptors, with different PI3K isoforms responding to different receptor types, including receptor tyrosine kinase (RTK), and G protein coupled receptors (GPCR). Catalytic subunits p110 α and p110 β bind p85 regulatory subunits (multiple isoforms and truncations), which bind to activated RTKs via their src homology 2 domain (SH2) and stimulate PI3K catalytic activity.¹ Conversely, p110 γ is activated by GPCRs and binds a p101 or p87 regulatory subunit, both of which are unrelated to p85.³ Optimal activation of p110 γ is dependent on its regulatory subunit, with p87 being highly expressed in the heart.⁷ Additionally, both p110 β and p110 γ can be activated by direct recruitment to G $_{\beta\gamma}$ subunits upon GPCR stimulation.⁸

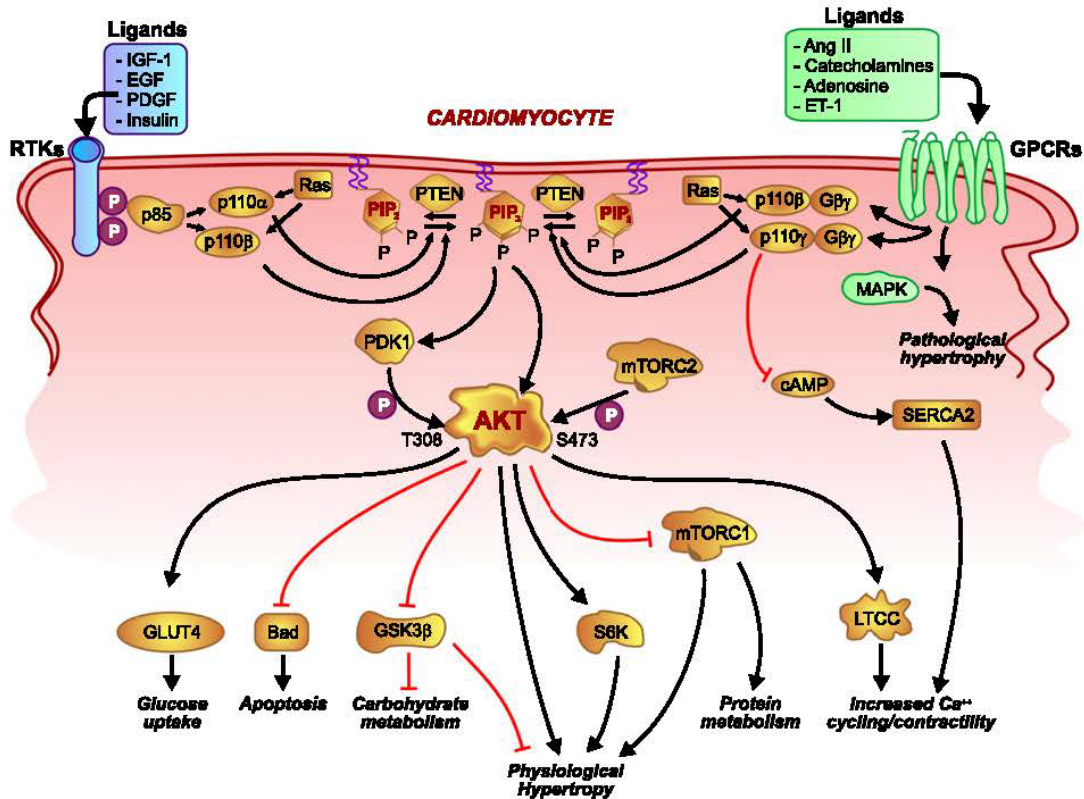


Figure 1.1. Schematic representation of the phosphatidylinositol 3-kinase signaling pathway. Ang II, angiotensin II; cAMP, cyclic adenosine monophosphate; EGF, epidermal growth factor; ET-1, endothelin-1; GLUT4, glucose transporter type 4; GSK3b, glycogen synthase kinase3b; IGF-1, insulin like growth factor; LTCC, L-type Ca^{2+} channels; mTORC1/2, mammalian target of rapamycin complex 1/2; PDK1, phosphoinositide-dependent kinase 1; PIP, phosphatidylinositol phosphate; PTEN, phosphatase and tensin homolog; RTK, receptor tyrosine kinase; S6K, ribosomal protein S6 kinase; SERCA2, sarcoendoplasmic reticulum Ca^{2+} adenosine triphosphatase.

The degree to which p110 β is a transducer of RTK or GPCR signals seems to vary between cell types,⁹ and the *in vivo* signaling role in the heart is currently poorly understood. A Ras binding domain (RBD) can be found on all class 1 PI3K catalytic subunits, but the importance of Ras mediated PI3K activation in the adult heart is unclear; one report shows that in neutrophils the RBD is more important for p110 γ activation than the p101 regulatory subunit,¹⁰ and mice with p110 α loss of RBD die perinatally, with impairment of lymphatic and vasculature development.^{3, 11}

1.2. PI3K in metabolic signaling

This thesis is primarily concerned with the p110 α (also referred to as PI3K α) isoform. Insulin mediated glucose uptake is an example of p110 α dependent signaling: insulin activates the insulin receptor, activating the insulin receptor substrate (IRS) adaptor protein, which recruits and activates PI3K α (p110 α +p85 regulatory subunit), which produces PIP₃, which leads to multiple subsequent signaling steps including Akt activation. Akt is recruited to membranes by PIP₃ and is phosphorylated at Thr³⁰⁸ by phosphoinositide-dependent protein kinase 1 (PDK1),¹² which is also activated by PIP₃.¹³ Akt can also be phosphorylated and further activated at Ser⁴⁷³ by mTORC2,¹⁴ which can also be activated by PI3K.¹⁵ Akt affects metabolism by increasing glucose uptake through AS160 inactivation and subsequent GLUT4 translocation to the cell membrane,¹⁶ and GSK3 β inhibition which promotes glycogenesis.¹⁷ Akt promotes cell growth through GSK3 β inhibition and its effects on NFAT, β -catenin and GATA4,¹⁸ and through mTORC1 activation, which causes increased S6K ribosomal subunits and promotes protein translation through inhibition of 4E-BP1.¹⁹ PI3K was originally discovered through its connection to cell transformation and cancer progression,^{20, 21} followed by its connection to insulin signaling and metabolism;²² regulation of cell metabolism and growth have been interrelated and enduring themes in PI3K research.

1.3. PI3K inhibition a target in cancer therapy

Gain-of-function mutations in various nodal points in the PI3K pathway play a critical causative role in many malignancies.²³⁻²⁹ PI3K α mutations are frequently found in human tumors, and its inhibition represents a direct target that is highly sought after for cancer therapy.^{30, 31} The PI3K pathway is frequently aberrantly activated in breast cancer with mutations occurring in up to one quarter of breast cancers. These mutations increase enzymatic function, enhance downstream signaling elements including Akt, and promote oncogenic transformation.³² Akt activation has a pro-survival effect through the interactions with caspases and Bcl-2 proteins, including the BH3-only proteins Bax and Bad.³³ The majority of PI3K mutations are correlated with cancer are in the p110 α gene *PIK3CA* in its helical domain, where the p85 subunit binds with an inhibitory effect,³⁴ and a

mutation in the C-terminal kinase domain that promotes greater association with membranes, causing increased catalytic activity.³⁵ There are multiple levels of PI3K activation (recruitment to receptors, interactions between PI3K subunits, catalytic activity, etc), and likewise, many points at which this system can be dysregulated: membrane binding combinations including Ras, Gβγ, and pY (phospho tyrosine) combine to cause more or less membrane recruitment. Also, inhibition as well as activation by regulatory subunits affects localization and catalytic activation, and negative regulation by the PTEN phosphatase may be altered.³⁶ While PI3Kα mutations are associated with favorable outcomes in breast cancer patients,³⁷ these mutations have also been linked to reduced efficacy of trastuzumab and lapatinib treatment,³⁸ likely because activated PI3Kα bypasses the receptors that these drugs inhibit. On the other hand, PI3Kβ inhibition may be more relevant for cancer driven by a loss of function mutation in PTEN.³⁹ In this case, PI3Kβ, which contributes more to the basal constitutive PIP₃ pool, can cause high PIP₃ signaling and drive cancer growth.⁴⁰ Cancers with loss of PTEN function are often not correlated with increased RTK signaling; rather, it is the loss of PTEN that amplifies the basal activity of PI3Kβ/δ.^{40, 41}

1.4. Development of PI3K Inhibitors

The majority of PI3K inhibitors have been designed to bind somewhere in the active site of the enzyme, which causes effective inhibition of activity.⁴²⁻⁶⁰ However, the enzymatic active site is the most conserved domain among kinases which may lead to some degree of inhibition of several other enzyme targets, despite attempts to improve target specificity.⁶¹ This lack of specificity can make it difficult to predict and minimize treatment-related toxicity. A number of strategies have been devised to minimize non-specific effects, including targeting other points of the protein away from the active site. There is also the possibility of designing a drug that binds both the active site and an auxiliary site, which would give greater specificity for its target.⁶¹ Early PI3K inhibitors, such as wortmannin and LY294002 were not suitable for clinical use due to poor pharmacological properties and off target effects. However, several compounds that are now in clinical trials have used

wortmannin and LY294002 as parent compounds to design PI3K inhibitors with greater selectivity and improved pharmacokinetics.⁴⁴⁻⁶⁰ Examples include GDC-0941, which is a highly selective, reversibly binding, inhibitor for p110 α / δ derived from LY294002,⁶² and PX866, an irreversibly binding pan PI3K inhibitor derived from wortmannin. Isoform selective inhibitors are also of great interest; if one PI3K isoform is predominant in a particular tumor, selective inhibition of that PI3K isoform and not other isoforms should reduce the risk of unwanted systemic effects. PI3K α is a common mutation in cancer cells and tumors; the rational design of a selective PI3K α inhibitor led to the development of the small molecule inhibitor BYL719,⁶³ which I have used in experiments looking at effects on the heart (Chapters 5 and 6).

1.5. PI3K signaling in heart hypertrophy

PI3K α signaling was first investigated in the heart through use of mice carrying transgenes under the regulation of the heart specific alpha myosin heavy chain (α MyHC) promoter.⁴ Increased and decreased PI3K α activity was achieved by a constitutively active (PI3K α -CA) and catalytically inactive dominant negative (PI3K α DN) transgene respectively. This study established the importance of PI3K α in normal heart growth: PI3K α -CA hearts and cardiomyocytes were enlarged compared to controls, whereas PI3K α DN hearts and cardiomyocytes had reduced size. PI3K α was further established as a mediator of non-pathological, adaptive hypertrophy important for physiological adaptation such as hypertrophy in response to exercise.⁶⁴

Signaling through PI3K α , induced by growth factors such as IGF-1 and insulin through RTKs, has been associated with adaptive physiological hypertrophy,^{64, 65} and in the setting of heart failure, is responsible for an initial phase of adaptive hypertrophy which helps the failing heart maintain function.^{64, 66} A recent survey of genetic mutations correlating with pathological LV hypertrophy identified mutations in the IGF-1 receptor gene.⁶⁷ Also, cardiomyocyte-specific over-expression of IGF-1 receptors resulted in beneficial hypertrophy in a PI3K α -dependent manner.⁶⁸ Interestingly, circulating levels of IGF-1 are reduced in men with chronic heart failure and correlates

with adverse prognosis.⁶⁹ IGF-1 signaling is required for exercise induced hypertrophy, which was blocked in a PI3K α dominant negative (PI3K α DN) model⁷⁰ as well as p85 deletion,⁷¹ with both models having reduced baseline heart size. PI3K signaling is highly active in the pre and post-natal rat heart compared to the adult,⁷² consistent with a central role for PI3K signaling in developmental growth. This may be an important consideration if PI3K inhibitors are to be used to treat juvenile cancer patients who are still undergoing developmental heart hypertrophy as a component of normal development.

1.6. PI3K signaling in heart failure

Over expression of PI3K α in the heart was protective against pressure overload (aortic banding) induced heart failure,⁷³ whereas the PI3K α DN model showed enhanced susceptibility to aortic banding, with rapid progression to a dilated cardiomyopathy.⁶⁵ In the absence of pathological stimuli, PI3K α DN hearts had normal function⁵ and actually showed reductions in markers for cardiac aging at time points greater than 20 months, such as reduced lipofuscin accumulation⁷⁴, although the same model was reported to have reduced cardiac output at 45 weeks of age.⁷⁵ This evidence suggests that although PI3K α signaling may be dispensable in the healthy adult heart, the adaptive response to pathological stressors, such as hypertension, may require intact PI3K α signaling; also, cardioprotective signaling, such as growth factors released during exercise, may be attenuated with PI3K inhibition.

With the progression of heart failure, defined as excessive hemodynamic workload relative to the heart's capacity, neuro-hormonal stimulants such as angiotensin (Ang) II and epinephrine activate GPCRs in cardiomyocytes, which stimulate PI3K γ signaling.⁷⁶ Serum and glucocorticoid-regulated kinase (SGK1) is also activated by PI3K γ , and can have short term beneficial anti-apoptotic effects, but promote adverse myocyte remodeling when chronically stimulated.⁷⁷ Inhibition of PI3K γ has a number of possible benefits for cardiovascular disease; the hypertrophic remodeling normally associated with the adrenergic stimulant isoproterenol was blocked in PI3K γ ^{-/-}

mice.⁷⁸ Also, PI3K γ has an important role in inflammation,⁷⁹ which is a critical step for the formation of atherosclerotic plaques; mice prone to atherosclerosis had reduced plaque development when crossed with PI3K γ ^{-/-} mice.⁸⁰ Activation of the catalytic p110 γ subunit through p87 causes the binding of RII α , the regulatory subunit of PKA, to the RBD of 110 γ resulting reduced PKA activity.⁸¹ In addition, PI3K γ causes reduced PKA activity through activation of PDE4, which degrades cAMP, a key activator of PKA.⁸² However, there are detrimental effects associated with long-term suppression of PI3K γ signaling⁸³ due to increased MMP activity which resulted in a loss of cell adhesion integrity in response to pressure-overload⁸⁴ and myocardial infarction.^{83, 85} Although PI3K γ is not a specific target for cancer therapies, several of the PI3K inhibitors block all PI3K isoforms, so inhibition of PI3K γ may contribute to the cumulative effect on cardiac physiology of these drugs.

1.7. Negative regulation of PI3K through PTEN

The lipid phosphatase PTEN is a negative regulator of PI3K signaling by converting PIP₃ to PIP₂, and loss of function mutations in PTEN are among the most common mutations in cancer leading to PI3K gain of function.⁸⁶ In the heart, loss of PTEN results in physiological hypertrophy similar to exercise training,⁵ reduced heart and cardiomyocyte contractility,⁴ resistance to pressure-overload induced heart failure⁸⁷ and improved functional recovery after *ex vivo* ischemia reperfusion (IR) injury.⁸⁸ Numerous other phosphoinositide phosphatases are also expressed in the heart and likely contribute to the close regulation of PIP₃ levels in the heart.⁸⁹ Distinct effects on heart size and contractility were first distinguished by crossing PTEN knockout mice with the PI3K α DN, which caused the phenotype to revert to a reduced heart size, and second, by crossing PTEN knockout mice with a p110 γ knockout mouse.⁵ The p110 γ knockout has increased contractility due to p110 γ negative regulation of cAMP downstream of GPCR receptors. The PTEN knockout went from reduced heart function to super physiological heart function with p110 γ knockout. This study established distinct roles for PI3K

isoforms, despite the common PIP₂ substrate and PIP₃ product, although cross signaling between different PI3K isoforms has also been suggested in following studies.

1.8. Ischemia Reperfusion (IR) injury and PI3K α signaling

Ischemic heart disease, wherein blood flow to the myocardium is interrupted, causing cell death from reduced ATP production and acidosis due to the lack of oxygen, as well as damage from the flood of oxygen radicals that result from reperfusion,⁹⁰ is a common cause of heart injury and death. Patients that survive an ischemic event have a significant risk of developing heart failure due to loss of functional myocardium and subsequent remodeling and fibrosis.⁹¹ Clinical treatment surrounding occluded myocardial blood flow, called acute coronary syndrome (ACS) centers around timely reperfusion, either by percutaneous coronary intervention (PCI) or coronary artery bypass graft (CABG). Ischemic injury is thought to be caused by both the ischemic event as well as reperfusion injury upon reperfusion.⁹⁰ Common animal models of ischemic heart disease represent different aspects of clinical ischemic heart disease, and include surgical myocardial infarction (MI), where a coronary artery is permanently occluded, and ischemia reperfusion (IR), where perfusion of a coronary artery (*in vivo*) or the entire heart (*ex vivo*), is temporarily stopped, and then resumed.

There has been a concerted effort to understand IR injury and mechanisms whereby myocardial damage can be prevented or reduced.⁹² The PI3K pathway has been extensively studied in connection to preventative measures for reducing IR injury as part of a Reperfusion Injury Salvage Kinase (RISK) signaling axis, which includes PI3K, Akt and ERK with proposed beneficial end effects on maintaining mitochondrial function upon IR injury.⁹³ IR therapies have been largely disappointing when tested in real-world clinical applications, and activators of PI3K pathway signaling are an example of this. Insulin is a robust activator of PI3K α signaling and activation of Akt, but treatment with glucose-insulin-potassium (GIK) did not improve outcomes in ST-segment elevation myocardial infarction (STEMI) patients in a large clinical trial.⁹⁴

Furthermore, cyclophilin-D (Cyp-D), which is postulated as an important end target of RISK signaling as well as other protective strategies, is inhibited by cyclosporine, but cyclosporine showed no benefit when given in a bolus to STEMI patients undergoing PCI.⁹⁵ Clearly, there is still a need for a greater mechanistic understanding of PI3K and RISK signaling and their role in cellular mechanisms of IR injury or protection.

It was first reported in 2008 that PI3K α DN hearts are resistant to IR injury.⁹⁶ This finding, which contradicts the RISK paradigm, was nevertheless originally harmonized to the RISK paradigm by suggesting that there was compensatory upregulation of PI3K γ signaling and enhancement of Akt activation in the PI3K α DN hearts upon IR.⁹⁶ Also, loss of PI3K γ caused increased infarct size post in vivo IR, and had reduced activation of Akt after reperfusion.⁸⁵ This is in contrast to earlier evidence that these pathways are distinct.⁵ In chapters 3 and 4 of this thesis, I present my investigation into the mechanisms underlying this finding that loss of PI3K α is protective against IR injury. Chapter 3 shows our findings when we cross bred the PI3K α DN mice with PI3K γ knockout mice to see if the protective phenotype is PI3K γ dependent. We then look at metabolic changes and signaling pathways that may provide an explanation of PI3K α DN IR protection. We published these findings without ever finding the underlying mechanism of PI3K α DN IR protection. Chapter 4 shows some of my ongoing attempts to find the elusive mechanism underlying this phenotype. My first approach was to acutely inhibit the Akt and ERK pathways, important nodes in the RISK signaling system, to see if this could impair PI3K α DN IR recovery. I also found that the cardiomyocyte inducible PI3K α deletion model using tamoxifen/Cre was protected under IR injury. Following this, I adopted a new strategy: characterize the end injury process and investigate known molecular regulators of those processes, especially regulators with possible connections to PI3K signaling based on the published literature. I could then work back from these cellular processes to their intersection with PI3K α regulation. I found that control hearts sustained severe necrotic cell death in our IR protocol, which was dramatically reduced in PI3K α DN. Regulated necrosis is an expanding field

of research,⁹⁷ with several reports connecting necrotic regulators to myocardial ischemic injury.⁹⁸⁻¹⁰² A common end mechanism for a large number of IR protection strategies is maintenance of the mitochondrial permeability transition pore (mPTP), which can disrupt mitochondrial membrane potential, which is essential for ATP production via oxidative phosphorylation. I did live tissue imaging to measure post-IR mitochondrial membrane potential, and then looked for altered regulation of cyp-D as well as Bcl-2 family proteins Bax and Bak, which have also been implicated in necrotic death via disruption of mitochondrial membrane potential.⁹⁸

1.9. PI3K α signaling and heart function

The initial distinction between PI3K α controlling developmental hypertrophy, and PI3K γ influencing heart function⁵ was subsequently challenged by a report showing that an inducible, cardiomyocyte specific knockout of p110 α caused a contractility defect.¹⁰³ These authors propose that the lack of contractile effects in the PI3K α DN hearts may be due to compensation in development, and expect that their model better captures the effects of PI3K α loss in adult hearts. Cardiomyocyte specific p110 α knockout mice were generated through insertion of LoxP sites that flank the gene of interest. These mice can then be crossed to commercially available mice expressing Cre recombinase (Cre) under the α MHC promoter. To conditionally target these genes in only the adult heart, a Cre chimera is utilized in which Cre is fused to a mutated estrogen receptor (MER) (MCM; MER-Cre-MER) which keeps Cre in the cytosol. Administration of the drug tamoxifen causes nuclear localization and activation of Cre. A constitutively active Cre can also be employed which does not require tamoxifen for activation, but does not allow for the same level of temporal control of the gene deletion. In sharp contrast to PI3K α DN hearts, which have normal function at baseline conditions,^{4, 5, 64} the PI3K α ^{fix/fix} MCM (PI3K α Mer) mice were reported to display reduced contractility, with L-type Ca⁺⁺ channels (LTCC) membrane depletion, suggesting a specific role for PI3K α in maintaining normal contractility.¹⁰³

Interpretation of cardiac phenotypes from mice using the MCM model is complicated by the cardiotoxic effects from the combination of the Cre recombinase enzyme and tamoxifen.^{104, 105} Oral administration of tamoxifen sufficient to cause a reporter gene deletion was previously shown to cause a transient reduction in cardiac function at 10 days after starting the drug (80mg/kg/day for 7 days PO), with full recovery of function at 28 days.¹⁰⁵ Subsequent reports have shown that even a single dose dose of 40mg/kg IP injection caused gene deletion and avoided heart toxicity,¹⁰⁶ although the precise amount of tamoxifen required to delete any one specific gene may vary and should be confirmed for each case. The ideal control for Cre/tamoxifen induced toxicity is mice bearing the Cre transgene, but without a gene being targeted by LoxP sites administered the same amount of tamoxifen used in the knockout model of interest. I have argued that in addition to using this control cohort, the dose of tamoxifen should be kept minimal because even without overt toxicity in the control group, a phenotype in a knockout model may emerge or be exacerbated when combined with tamoxifen/Cre toxicity.¹⁰⁷ The previous study of inducible p110 α deletion used daily tamoxifen injections of 1mg for 28 days (40mg/kg for 25g mouse);¹⁰³ this study, published in *Circulation*, was released at almost the same time as the *Circulation Research* paper showing tamoxifen/Cre toxicity.¹⁰⁵ Chapter 5 of this thesis details my efforts to parse out the effects of p110 α deletion on heart function apart from influence of the tamoxifen/Cre transgenic system.

1.10. Potential for heart toxicity of PI3K α inhibition in cancer patients

Numerous cancer therapies may contribute to the cumulative risk for heart disease, including chemotherapeutic agents such as anthracyclines and targeted therapies such as HER2 inhibitors (trastuzumab) and VEGF pathway inhibitors,¹⁰⁸⁻¹¹³ which may exacerbate traditional cardiovascular risk factors often highly represented in cancer patients. Downstream of HER2, VEGF, and other growth factor receptors, the PI3K family of lipid kinases and associated phosphatases are among the most commonly occurring sites of mutations in cancer patients,

including gain of function mutations in the p110 α class 1A catalytic subunit (gene name: PIK3CA) in women with breast cancer.^{3, 114} PI3K inhibition is particularly of interest in women with breast cancer, where PI3K pathway mutations, including in HER2 are common.^{115, 116} Numerous inhibitors of the PI3K pathway have been developed with hundreds of clinical studies currently in progress on the safety and efficacy of isoform-specific and pan-PI3K inhibitors, often in combination with other therapies.^{117, 118} PI3K inhibition is likely to slow, but not kill cancer cells, so combination therapies with cytotoxic drugs will likely be required.¹¹⁹ Similarly, trastuzumab in combination with cytotoxic anthracycline (example: doxorubicin) therapy both has enhanced therapeutic efficacy against breast cancer as well as increased heart toxicity.^{108, 112}

As a master transduction node for growth factor signaling, PI3K inhibition may promote skeletal muscle loss,¹²⁰ but effects on the myocardium are less clear. People who die from cancer have lower heart weights than people who die of non-cancer or cardiac causes.¹²¹ The nature of adverse cardiac remodeling and atrophy, in conjunction with cancer cachexia and the potential for adverse cardiac effects of extended PI3K inhibition in these vulnerable populations remains unknown.

Ongoing pre-clinical investigations using animal models of cancer therapy toxicity are important for anticipating potential adverse effects of new cancer therapies.^{111, 122} Furthermore, the need to study heart disease among women, and not simply extrapolate findings from men and male animal models is being more fully appreciated within the cardiovascular community.^{123, 124} These pitfalls also need to be avoided in the growing field of cancer related cardiotoxicity. Displayed in chapter 6 of this thesis, I investigate the effect of PI3K α inhibition on the cardiac structure and function in female murine models receiving cytotoxic anthracycline (Dox) treatment.

Anthracyclines, such as Dox, have been recognized to potentially cause heart damage, which can lead to adverse heart remodeling and dysfunction, and potentially cause overt heart failure.¹²⁵ This has been a limiting factor in the maximum allowable dose of anthracyclines. Early detection, limitation of anthracycline dose, and treatment with traditional heart failure medications

have been strategies to limit adverse effects of anthracyclines on the heart.¹¹⁰ A significant effort has been made to understand the mechanisms of anthracycline effects on the heart, to potentially find ways to mitigate risks to the heart, thereby allowing greater utilization of anthracyclines for their antineoplastic effects. Proposed mechanisms of anthracycline toxicity include DNA damage as well as increased reactive oxygen species and mitochondrial dysfunction, leading to cardiomyocyte dysfunction and death, resulting in a cardiomyopathy.¹¹¹ It is unknown if the use of PI3K inhibitors will add additional, and possibly synergistic risk for adverse heart effects in patients who have also been exposed to anthracycline therapies.

2. General Methods

2.1 Experimental animal use

Mice used in this study were in a C57Bl/6 (wildtype) genetic background. Mice were housed on a 12-h light/12-h dark cycle with ad libitum access to chow diet (#5001 from Lab Diet, St. Louis, MO, with 13.5% kcal from fat) and water. Experiments were performed in accordance with the Canadian Council of Animal Care (CCAC) with approval from a University of Alberta Animal Care and Use Committee (ACUC). Animal husbandry was performed with the services and oversight of Health Sciences Laboratory Services (HSLAS).

2.1.1. Chapter 3 animal use

Male PI3K γ KO, cardiac-specific PI3K α DN mice, and double mutant (DM) mice (PI3K γ KO/PI3K α DN), which were generated by breeding female PI3K γ KO with male PI3K α DN mice as described previously.^{4, 5, 84, 96} PI3K α DN mice were originally created by cloning a truncated p110 α gene with a disrupted kinase domain into a α MHC promoter construct.⁴ Immunoprecipitation of the regulatory p85 subunit pulled out only 20% of endogenous p110 α compared to the control group. PI3K γ KO were produced as a whole body germline knockout.¹²⁶ PI3KDM mice were generated at the expected Mendelian frequency.

2.1.2. Chapter 4 animal use

Male mice models used include PI3K α DN mice described above and inducible p110 α cardiomyocyte specific knockout mice. Mice with conditionally active transgenic Cre recombinase (MCM) under the control of the α MHC promoter (purchased from Jackson Lab: Tg(Myh6-cre)1Jmk/J; No: 005650) were crossed with mice carrying loxP sites targeting PI3K α as previously described (kindly shared by Dr. Bart Vanhaesebroeck, University College London).^{9, 127} Male mice 10-14 weeks old were given tamoxifen (Sigma), dissolved in corn oil

(concentration calculated for 4mL/kg), by oral gavage daily for 2 days. Mice were used for terminal experiments 7-14 days after the last tamoxifen administration.

2.1.3. Chapter 5 animal use

Mice with transgenic Cre recombinase either conditionally active (MCM) or constitutively active (Cre) under the control of the α MHC promoter (Jackson Lab: Tg(Myh6-cre)1Jmk/J; No: 009074) were crossed with mice carrying loxP sites targeting either the PI3K α or PI3K β genes (*PIK3CA*, *PIK3CB* respectively) as previously described (kindly shared by Dr. Bart Vanhaesebroeck, University College London).^{9, 127} Male mice 10-11 weeks old were given tamoxifen (Sigma), dissolved in corn oil (concentration calculated for 4mL/kg), by oral gavage daily for 4 days. The high dose (HD) of tamoxifen was 60mg/kg/day and the low dose (LD) was 40mg/kg/day. Male mice 16-18 weeks old were given 30mg/kg/day BYL-719 dissolved in corn oil (concentration calculated for 8mL/kg) by oral gavage daily for two weeks, 5 days/week or acutely once per day for four days. The dose of 30mg/Kg/day was previously shown to reduce the size of PI3K α driven tumors in mice.¹²⁸

2.1.4 Chapter 6 animal use

All animals used were female in a C57BL/6 background. Female WT mice were treated daily, five days/week, with BYL719 (BYL; trade name Alpelisib) suspended in corn oil (3.75mg/mL), or equal volume vehicle, by oral gavage (30mg BYL719/kg/day), based on dosing previously shown to cause tumor regression by BYL-719 in murine models.¹²⁸⁻¹³⁰ Mice were treated once weekly with doxorubicin dissolved in DMSO (5% final) and diluted in saline (1.25mg/mL), or equal volume vehicle, by intraperitoneal (IP) injection (10 mg doxorubicin/kg/week). For p38 inhibition, mice were treated daily, five days/week, with SB202190 dissolved in DMSO (5% final) and diluted in saline (1.25mg/mL) given by IP injection (5mg/kg), a dose previously used to limit weight loss in tumor bearing mice.¹³¹

Heart specific genetic deletion of p110 α was achieved by breeding mice homozygous for loxP sites (flx) at the p110 α gene (*PIK3CA*), as previously described above, with Cre recombinase under the control of the α MHC promoter (The Jackson Laboratory: Tg(Myh6-cre)1Jmk/J; No: 009074).

2.2. Heart functional assessment

2.2.1. Echocardiography

Noninvasive functional heart assessment was performed on mice for chapters 3, 5 and 6 by transthoracic echocardiography (ECHO) using a Vevo 770 or 3100 high resolution imaging system with 30 MHz transducer (RMV-707B; VisualSonics) under isoflurane anesthetic (1.5-2%) as previously described.^{132, 133} Systolic function of the LV and RV was assessed by dimensional changes viewed in the short axis m-mode. Pulse wave Doppler imaging was used to characterized transmitral filling during passive LV filling (E wave) and active filling during atrial systole (A wave). The pulse wave Doppler was also analyzed for isovolumetric relaxation and contraction times, as well as ejection time. Tissue Doppler imaging of mitral annulus movement was also analyzed for relative movement in passive filling (E') and active filling (A').

2.2.2 Invasive hemodynamic assessment

Hemodynamic assessment was performed with a pressure transducer catheter (1.2F admittance catheter; Scisense Inc.) under isoflurane anesthetic (1.5-2%) with the closed chest model previously described.¹³⁴ The catheter was inserted into the right carotid and advanced into the left ventricle as indicated by the pressure reading using the ADVantage Pressure-Volume System (TCP-500, Scisense Inc.) with iworx LabScribe2 software for data recording and analysis (iWork Systems Inc.). The end diastolic pressure-volume relationship was measured by transiently clamping the inferior vena cava to cause varying preload in the heart.

For right ventricle measurements, the catheter was inserted at the right jugular vein and advanced into the right ventricle, using the pressure trace to indicate when the catheter reached the right ventricle. Due to the irregular chamber shape of the right ventricle, absolute volumes could not be measured, so volumes are compared as relative changes in magnitude.

2.3. Blood glucose measurements

Blood glucose was measured in fasted mice from a tail vein prick using the Ascensia Contour Blood Glucose Monitoring System (Bayer).

2.4. Body weight, composition and food consumption

For chapter 6, body weight was measured once per week and drug dosing adjusted. Body composition was measured in live, conscious mice using a NMR-MRI scanner (EchoMRI). Food consumption was estimated by weighing food in a cage at 24hr intervals, with care taken to find any fragments that may have fallen into the bedding. Food consumption was then expressed relative to the total body weight of the animals in that cage (2-3 animals/cage).

2.5. Electrocardiogram (ECG)

For chapter 6, surface electrocardiogram was recorded with mice under light anesthesia (1% inhaled isoflurane) on a heated pad to maintain body temperature using DSI Ponema P3Plus version 5 with measurements recorded in lead I. P and QRS waves were identified by the software, and T waves were manually marked where the wave returned to the isoelectric line.

2.6. *Ex vivo* heart perfusions

2.6.1. Isolated Langendorff heart perfusion and ischemia–reperfusion protocol

Retrograde Langendorff heart perfusion was used to study heart contractile function. Mice were heparinized, anesthetized (isoflurane 2%) and hearts were excised and mounted on the Langendorff system and perfused at a constant pressure of 80 mm Hg with modified Krebs–Henseleit solution (116 mM NaCl, 3.2 mM KCl, 2.0 mM CaCl₂, 1.2 mM MgSO₄, 25 mM NaHCO₃,

1.2 mM KH_2PO_4 , 11 mM glucose, 0.5 mM EDTA and 2 mM pyruvate), which was kept at 37°C and continuously oxygenated with 95% O_2 and 5% CO_2 to maintain a pH of 7.4 as previously described.⁹⁶ By inserting a water-filled balloon into the LV chamber, which was connected to a pressure transducer, the pressure changes were recorded by a PowerLab system (AD Instruments, US). After stabilization and 10 min baseline recording (approximately 30min total), global ischemia was induced by stopping the perfusion for 30 min followed by 40 min reperfusion. Following reperfusion, atria were removed and ventricles were snap-frozen in liquid nitrogen and stored at -80 °C until further processing.

For live tissue imaging following the above IR protocol, fluorescent probes (tetramethylrhodamine, ethyl ester) TMRE, Hoechst and Sytox green were added at specific times to the perfusion buffer in the reperfusion phase (Figure 2.1) with 10min of washout before a longitudinal slice of the left ventricle free wall was cut for confocal imaging.

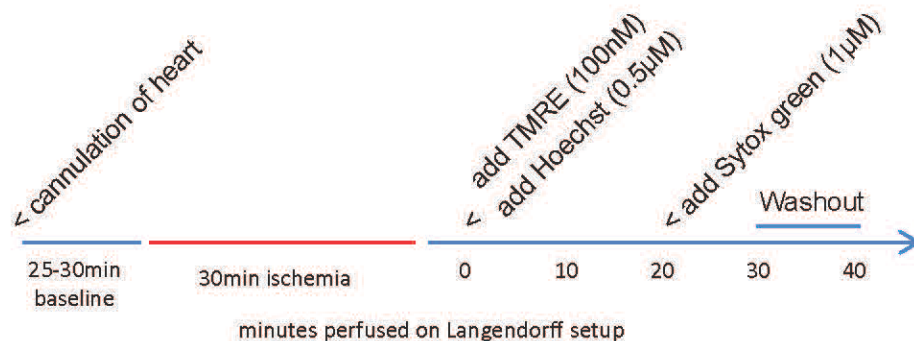


Figure 2.1 Perfusion for live tissue imaging

2.6.2. Working heart perfusion and ischemia–reperfusion protocol

Hearts from anesthetized mice were perfused in working mode with Krebs–Henseleit buffer containing 5 mmol/L [5-3H/U-14C] glucose, 1.2 mM palmitate prebound to 3% delipidated bovine serum albumin, and 50 $\mu\text{U}/\text{mL}$ insulin as described previously.¹³⁵ Hearts were perfused aerobically at a constant left atrial preload pressure of 11.5 mmHg and a constant aortic afterload pressure of 50 mm Hg for 30 min, followed by 18 min of no-flow ischemia, and 40 min

of aerobic reperfusion. Determination of glucose oxidation and glycolysis was carried out as previously described.^{135, 136} Following perfusion, atria were removed and ventricles were snap-frozen in liquid nitrogen and stored at -80 °C until further processing.

2.7. Adult mouse and human cardiomyocyte isolation, function and culture

2.7.1. Adult mouse cardiomyocyte isolation

For isolation of mouse cardiomyocytes, the mouse was anesthetized with inhaled isoflurane (2%). The heart was removed and promptly perfused with a collagenase solution and myocytes isolated and cultured as previously described.¹³⁷ We modified the protocol by adding (S)-blebbistatin (25 µM; Toronto Research Chemicals) used in 'stopping buffer' to inhibit cardiomyocyte contraction after isolation; also, ATP and BDM supplements were not used in media or buffers.¹³⁷

2.7.2. Adult human cardiomyocyte isolation

Human cardiomyocytes were isolated from non-failing human donor hearts which was obtained by the *Human Organ Procurement and Exchange* (HOPE) program. The mouse perfusion based protocol was modified as follows: fresh, explanted LV tissue was pulled apart with fine forceps and stirred in digestion buffer with blebbistatin (25 µM) at 36°C. After 20 min, digestion buffer was periodically removed and suspended cells were pelleted to determine the progress of the tissue digestion. Pelleted cells with rod shape morphometry were pooled as digestion continued (approximately 1hr), and fresh digestion buffer was added. Calcium reintroduction, plating and culture were performed as for murine cardiomyocytes.

After plating cells in media containing 10% serum, cardiomyocytes were cultured in serum free media with ITS supplement (Sigma) containing 10mg/L insulin. For addition to culture media, BYL-719 (100nM final concentration) dissolved in dimethyl sulfoxide (DMSO) was serially diluted to give final concentration of 0.005% DMSO in treated or vehicle control.

2.7.3. Measurement of cardiomyocyte contractility

Cardiomyocytes were isolated as described above, but blebbistatin was omitted to preserve contractile function. Following isolation, cardiomyocytes were kept in perfusion buffer solution (pH 7.4). An aliquot of isolated cardiomyocytes were transferred in a glass-bottomed recording chamber on top of inverted microscope (Olympus IX71) and allowed to settle for 5-6 min. Cells were superfused at a rate of 1.5-2 ml/min with modified Tyrode's solution (containing in mM): 135 NaCl, 5.4 KCl, 1.2 CaCl₂, 1 MgCl₂, 1 NaH₂PO₄, 10 Taurine, 10 HEPES, 10 glucose; pH 7.4 with NaOH). The superfusion solutions were heated to in-bath temperature of 35-36°C using in-line heater (SH-27B, Harvard Apparatus) controlled by automatic temperature controller (TC-324B, Harvard Apparatus). Quiescent rod-shaped cardiomyocytes with clear striations were selected for study. Platinum-wire electrodes were placed near the cell just outside of the microscope view at 400X magnification. Cardiomyocytes were paced at 1 or 3 Hz with voltage of 3-4 V (ca. 50% above threshold) and pulse duration of 2.5 ms using S48 stimulator (Grass Technology). Sarcomere length was estimated in real time from images captured at a rate 200 frame/sec via 40X objective (UAPO 40X3/340, Olympus) using high-speed camera (IMPERX IPX-VGA-210, Aurora Scientific) as we have previously described.¹³⁸ At about 2 min of stimulation time, 5-10 consecutive contractions were selected and averaged to reduce noise and make calculations of derivatives more precise. Averaged contraction was used to calculate fractional shortening (FS) and $\pm dL/dt$. Calculations were performed in Origin 8.5 (OriginLab) using custom-made script of built-in LabTalk language.

2.8. cAMP measurements

Measurements of cAMP in the left ventricle tissue were made using a competitive enzyme immunoassay; briefly, fragmented beta-galactosidase enzyme complementation is inhibited by a cAMP antibody, but when cAMP binds to the antibody, this competitive inhibition is lost, leading

to beta-galactosidase activity, which is detected through the enzymatic reaction with a substrate (GE Healthcare, Amersham Biosciences).

2.9. Histology

Hearts were arrested in saline with 1M KCl to stop the heart in diastole, then fixed in 10% buffered formalin. Hearts were then embedded in paraffin, and tissue slices (5 μ m thick) mounted to glass slides.

2.9.1. PSR

Picro-sirius red (PSR) and trichrome staining was performed to assess fibrosis. Deparaffinization of slides was performed by heating (65°C for 10min), followed by Xylene and then alcohol gradient rehydration, followed by staining with Celestine Blue (5min), wash in distilled water, hematoxylin (5min), wash with tap water, acid alcohol (5min), wash in tap water and then Scott's tap water (2min), wash in distilled water, 0.2% PMA (25min), PSR dye (90min), wash in acid alcohol, then ethanol (5min) and Xylene (5min) and apply mounting media and cover slip to image.

2.9.2. WGA staining

Wheat germ agglutinin (WGA) staining was performed to visualize the outline of cells to measure cross sectional area. Rehydration was performed as with PSR staining followed by incubation with fluorescent conjugated WGA in 1.5%BSA solution (25min), followed by washing with PBS and mounting media and coverslip before imaging.

2.9.3. TUNEL staining

Terminal-deoxynucleotidyltransferase-mediated dUTP nick-end labeling (TUNEL) assay kit was performed on formalin fixed sections according to the manufacturer's directions (Invitrogen).

2.9.4. DHE staining

Dihydroethidium (DHE) staining was performed on frozen sections cut from tissue frozen in OCT freezing medium. Thawed slides were covered with Hanks Buffered Salt Solution (HBSS) (5min), then incubated with DHE dye for 20min at room temperature followed by 30min at 37°C, followed by washing with HPSS, mounting media and coverslip before imaging fluorescence.

2.10. Quantitative PCR for gene expression

RNA was extracted by homogenizing (TissueLyser II) frozen tissue samples in TRIzol according to the manufacturer's instructions, and cDNA was synthesized. Gene expression was measured by cDNA quantification using real-time PCR primers and probes (TAQMAN) using a Lightcycler 480 (Roche). Primers (forward and reverse) and probes (all ThermoFisher) are as follows:

Protein(gene) Type	Sequence	
β - MHC (<i>Myh7</i>)	Forward: Reverse: Probe:	5'-GTGCCA AGG GCC TGA ATG AG-3' 5'-GCA AAG GCT CCA GGT CTG A-3' 5'-FAM-ATC TTG TGC TAC CCA GCT CTA A-TAMRA-3'
ANF (<i>Nppa</i>)	Forward: Reverse: Probe:	5'-GGA GGA GAA GAT GCC GGT AGA-3' 5'-GCT TCC TCA GTC TGC TCA CTC A-3' 5'-FAM-TGA GGT CAT GCC CCC GCA GG-TAMRA-3'
BNP (<i>Nppb</i>)	Forward: Reverse: Probe:	5'-CTG CTG GAG CTG ATA AGA GA-3' 5'-TGC CCA AAG CAG CTT GAG AT-3' 5'-FAM-CTC AAG GCA GCA CCC TCC GGG-TAMRA-3'
α -skeletal muscle actin (<i>ACTA1</i>)	Forward: Reverse: Probe:	5'-CAGCCGGCGCCTGTT-3' 5'-CCACAGGGCTTTGTTTGAAAA-3' 5'-FAM- TTGACGTGTACATAGATTGACTCGTTTTACCTCATTG- TAMRA-3'
Atrogin-1 (<i>Fbxo32</i>)		ThermoFisher catalogue # 4331182
TNF- α (<i>Tnfa</i>)	Forward: Reverse: Probe:	5'- ACAAGGCTGCCCGACTAC-3' 5'- TTTCTCCTGGTATGAGATAGCAAATC-3' 5'-FAM-TGCTCCTCACCCACACCGTCAGC-TAMRA-3'
IL-6 (<i>Il6</i>)	Forward: Reverse: Probe:	5'-ACAACCACGGCCTTCCCTACTT-3' 5'-CACGATTTCCAGAGAACATGTG-3' 5'-FAM-TTCACAGAGGATACCACTCCCAACAGACCT- TAMRA-3'
IL-1 β (<i>Il1B</i>)	Forward: Reverse: Probe:	5'-AACCTGCTGGTGTGTGACGTTT-3' 5'-CAGCACGAGGCTTTTTTTGTTGT-3' 5'- FAM-TTAGACAGCTGCACTACAGGCTCCGAGATG- TAMRA-3'

2.11. Tissue homogenization and Protein analysis

2.11.1. Tissue homogenization

Heart tissue was homogenized using a TissueLyser II in CellLytic M Cell Lysis Reagent (Sigma) with cOmplete and PhosSTOP inhibitors (Roche). Protein concentrations were standardized using a Bradford assay (Bio-Rad); samples were boiled in a denaturing Laemmli load dye (Bio-Rad).

2.11.2. Western blot

Samples were separated using SDS-PAGE to Immobilon PVDF membranes (Millipore). PVDF membranes were stained for total protein as a loading control using MemCode (Thermo). Membranes were probed using the following list of antibodies at 1:1000-1:2000 concentration in Tris buffered saline solution with 1.5% BSA, followed by HRP conjugated secondary antibodies (Cell Signaling) at 1:5000 concentration and imaged with ECL (GE Amersham) Chemiluminescence using an ImageQuant TL (GE).

Antibody target	Company	Product ID
P110 α	Cell Signaling	4255
Akt total	Cell Signaling	9272
P-Akt Ser 473	Cell Signaling	9271
P-Akt Thr 308	Cell Signaling	9275
ERK 1/2 total	Cell Signaling	4695
P-ERK 1/2	Cell Signaling	4377
Caspase 3	Cell Signaling	9662
Caspase 8	Cell Signaling	4927
RIP-1	Cell Signaling	3493
RIP-3	Cell Signaling	75702
P-CaMKII (Thr 286)	Cell Signaling	12716

Bax	Cell Signaling	2772
Bak	Cell Signaling	12105
Cyp-D (Cyclophilin F)	abcam	Ab110324
Cox4	Cell Signaling	4850
Acyl-Lysine	Millipore	05-515
P-Ser	abcam	Ab9332
Calpain 1	Cell Signaling	2556
Calpain 2	Cell Signaling	2539
PDE5a	Abcam	ab14672
P-PDH	EMD Millipore	AP1062
P-p38	Cell Signaling	4511
p38 total	Cell Signaling	9212
FOXO1	Cell Signaling	2880
FOXO3A	Cell Signaling	12829
SMAD 2/3	Cell Signaling	5678
Histone H3	Cell Signaling	4499
IRS-1	Cell Signaling	3407
P-p38	Cell Signaling	9215
P38 total	Cell Signaling	9212
Histone H3	Cell Signaling	4499
P-ERK	Cell Signaling	4377
ERK total	Cell Signaling	4695
Phospholamban	Badrilla	A010-14
P-Phospholamban (Ser 16)	Badrilla	A010-12
P-AMPK α 2 (Thr 172)	Cell Signaling	2531
AMPK α 2 total	Santa Cruz	sc-25792
P-AS160	ThermoFisher	44-1071
CD36	Novusbiologicals	NB400

2.11.3. Subcellular fractionation

For chapter 4, subcellular fractionation of frozen tissue was performed to obtain mitochondria and cytosolic fractions was adapted from a published protocol.¹³⁹ Alterations include: phosphatase and protease inhibitors from Roche were used; tissue was homogenized using a TissueLyserII (Qiagen; 3min, 25 cycles/sec); final mitochondrial and cytosolic pellets were resuspended in CellLytic buffer (Sigma) with Roche inhibitors.

Fractionation of cell nuclei from heart tissue for chapter 6 was performed as previously described.¹³⁴ Tissue was homogenized in hypotonic lysis buffer, spun 5min at 100g, then SN spun 10min at 2,000g. The resulting SN was considered the non-nuclear fraction, and the pellet was considered the rough nuclear fraction. The rough nuclear fraction was further purified by ultracentrifugation loaded onto hypotonic lysis buffer + 2.4M sucrose and spun 90min at 100,000g. The pellet was then collected as the final nuclear fraction. The non-nuclear fraction was not further separated into membrane and cytosolic fractions.

2.11.4. Co-immunoprecipitation

For chapter 4, co-immunoprecipitation (Co-IP) of Cyp-D was performed using Dynabeads (Invitrogen) according to the manufacturer's instructions. Briefly, magnetic beads with protein G surface coating were incubated with the Cyp-D antibody. Beads were then incubated with tissue homogenates. The unbound homogenate was removed, and the beads were washed. Finally, bound proteins were released by suspending the beads in lysis buffer with denaturing load dye and boiling the samples as with standard Western blots.

2.12. Statistics and graphing

Unpaired two-tailed Student t-test was used to test for differences between two experimental groups. One-way analysis of variance (ANOVA) with Student Newman Keuls post hoc test was used for three or more groups. Two way ANOVA was used for two groups with two subgroups

(i.e. two genotypes with two treatments). If no combination effect was observed, main effects of individual treatments/genotype were considered. Cox regression was used for survival analysis.

Data was graphed using bar graphs showing mean values +/- standard error of the mean (SEM) or box and whisker plots dividing the data into quartiles with the box representing the first and third quartile and the internal band representing the second quartile (median) (Origin 2016); the mean was indicated by a small square, and whiskers maximum and minimum values, except for outliers indicated when greater than 1.5x the interquartile range from the upper or lower limit of the box. Statistical analysis was performed using Microsoft SPSS (version 23). Statistical significance was considered to be $P \leq 0.05$.

3. PI3K α in Ischemia Reperfusion Injury Part I: Published Work

Adapted from previously published: Enhanced recovery from ischemia-reperfusion injury in PI3K α dominant negative hearts: investigating the role of alternate PI3K isoforms, increased glucose oxidation and MAPK signaling. J Mol Cell Cardiol. 2013 Jan;54:9-18.

3.1 Introduction

This chapter details our study of PI3K signaling in an *ex vivo* ischemia/reperfusion (IR) injury model introduced in chapter 1.8. This study follows on the previous findings that PI3K α DN hearts are resistant to IR injury, and proposed that enhanced PI3K γ activity explains this phenotype.⁹⁶ This chapter has three main themes: (1) cross breeding PI3K α DN and PI3K γ knockout (KO) mice to see if the PI3K α DN phenotype is lost, (2) characterization of altered metabolic substrate utilization as a possible mechanism and (3) investigation of related signaling pathway changes that could explain the PI3K α DN phenotype.

3.2 Results and discussion

3.2.1. Independent basal effects of PI3K α and PI3K γ

It was previously shown that PI3K α and PI3K γ play different roles in the myocardium from mice with a PTEN null background.⁵ Here we tested the hypothesis that PI3K α and PI3K γ mediate independent effects in the heart when both isoforms are mutated in mice with a wildtype (WT) background (non-transgenic littermates to PI3K α DN mice). We found that cross bred PI3K α DN and PI3K γ KO mice, here referred to as PI3K double mutant (PI3KDM) mice mimic the PI3K α DN phenotype with smaller hearts based on the decreased ratios of heart weight to body weight and left ventricle (LV) weight to tibial length (Table 3.1). PI3K γ KO mice have increased myocardial cAMP resulting in enhanced cardiac contractility^{5, 84}.

We found that cAMP concentrations were also elevated in the PI3KDM hearts (Figure 3.1A), which corresponded to increased phosphorylation of phospholamban (serine-16) (Figure

3.1B and C) with similar values seen in PI3K γ KO hearts (Figure 3.1A–C). These molecular alterations are expected to increase basal myocardial contractility as was observed previously in PI3K γ KO mice. Echocardiographic and invasive hemodynamic measurements confirmed

Table 3.1 Hemodynamic and morphometric parameters

	WT	PI3K α DN	PI3K γ KO	PI3KDM
N	10	10	10	10
HR (bpm)	494 \pm 14	503 \pm 12	491 \pm 12	508 \pm 15
PWT (mm)	0.68 \pm 0.06	0.65 \pm 0.05	0.67 \pm 0.05	0.66 \pm 0.10
LVEDD (mm)	3.71 \pm 0.11	3.47 \pm 0.08	3.69 \pm 0.12	3.49 \pm 0.13
LVESD (mm)	2.55 \pm 0.09	2.43 \pm 0.07	2.34 \pm 0.08	2.24 \pm 0.10
FS (%)	31.3 \pm 1.8	30 \pm 2.1	36.5 \pm 2.2*	35.8 \pm 1.9*
VCF _c (circ/s)	6.13 \pm 0.12	6.02 \pm 0.14	7.93 \pm 0.15*	7.88 \pm 0.12*
+dP/dt _{max} (mm Hg/s)	10131 \pm 301	9984 \pm 323	12893 \pm 276*	12744 \pm 330*
- dP/dt _{min} (mm Hg/s)	9845 \pm 252	9683 \pm 273	11967 \pm 281*	12006 \pm 343*
LVEDP (mm Hg)	5.23 \pm 1.96	4.06 \pm 1.82	6.52 \pm 2.1	3.83 \pm 2.2
LVW/TL (mg/mm)	4.11 \pm 0.04	3.38 \pm 0.07*	4.15 \pm 0.07	3.46 \pm 0.06*
HW/BW (mg/g)	5.26 \pm 0.11	3.96 \pm 0.12*	5.29 \pm 0.15	4.02 \pm 0.13*

HR, heart rate; PWT, posterior left ventricular wall thickness; LVEDD, left ventricular end diastolic diameter; LVESD, left ventricular end systolic diameter; FS, fractional shortening; VCF_c, velocity of circumferential shortening corrected for heart rate; +dP/dt_{max}, maximum first derivative of the change in left ventricular pressure; and - dP/dt_{min}, minimum first derivative of the change in left ventricular pressure; LVEDP, left ventricular end-diastolic pressure; LVW, LV weight; TL, tibial length; HW, heart weight; BW, body weight. *p =0.05 compared with the WT group.

increased basal myocardial contractility in PI3KDM mice characterized by increased velocity of circumferential fiber shortening (VCF_c), +dP/dt_{max} and -dP/dt_{min} compared to WT mice (Table 3.1). These results show that basal PI3K α and PI3K γ isoforms are independent and the dual loss of PI3K α and PI3K γ signaling results in smaller and hypercontractile hearts.

3.2.2. Loss of PI3K γ does not reverse protection in PI3K α DN hearts

PI3K γ controls GPCR-mediated downstream signaling,^{140, 141} and loss of PI3K γ impairs ischemic preconditioning and prevents adenosine-mediated phosphorylation of Akt.⁹⁶ We hypothesized that loss of PI3K γ would abrogate the protective effect of PI3K α inactivation on the functional recovery of PI3K α DN hearts following IR, and as such we subjected PI3KDM hearts to IR using the classic Langendorff model. Contrary to our hypothesis, PI3KDM hearts showed a marked

protection from myocardial IR injury using a standard ischemic–reperfusion protocol. Left ventricular developed pressure (LVDP), +dP/dtmax, –dP/dtmin and rate–pressure product (RPP) (Figure 3.1D–G) collectively showed a significantly greater recovery in the PI3KDM compared with WT hearts.

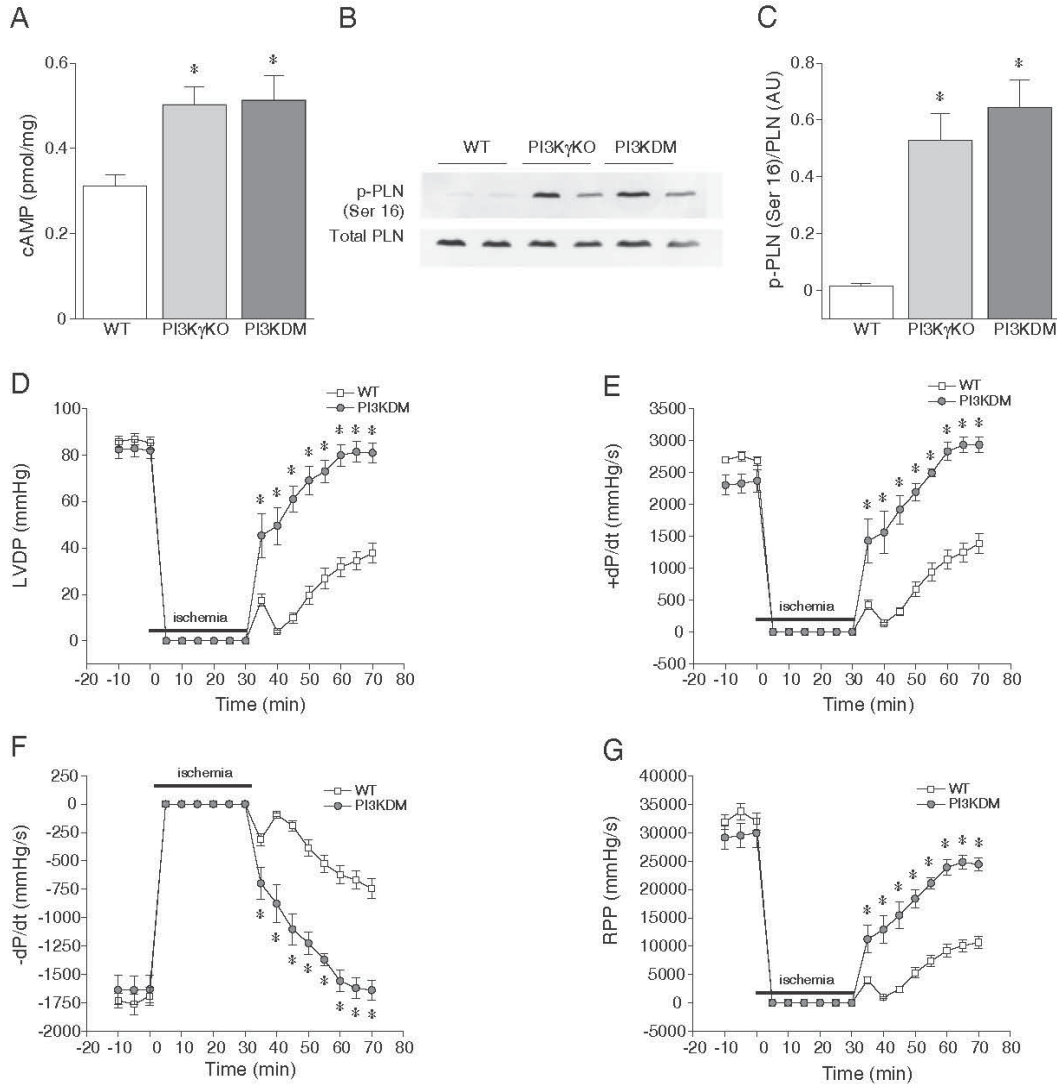


Figure 3.1. PI3KDM hearts retain increase in cAMP signaling, characteristic of PI3K γ KO, and robust recovery from IR, characteristic of PI3K α DN. Measurement of cAMP (A) and phospholamban (PLN) representative western blots (B) and densitometry results (C) obtained directly from WT, PI3K γ KO and PI3KDM heart tissue. Functional recovery from after ischemia for WT and PI3KDM hearts after 10 min baseline, 30 min ischemia and 40 min reperfusion: LV developed pressure (LVDP; D), maximum (+dP/dtmax; E) and minimum (-dP/dtmin; F) rate of change in LV pressure, and rate–pressure product (RPP; G). Values are mean \pm SEM; n=6 per group; *p \leq 0.05 compared to WT.

3.2.3. Signaling through Akt and GSK3 β is reduced in PI3KDM hearts

Western blot analysis showed that WT hearts had significantly increased phosphorylation of Akt following IR when compared to baseline (aerobic perfusion) (Figure 3.2A–C). Basal Akt phosphorylation in the PI3KDM hearts was reduced compared to WT; Akt phosphorylation increased, although not significantly in the PI3KDM hearts after IR treatment, but was still reduced compared to IR WT hearts based on phospho-Akt/total ratio (Figure 3.2A–C).

Accordingly, GSK3 β phosphorylation was also reduced in PI3KDM hearts compared to WT at baseline (Figure 3.2A and D), but phosphorylation of GSK3 β was not significantly different between PI3KDM and WT in IR groups (Figure 3.2A and D). The robust phosphorylation of GSK3 β upon IR, despite the low Akt activation in the PI3KDM model may be partially caused by other pathways that can also phosphorylate GSK3 β , such as PKA¹⁴², which may be activated by the increased cAMP levels in the PI3KDM model (Figure 3.1A). PI3K α DN hearts have higher Akt phosphorylation than WT after IR,⁹⁶ but have reduced basal Akt phosphorylation.⁴ These results support a role of PI3K γ mediated signaling in the phosphorylation of Akt in response to myocardial IR injury. However, the marked protection against myocardial IR injury despite the relative lack of Akt phosphorylation in the PI3KDM hearts compared to WT both at baseline and upon IR, and the similar level of GSK3 β phosphorylation between PI3KDM and WT upon IR, implies other mechanism(s) are responsible for the cardioprotection in these hearts.

3.2.4. PI3K α DN hearts are resistant to myocardial I/R injury in the ex vivo working heart perfusion model

We next investigated whether cardioprotection seen in the PI3K α DN hearts perfused in the Langendorff mode can be recapitulated in an ex vivo working heart perfusion model.

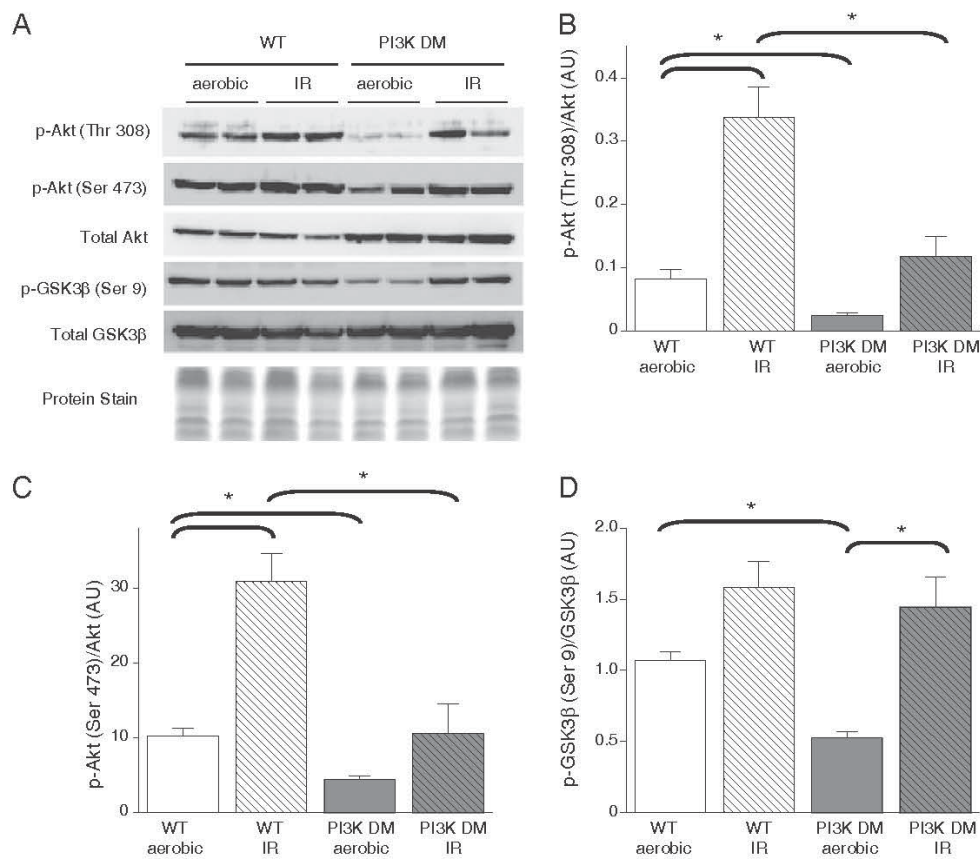


Figure 3.2. Phosphorylation of Akt was reduced in PI3KDM compared to WT hearts both at baseline and following IR at 40 min reperfusion using the ex vivo Langendorff system; GSK3 β phosphorylation was also reduced at baseline but was not significantly reduced from WT upon reperfusion. Representative western blots (A) and densitometric analysis for Akt (Thr 308) (B) and (Ser 473) (C), and GSK3 β (Ser 9) (D). Values are mean \pm SEM; n=4 per group; *p \leq 0.05 compared to the corresponding group indicated.

We had three reasons for utilizing the working heart model: first, to see if the IR protection of the PI3K α DN hearts would be maintained in the ejecting, working heart mode and not only in the Langendorff isovolumic system; second, to directly compare PI3K α DN and PI3KDM hearts to see if there is any effect on PI3K α DN IR recovery with the loss of PI3K γ ; and third, the working heart model allows the use of dual energy sources (palmitate and glucose) and assessment of cardiac metabolism in the presence of physiological levels of insulin. While the product of heart rate and peak systolic pressure (HR \times PSP) and cardiac power were not significantly different at baseline between the three groups, both PI3K α DN and P3IKDM hearts had significantly

stronger recovery after IR than WT with no difference between PI3K α DN and PI3KDM (Figure 3.3A–D).

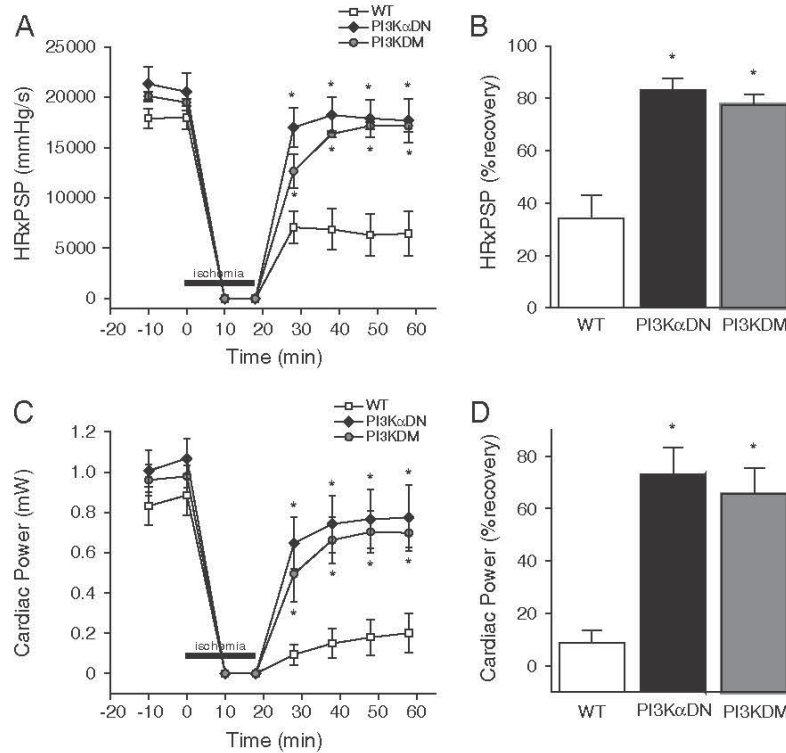


Figure 3.3. Functional recovery in ex vivo perfused working hearts is similarly increased from WT in PI3K α DN, and PI3KDM hearts. Recovery of the product of heart rate and peak systolic pressure (HRxPSP; A and B) and cardiac power (C and D) following 30 min baseline perfusion, 18 min ischemia and 40 min reperfusion. Values are mean \pm SEM; n= 6-8; *p \leq 0.05 compared to WT.

Taken together, these results confirm that chronic loss of PI3K α protects the heart from myocardial IR injury in a setting of afterload and with dual substrate (glucose and palmitate) utilization, and this protection is independent of PI3K γ signaling.

3.2.5. Akt and GSK3 β in PI3K α DN and PI3KDM from the working heart perfusion

PI3K α DN hearts have enhanced phosphorylation of Akt and GSK3 β after IR treatment using the Langendorff model,⁹⁶ and we have obtained similar results using the working heart model (Figure 3.4A–C and E). Interestingly, both PI3K α DN and PI3KDM hearts had increased mean total Akt protein levels, with the PI3KDM model reaching significance (Figure 3.4D), and PI3KDM hearts had increased GSK3 β protein levels (Figure 3.4F). Increased expression of total

Akt was also reported for a cardiac PI3K α knockout using the flox/ Cre transgenic system¹⁴³. Due to the increased protein levels of Akt and GSK3 β , PI3KDM has a phospho/total ratio for Akt and GSK3 β that is similar to WT. When comparing PI3KDM to WT, there is a striking reversal in the total Akt and GSK3 β phosphorylation between Langendorff and working heart perfusions, but PI3KDM hearts recover from IR injury significantly better than WT in both perfusion systems, suggesting that although signaling through Akt and GSK3 β has IR protective effects, it is not the driving mechanism behind the IR protection of PI3K α DN hearts. In our study we did not investigate the different activation of the Akt isoforms (Akt1–3) which may explain the varying degrees of total Akt activation and the final effect on IR recovery, as Akt1 is known to have a greater role in IR protection compared to Akt2¹⁴⁴. In addition, we measured Akt and GSK3 β phosphorylation levels at the end of the reperfusion, but we did not assess their levels immediately after reperfusion, when Akt activation and GSK3 β inhibition may be more important for IR protection.

3.2.6 Altered metabolic substrate utilization in PI3K α DN and PI3KDM hearts

Metabolic reprogramming, which can shift the utilization of metabolic substrates, is known to have an important role in the heart's ability to minimize myocardial IR injury,^{145, 146} and either inhibition of FA oxidization or stimulation of glucose oxidization can cause a dramatic reduction in IR injury.¹⁴⁷ PI3K can play a key role in regulating cardiac metabolism^{75, 148} and PI3K α DN hearts have decreased FA oxidization⁷⁵ which may increase glucose oxidation due to the Randle effect.¹⁴⁹

Interestingly, both PI3K α DN and PI3KDM hearts showed an increase in basal glucose oxidation compared to WT hearts before ischemia and also upon reperfusion (Figure 3.5A), but glycolysis rates were not significantly different between the three genotypes at baseline or upon reperfusion (Figure 3.5B).

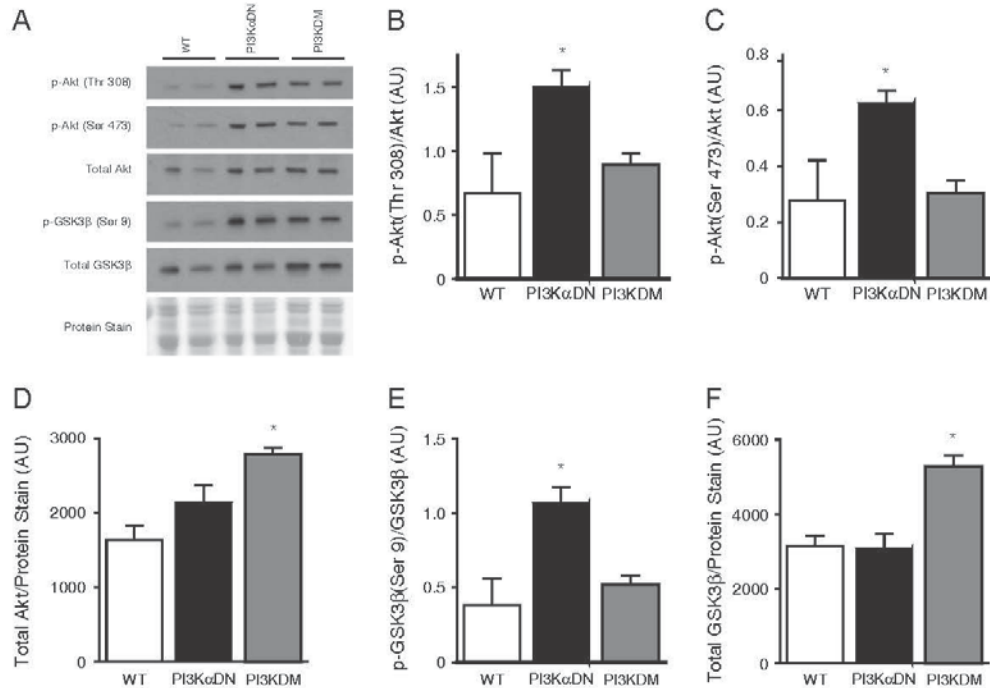


Figure 3.4. Phosphorylation of Akt and GSK3 β in reperused WT, PI3K α DN and PI3KDM hearts from the working heart model at 40 min reperfusion. Phosphorylation of Akt and GSK3 β was increased in PI3K α DN hearts compared to WT (A–C and E), but this was not the case in PI3KDM hearts, partly due to increased protein levels for both Akt and GSK3 β (A–F). Values are mean \pm SEM; n=6 per group; *p \leq 0.05 compared to WT.

AMP-activated protein kinase (AMPK) acts as a metabolic master switch for important aspects of cellular energy supply including the uptake of glucose and β -oxidation of fatty acids. Following a rise in the intracellular AMP-to-ATP ratio, AMPK switches off energy-consuming processes such as protein synthesis, whereas ATP-generating mechanisms, such as fatty acid oxidation and glycolysis are activated.^{150, 151} The low level of AMPK activation in the PI3K α DN and PI3KDM hearts following IR (Figure 3.5C-D) is indicative of maintained ATP production and is consistent with the increased levels of glucose oxidation in these models. Upon phosphorylation of AMPK, fatty acid oxidation increases via phosphorylation of acetyl-CoA carboxylase,^{152, 153} and fatty acid uptake is increased via activation of membrane translocation of the fatty acid transporter CD36. CD36 expression was decreased compared to WT in PI3K α DN and PI3KDM but only the former was significant (Figure 3.5E). AS160 is an important negative regulator of glucose uptake through inhibition of GLUT4 membrane translocation;

when phosphorylated by Akt, AS160 is inactivated and glucose transport is promoted.¹⁵⁴ Both PI3K α DN and PI3KDM hearts had increased levels of p-AS160 (Thr 642) (Figure 3.5C); PI3K α DN hearts had a coordinate increase in the ratio of phospho to total AS160 protein (Fig. 5F), but this was not the case with the PI3KDM model, due to an increase in the total protein level of AS160 (Figure 3.5G). Before further investigating the mechanism responsible for causing increased glucose oxidation in PI3K α DN, we first wanted to investigate the significance of this altered metabolic substrate utilization in the context of IR injury.

To test the significance of enhanced glucose oxidation for IR recovery in PI3K α DN hearts, we perfused hearts in the working mode with palmitate but in the absence of glucose. We did not continue at this point with PI3KDM model because we had established that PI3K γ signaling did not have an effect on PI3K α DN IR recovery. We hypothesized that if increased glucose was an important factor in PI3K α DN IR recovery, the benefit would be lost if the hearts were forced to metabolize only FAs. When perfused with only palmitate as a metabolic substrate, WT hearts had normal function after a 30min baseline perfusion; this was expected considering that FAs are a major source of energy for the heart *in vivo* (60-90%).¹⁵⁵ However, upon administration of 18min ischemia, WT hearts did not recover sufficiently to pump against the afterload (data not shown). We reduced the ischemic period to 9min in an attempt to have WT hearts regain some function, but WT hearts were still non-ejecting after 9min ischemia (Figure 3.5H-K). In contrast, PI3K α DN hearts had nearly complete recovery after 9min ischemia in the absence of glucose (Figure 3.5H-K). These results confirmed the importance of glucose oxidation for the recovery of WT hearts after ischemia, but suggested that increased glucose oxidation was not the primary mechanism of IR protection in PI3K α DN hearts.

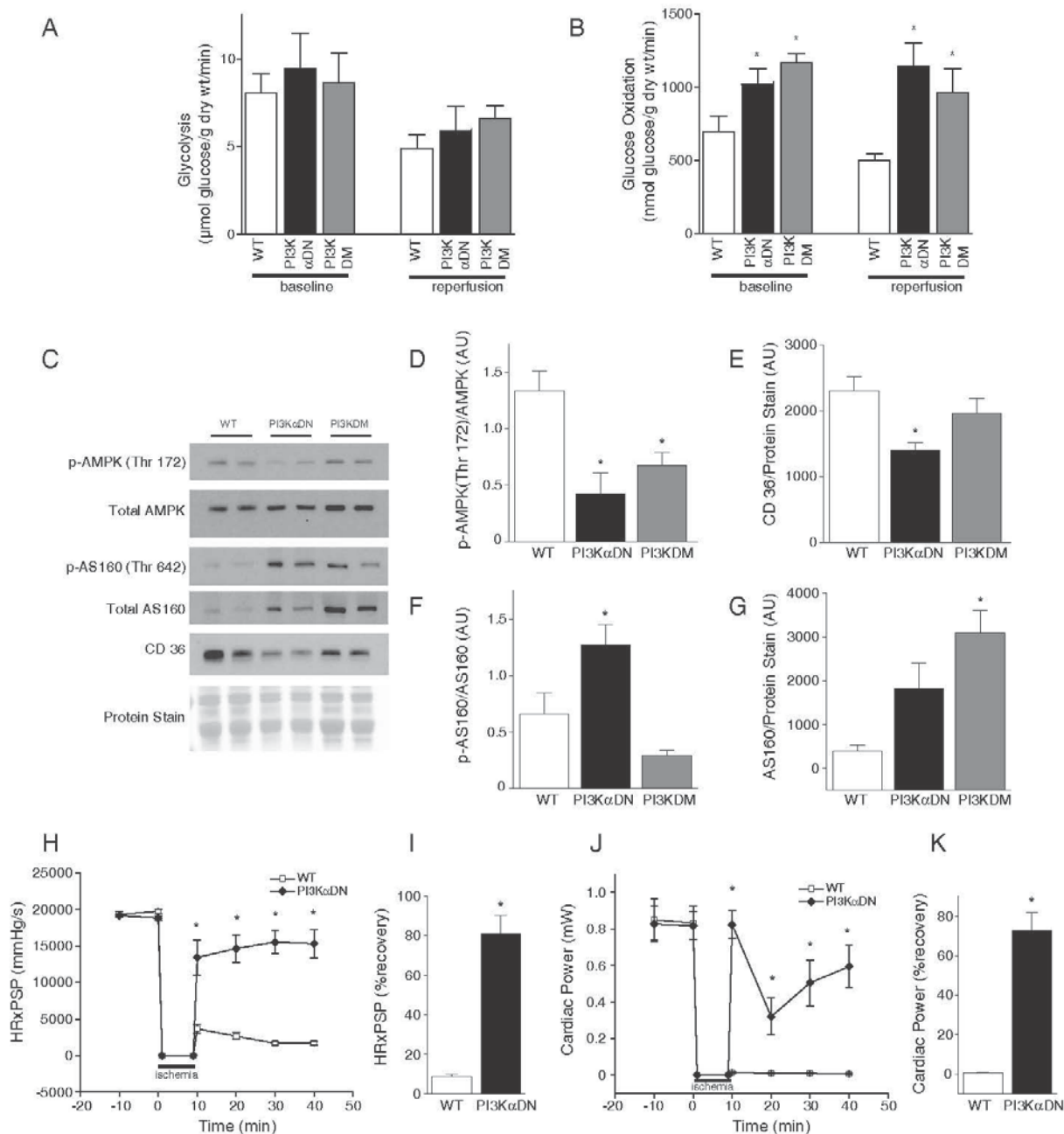


Figure 3.5. Glucose metabolism in *ex vivo* perfused working hearts from PI3KαDN and PI3KDM mice compared to WT at baseline and after reperfusion. Both PI3KαDN and PI3KDM hearts had similar rates of glycolysis to WT hearts at baseline and reperfusion (A), but significantly increased rates of glucose oxidation both at baseline and upon reperfusion (B). Western blots for regulators of metabolic substrate uptake and utilization in tissue from post-IR working hearts showed decreased AMPK phosphorylation in both PI3KαDN and PI3KDM hearts (C and D) and altered expression of the fatty acid transporter CD36 and AS160, a regulator of glucose uptake (C and E–G). PI3KαDN and WT hearts perfused in the working mode without glucose were treated with 9 min ischemia and assessed for recovery of the product of heart rate and peak systolic pressure (HR×PSP; H and I) and cardiac power (J and K). Values are mean±SEM; n=6–8 per group (A and B), n=6 per group (C–G) and n=5 per group H–K); *p<0.05 compared to WT.

3.2.7. Increased MAPK signaling in PI3K α DN hearts

Inhibition of the PI3K signaling axis can have effects on alternate signaling pathways that may contribute to the IR protection of PI3K α DN hearts; for example, pharmacological inhibition of PI3K causes a significant increase in MAPK signaling.¹⁵⁶ We looked at activation of three key nodes in MAPK signaling in hearts from our working heart model: ERK1/2, JNK and p38. ERK1/2 signaling is anti-apoptotic and protective in the setting of IR,^{157, 158} JNK has been associated with both protective and detrimental effects on IR recovery¹⁵⁹ while p38 activation is associated with reduced IR recovery.¹⁶⁰ Phosphorylation of both ERK1/2 and JNK was significantly increased (Fig. 6A-C), but p38 activation was unchanged between WT and PI3K α DN (Figure 3.6A and D). As noted previously, wortmannin collapsed PI3K α DN IR recovery to the same level as WT,¹⁶¹ but wortmannin has numerous targets outside of the PI3K family, including MAPK.¹⁶²

In order to explain this increase in ERK1/2 and JNK activation in PI3K α DN hearts, we looked to the large field of PI3K signaling in the context of cancer research. Deregulation of PI3K activation is a common driving factor in numerous cancers, and several PI3K inhibitors are in clinical trials and early development.³¹ An important complication that arises when inhibiting the PI3K pathway is the possibility for compensatory upregulation of parallel signaling pathways due to the relief of negative feedback mechanisms.¹⁶³⁻¹⁶⁵ For example, PI3K signaling activates the ribosomal subunit S6K, which promotes protein translation and cell growth. However, S6K also inhibits the expression of IRS-1, an important mediator between growth factor receptors and PI3K activation.¹⁶⁶ We investigated the expression and activation of IRS-1 in PI3K α DN hearts, and found that total IRS-1 expression was dramatically increased (Figure 3.6E-G), and phosphorylation of the activating Tyr 612 site was also increased. IRS-1 is able to cause strong activation of ERK1/2, as a result of rapamycin treatment, which causes relief of S6K inhibition of IRS-1.¹⁶⁷ This increase in IRS-1 expression and activation may also explain some of the differences in Akt phosphorylation between our Langendorff and working heart models: insulin was included in the working heart perfusate but was not used in the

Langendorff. Interestingly, the PI3KDM model had reduced Akt activation after IR in the Langendorff model compared to WT (Figure 3.2A-C), but in the working heart, PI3KDM hearts had similar ratios of phospho to total Akt compared to WT (Figure 3.4A-C), this result may be explained by an increased sensitivity to insulin due to increased IRS-1 activity.

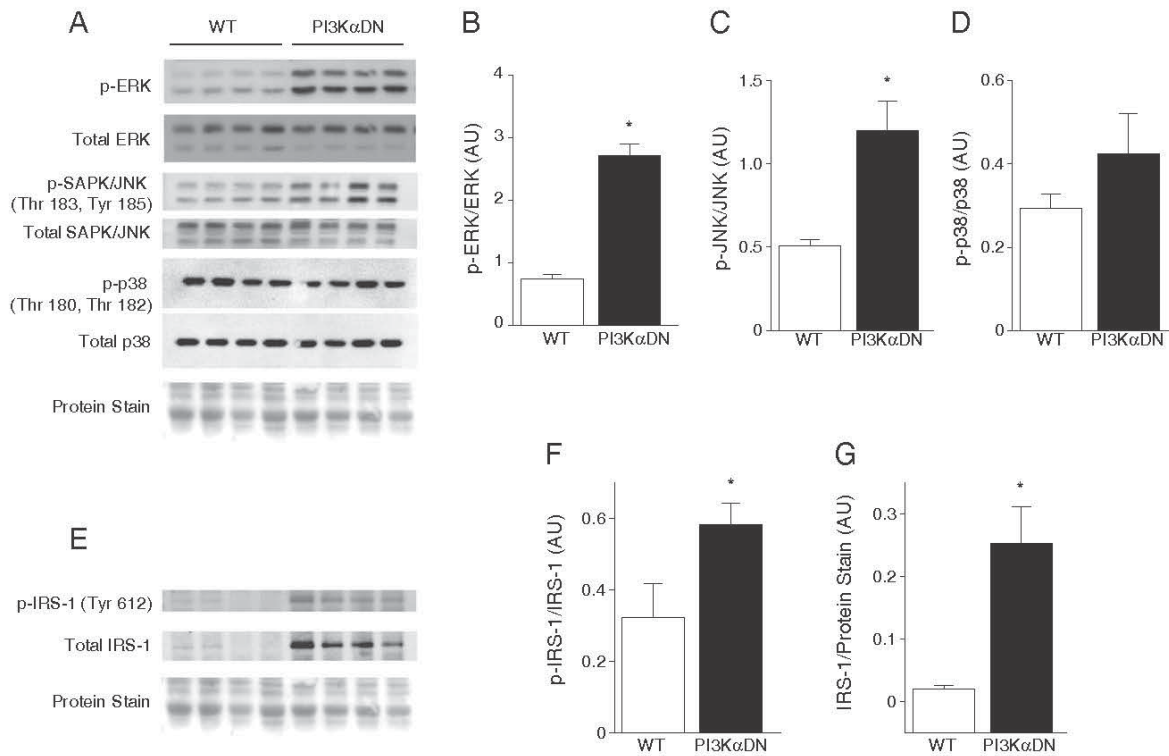


Figure 3.6. Western blot analysis showed activation of MAPK signaling (A–D) and IRS-1 (E–G) in PI3K α DN hearts from working heart IR perfusions. Values are mean \pm SEM; n=6 per group (A–D) and n=4 per group (E–G); *p \leq 0.05 compared to WT.

3.3 Conclusions

We have concluded that IR protection in PI3K α DN hearts was not due to increased signaling through PI3K γ isoform because PI3KDM hearts were still protected. We observed interesting variations in Akt activation, with robust Akt activation in PI3K α DN hearts perfused in the working model, and PI3KDM hearts also had high Akt activation in this model, although not different than WT when comparing phospho to total protein levels. Activation of Akt was reduced

in the PI3KDM when compared to WT hearts in the Langendorff model, but functional recovery for PI3KDM was significantly higher than WT in both Langendorff and working heart models, suggesting that the activation of Akt is not a critical mediator of the protection against IR injury in this model. Importantly, using both Langendorff and working heart models we have shown that both the PI3K α DN and PI3KDM hearts displayed similar and enhanced functional recovery in response to IR injury. Interestingly, PI3K α DN hearts have enhanced glucose oxidation during baseline and post-IR; this may be caused by a combination of increased glucose uptake into the cell or a decrease in FA uptake/utilization, possibly by altered expression and regulation of AMPK, AS160 and CD36. However, this preference for glucose oxidization does not seem to be important for PI3K α DN IR protection, because these hearts were still significantly protected from IR injury when hearts were forced to only metabolize FAs (palmitate). Interestingly, we found that MAPK signaling through ERK1/2 and JNK had increased activation in PI3K α DN hearts, possibly driven by an increase in IRS-1 activation and expression, although further work will be needed to determine the extent to which MAPK activation is responsible for the IR protection seen in PI3K α DN hearts. Our results illustrate the inherent complexity of signaling mechanisms in the heart and highlight an interesting intersection between PI3K and MAPK signaling.

4. PI3K α in Ischemia Reperfusion Injury Part II: Unpublished Work

4.1. Introduction

This chapter presents some of the further experiments I've performed following our previous publication (chapter 3).¹⁶⁸ This chapter has the following main topics: (1) testing the relevance of acute Akt and ERK activation in PI3K α DN hearts in IR injury by performing perfusions with inhibitors to those pathways, (2) testing IR recovery in an inducible PI3K α knockout model, (3) investigation of mitochondrial membrane potential and cell injury/death processes and (4) investigation of mediators of regulated necrosis.

Our overall goal with this ongoing project is to understand the cellular and molecular mechanisms that underpin the resistance of PI3K α DN hearts to IR injury, possibly leading to new understandings of PI3K signaling, IR injury mechanisms and possible new therapeutic targets.

4.2. Challenge of PI3K α DN hearts with inhibitors against MEK and AKT in IR model

4.2.1. Background and rational for experiments

There is a general consensus that IR protective signaling pathways converge through cellular mechanisms that cause maintained mitochondrial integrity and function. Intact mitochondria are essential for sufficient ATP production as well as maintenance of ionic homeostasis. Opening of the mitochondrial permeability transition pore (mPTP) Akt and ERK have been proposed as central nodes for IR protection.¹⁶⁹ To test my previous hypothesis¹⁶⁸ that the MAPK member ERK activation may cause enhanced IR recovery in PI3K α DN hearts, as well as the hypothesis that increased Akt signaling was responsible for this phenotype,⁹⁶ I performed Langendorff perfusions with inhibitors against either the Akt or ERK pathway. The Akt inhibitor MK2206 inhibits Akt isoforms 1-3 with IC₅₀ of 12-65nM,¹⁷⁰ and is currently in clinical trials as a cancer therapy (50 results for MK2206 on clinicaltrials.gov Oct. 2016). ERK is the substrate of the

kinase MEK; to reduce ERK activation, I used the potent MEK inhibitor MEK-162 (ARRY-162, Binimetinib; IC₅₀ 12nM; manufacturer supplied). This drug is in clinical trials as a cancer therapy and as an anti-inflammatory agent (43 results for MEK-162 on clinicaltrials.gov Oct. 2016). I hypothesized that one or both of these inhibitors would significantly reduce the functional recovery of PI3KαDN hearts after IR.

4.1.2. Results: Akt and ERK inhibition in PI3KαDN and Ctr hearts

Perfusion with MEK-162 significantly reduced ERK phosphorylation, but did not reduce functional recovery in PI3KαDN hearts (Figure 4.1A,B). Similarly, perfusion with the Akt inhibitor MK2206 significantly reduced phosphorylation of Akt at Thr308 and Ser473 residues (Figure 4.1D), but did not reduce functional recovery of PI3KαDN hearts (Figure 4.1C). Surprisingly, Akt inhibition had a beneficial effect on IR functional recovery in control hearts if only wildtype hearts were considered in an unpaired t-test (not shown).

4.2 IR recovery in an adult, inducible PI3Kα deletion model

4.2.1 Background and rationale for experiments

The PI3KαDN heart had a kinase dead p110α transgene expressed in the heart, which causes constitutively reduced PI3Kα activity, including throughout development, resulting in reduced heart size.⁴ Others have speculated that PI3KαDN phenotypes may be influenced by developmental processes, where adaptation to reduced p110α during development may cause a different phenotype than if p110α was inhibited/deleted in an adult heart.¹⁰³ To determine if the strong IR recovery seen in PI3KαDN hearts is unique to the PI3KαDN model or is found in other models of p110α deletion, I tested an inducible, cardiomyocyte specific p110α model. For control hearts, I used littermates which carry the LoxP sites on the p110α gene, but lack the Cre recombinase transgene. I also did not treat these mice with tamoxifen. These would not be ideal controls if tamoxifen/Cre toxicity was a concern, but I had already established a safe dose of

tamoxifen,⁶ and I was hypothesizing a beneficial phenotype for the conditional knockout mice. Also, these littermate control hearts gave a IR phenotype similar to wildtype mice.

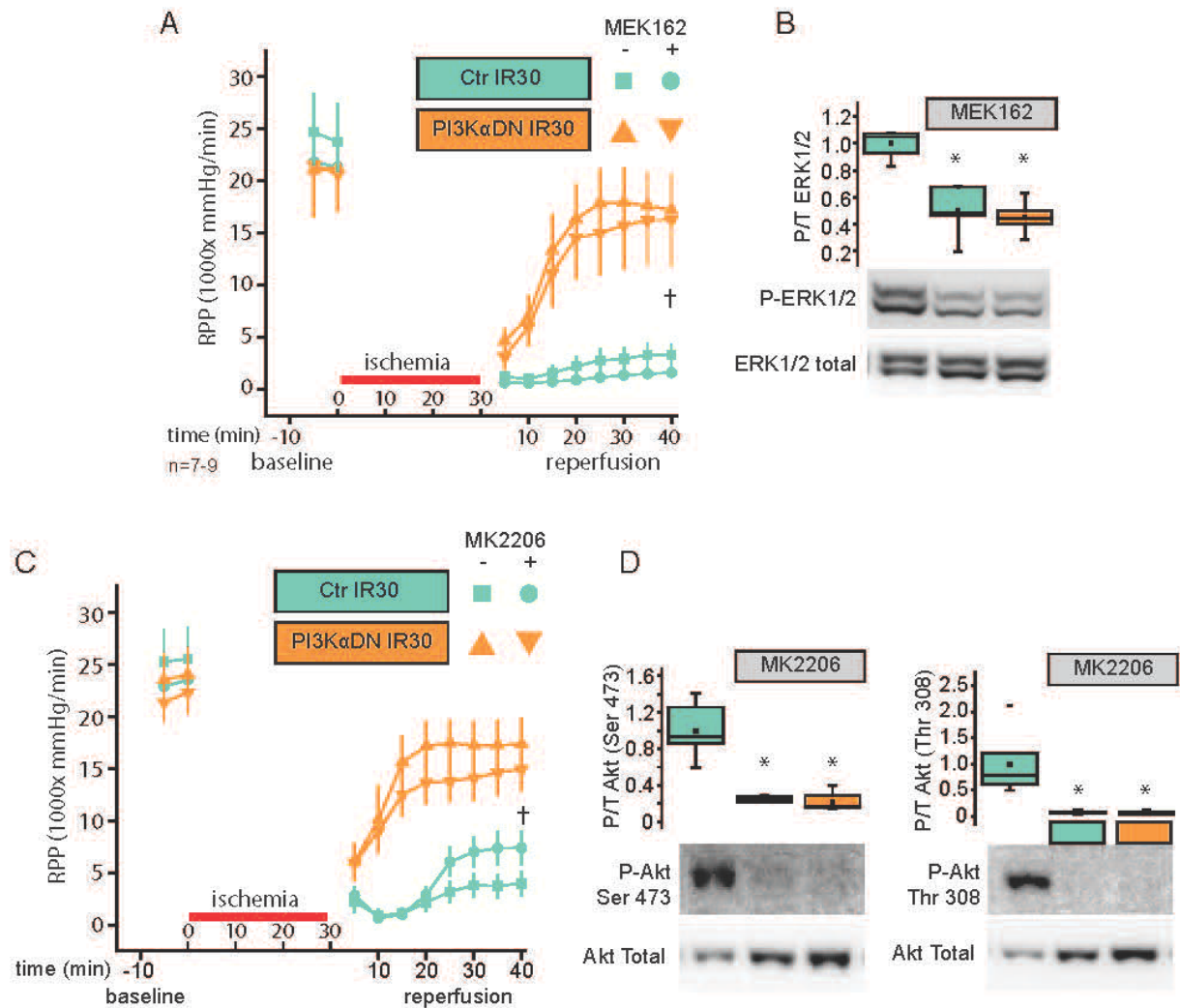


Figure 4.1. Langendorff perfusion with functional assessment of developed pressure and heart rate (RPP, rate pressure product) with 30min global, no flow ischemia (IR30) with 40min reperfusion for control (Ctr) and PI3KαDN hearts (A) with the MEK inhibitor MEK162 (100nM). B, Western blot confirmed significant reduction in phosphorylation of ERK1/2 (n=4-5). C, similarly, hearts were perfused with the Akt inhibitor MK2206 (1μM) and (D) Western blots showed reduced phosphorylation of Akt on Ser 473 and Thr 308 (n=4-6). *P<0.05 compared to untreated controls, 1 way ANOVA; † P<0.05 significant effect of genotype, 2 way ANOVA; ‡ P<0.05 significant effect of drug treatment, 2 way ANOVA.

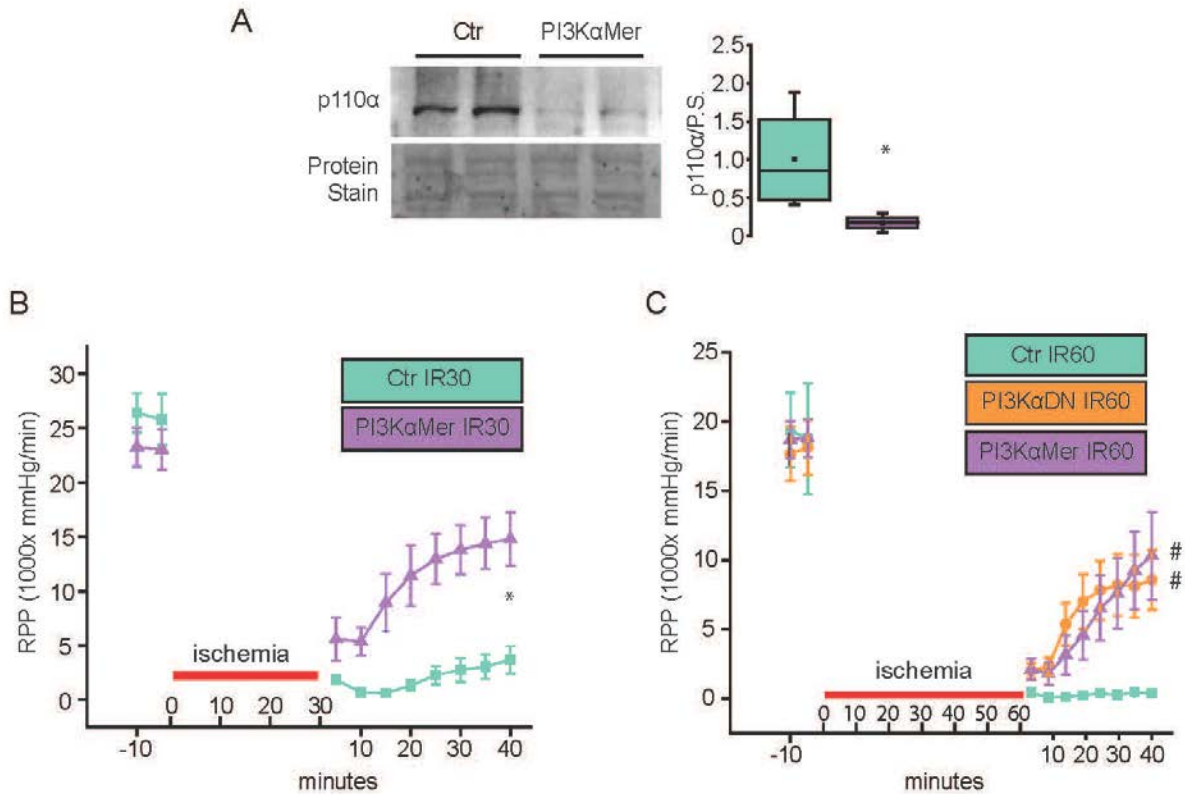


Figure 4.2. Deletion of p110 α was achieved after 2 days of tamoxifen treatment (40mg/kg) in PI3K α Mer compared to non-Mer littermate controls (A) (n=4) with 7-10 days follow-up allowed before perfusion experiments. Langendorff perfusions are shown with functional assessment of developed pressure and heart rate (RPP, rate pressure product) with 30min global, no flow ischemia (IR30) with 40min reperfusion for control (Ctr) or PI3K α Mer (n=7-9) (B). Additionally, 60min ischemia was tested in both PI3K α DN, PI3K α Mer and Ctr hearts (n=5-7) (C). *P \leq 0.05 in unpaired student t-test; #P \leq 0.05 one way ANOVA compared to Ctr group.

4.2.2 Results: PI3K α Mer, 60min ischemia, p110 α inhibition with BYL719

Deletion of p110 α was achieved after 2 days of tamoxifen treatment (40mg/kg) with 7-10 days follow-up allowed before perfusion experiments (Figure 4.2A). Under our standard 30min ischemia and 40min reperfusion protocol, knockout hearts had significantly improved functional recovery compared to controls (Figure 4.2B). With 60min ischemia, both PI3K α DN and PI3K α Mer had similar, higher functional recovery compared to Ctr hearts (Figure 4.2C). These results showed that reduction of myocardial PI3K α through distinct transgenic models both resulted in similar IR protection compared to control hearts.

4.3 Assessment of mitochondrial membrane potential and cell injury after IR injury

4.3.1 Background and rationale for experiments

Mitochondrial membrane potential (MMP) is required for the proton gradient that drives mitochondrial oxidative respiration. Loss of the MMP causes lost production of ATP from the mitochondria, and can lead to cell death. We hypothesized that PI3K deletion models likely have an end effect of maintaining MMP after IR compared to Ctr hearts. We performed live tissue imaging after IR by perfusing hearts with fluorescent probes during reperfusion (Figure 4.3A).

4.3.2 Results: reduced PI3K α models have higher MMP and reduced cell death after IR

TMRE fluorescence was significantly higher in PI3K α deletion models after IR than controls (Figure 4.3B). This corresponded to reduced levels of Sytox green positive cells (Figure 4.3C), showing that maintenance of mitochondrial function closely correlated with functional recovery (Figure 4.1-2), whereas control hearts not only had reduced function, but severe cell injury and death.

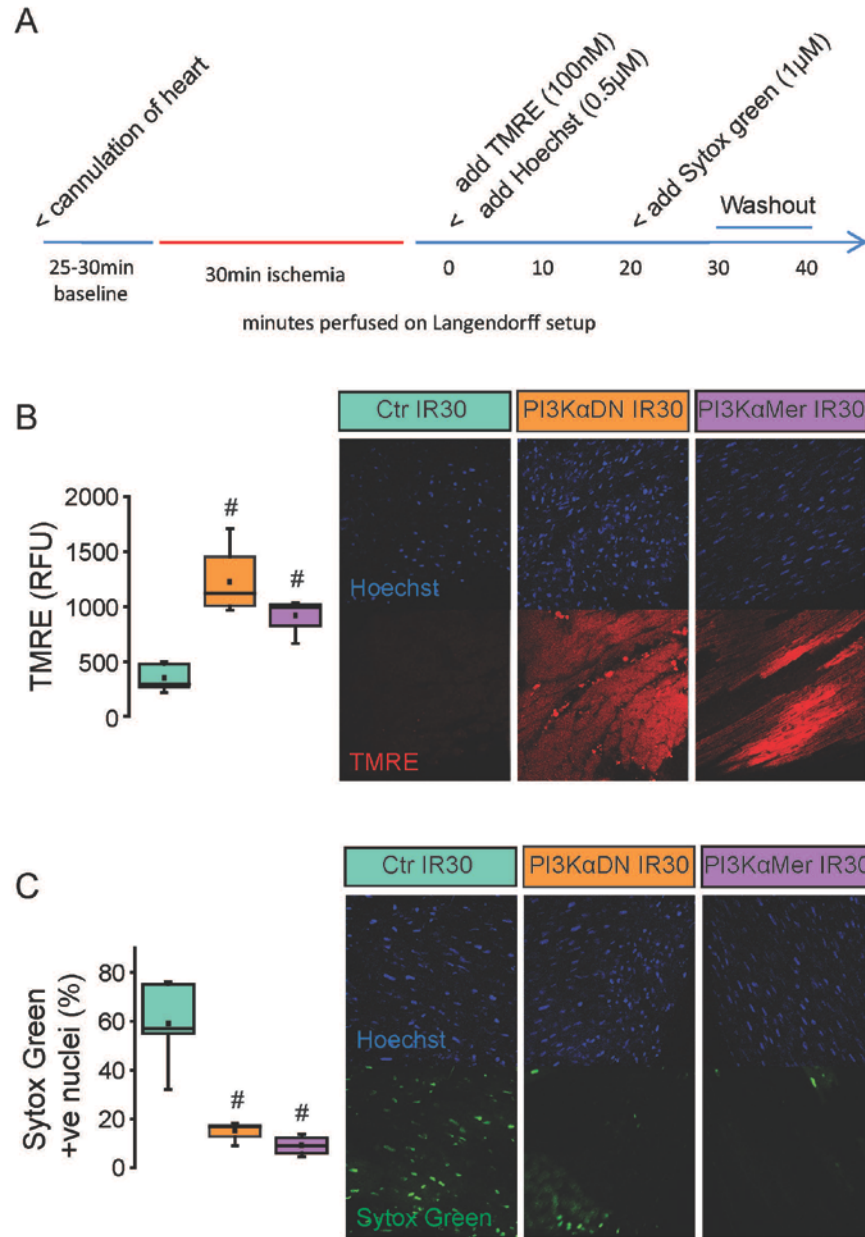


Figure 4.3. Live tissue imaging of mitochondrial membrane potential, nuclei and cell death after IR. Standard Langendorff perfusion was used with fluorescent probes added at the indicated times to the perfusion bath (A). tetramethylrhodamine, ethyl ester (TMRE) red fluorescence indicated functional mitochondrial membrane potential in live tissue (RFU; relative fluorescence units) (B). Sytox green is a cell death marker that is only taken up by permeable cells; Hoechst is a nuclear marker. (n=4-5). #P≤0.05 one way ANOVA compared to Ctr group.

4.4 Investigation of cellular injury processes: apoptosis or necrosis

4.4.1 Background and rationale for experiments

Both apoptosis and necrosis have been reported as cellular injury processes responsible for cellular damage in IR injury.¹⁷¹⁻¹⁷³ IR protection in PI3K α DN hearts was originally hypothesized to be due to anti-apoptotic signaling,⁹⁶ so I first investigated activation of apoptosis in our models. Necrosis is distinctive from apoptosis because it does not require caspase cleavage and involves cellular rupture with cellular contents released from the cell, whereas apoptosis contains cellular contents in apoptotic vesicles. Apoptosis can be a rapid process that could fit within our time period of 30min ischemia and 40min reperfusion: the key mechanisms of apoptosis have been shown to be activated within 10minutes.¹⁷⁴ Apoptosis is also an ATP dependent process, whereas necrosis is not;¹⁷⁵ the loss of MMP in Ctr hearts in our IR injury model likely leads to a low ATP environment that may favor necrosis. Increasingly, acute IR injury is thought to be primarily a regulated necrotic injury process known as necroptosis.^{98, 176,}

177

4.4.2 Results: Apoptosis not detected, evidence for necrosis

Initiator caspase 8, as well as executioner caspase 3 were not cleaved, but greater protein levels were detected in PI3K α DN hearts compared to Ctr in post IR heart tissue (Figure 4.4A,B,D). TUNEL staining was also not detected in post IR hearts. High levels of protein were detected in effluent from WT hearts post IR, but not PI3K α DN; this included cytosolic proteins Akt and caspase 3; this may explain the reduced levels of caspase 3 in Ctr hearts, and observed lower levels of Akt in WT compared to PI3K α DN hearts.¹⁶⁸

4.5 Investigation of molecular mechanisms of IR necrosis and protection in PI3K α DN

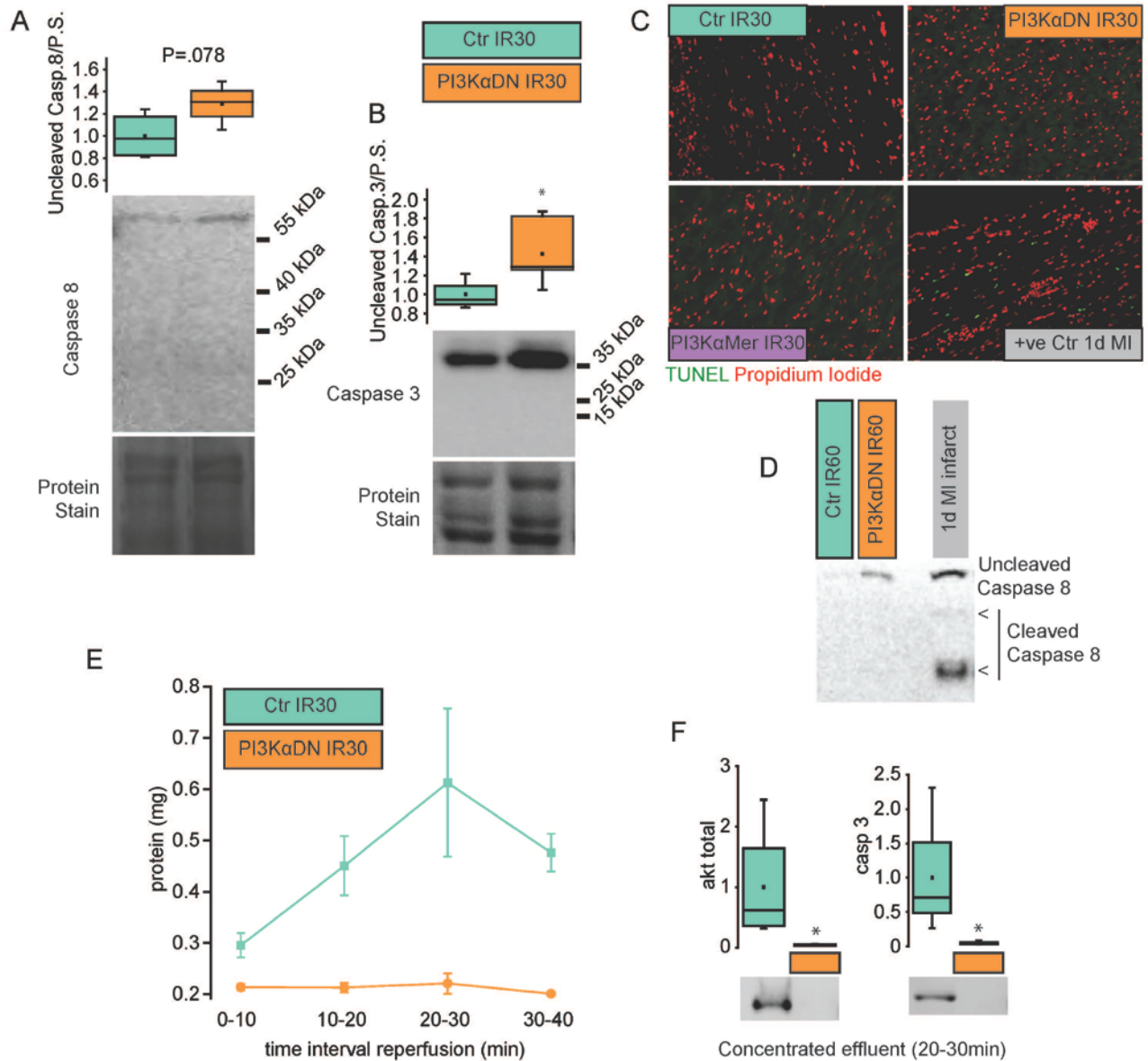


Figure 4.4. Mediators of apoptosis caspase 8 (A) and caspase 3 (B) were only detected in their uncleaved form in post IR heart tissue, but total levels of caspase 3 were elevated in PI3KαDN hearts (n=4). The lack of apoptosis involvement was confirmed in Ctr and both PI3KαDN and PI3KαMer post IR hearts (representative of n=3 hearts), with 1 day post MI heart used as a positive control. Caspase 8 was also not cleaved under the 60min ischemia protocol; 1 day post MI infarct tissue was used as a positive control (representative of n=4 for IR hearts) (D). Effluent released from the heart after reperfusion was collected (n=4-6 hearts) in 10min intervals and protein concentrated with all samples reduced to 250μL and protein concentration measured (E). Samples from 20-30 were probed for cytosolic proteins Akt and Caspase 3 (n=4) (F). *P≤0.05 in unpaired student t-test.

4.5.1 Justification of experiments

Necrotic cell death can occur as an unregulated process, such as through traumatic cellular injury such as freezing, but regulated necrotic cell death is increasingly being recognized, and has been proposed as a driving process in myocardial IR injury.^{98, 176, 177} I hypothesized that PI3K α may regulate mediators of regulated necrosis. Therefore, I next investigated proposed mediators of regulated necrosis. Receptor interacting proteins (RIP) 1 and 3 can activate apoptosis pathways when cleaved, or can induce regulated necrosis as intact proteins through formation of a necrosome complex.^{176, 177} The RIP-1 inhibitor necrostatin has been reported to be protective against myocardial IR injury, including in pig and mouse IR models.^{100, 178, 179} RIP3 overexpression induced cell death, and RIP3 knockout had greater heart function after MI.¹⁰² Moreover, a recent publication has reported that RIP3, and not RIP1 is critical for myocardial IR necrotic injury, and CaMKII (activated by phosphorylation) is the final mediator of cell membrane permeability and rupture.¹⁰¹

The mitochondria, long connected to intrinsic induction of apoptosis through cytochrome C release, can also play a role in necrosis induction; if mitochondrial membrane potential is lost and cellular energetics are impaired, apoptosis induction can be impaired because it requires ATP, and necrotic cell death becomes the dominant process. Bcl-2 family members Bax and Bak, commonly associated with apoptosis induction when localized to mitochondrial membranes, were also required for necrotic cell death in cell models of necrotic cell death, and mitochondrial swelling when challenged with increasing Ca⁺⁺ concentrations.^{180, 181} These Bcl-2 proteins can be regulated by PI3K signaling, so they are good candidates for altered regulation in PI3K α DN hearts.¹⁸²

Cyclophilin-D (Cyp-D) is an end effector of mitochondrial damage; Cyp-D knockout models are protected from IR injury, and many IR protective processes are thought to converge on inhibition of Cyp-D. Acetylation¹⁸³ and Ser residue phosphorylation¹⁸⁴ have both been proposed as regulatory post translational modifications of Cyp-D that block mitochondrial

disruption. A report shows that Cyp-D is stabilized by HSP90, and this interaction maintains the ability of Cyp-D to interrupt mitochondrial membrane potential.¹⁸⁵ Considering the understanding of lost mitochondrial membrane potential as a critical step in IR injury and regulated necrosis, we were intrigued to find a report that PI3K inhibition caused mitochondrial protection in a cancer study,¹⁸⁴ and hypothesized that a similar mechanism could explain the PI3K α DN heart IR phenotype. Interestingly, this study also showed that HSP90 inhibition enhanced the cytotoxicity of PI3K inhibition in tumor cells, citing HSP90 mediated maintenance of mitochondrial protein folding and Cyp-D inactivation.

4.5.2 Results: RIP protein; Bak protein levels, localization; Cyp-D modifications and interactions

Both RIP1 and RIP3 levels were increased in non-perfused PI3K α DN hearts compared to controls and levels of both proteins were barely detectible in both groups after IR (Figure 4.5A,B). This could be either due to release from the cell, or protein degradation. RIP1,3 were equally reduced in PI3K α DN hearts, which showed reduced rupture and release of cellular contents (Figure 4.4), suggesting that RIP1,3 are cleaved/degraded. Furthermore, the similar cleavage/degradation of RIP1 suggests that this is unlikely to be a regulatory step that distinguishes PI3K α DN hearts from controls in IR injury. Despite several studies investigating RIP1 and RIP3 in the heart, I do not know of any report showing protein levels in an acute IR protocol, so this cleavage/degradation of RIPs in IR is not well characterized. To further investigate the timing of RIP cleavage/degradation, I perfused control hearts and collected hearts at 4 different time points: 1) aerobic baseline period, 2) end of ischemia, 3) 10min into reperfusion and 4) 40min of reperfusion (regular protocol). I found that RIP1 was largely lost at the end of ischemia, and RIP3 levels declined within the first 10min of reperfusion (Figure 4.5C). Furthermore, phosphorylation of CaMKII, which was proposed as the end effector of RIP mediated cell rupture,¹⁰¹ had higher mean values in PI3K α DN hearts after IR (Figure 4.5D). I

contacted the corresponding author of this paper, who told me that CaMKII phosphorylation was not consistent at shorter reperfusion time points, only at 2hrs of reperfusion shown in the paper, is CaMKII activated.

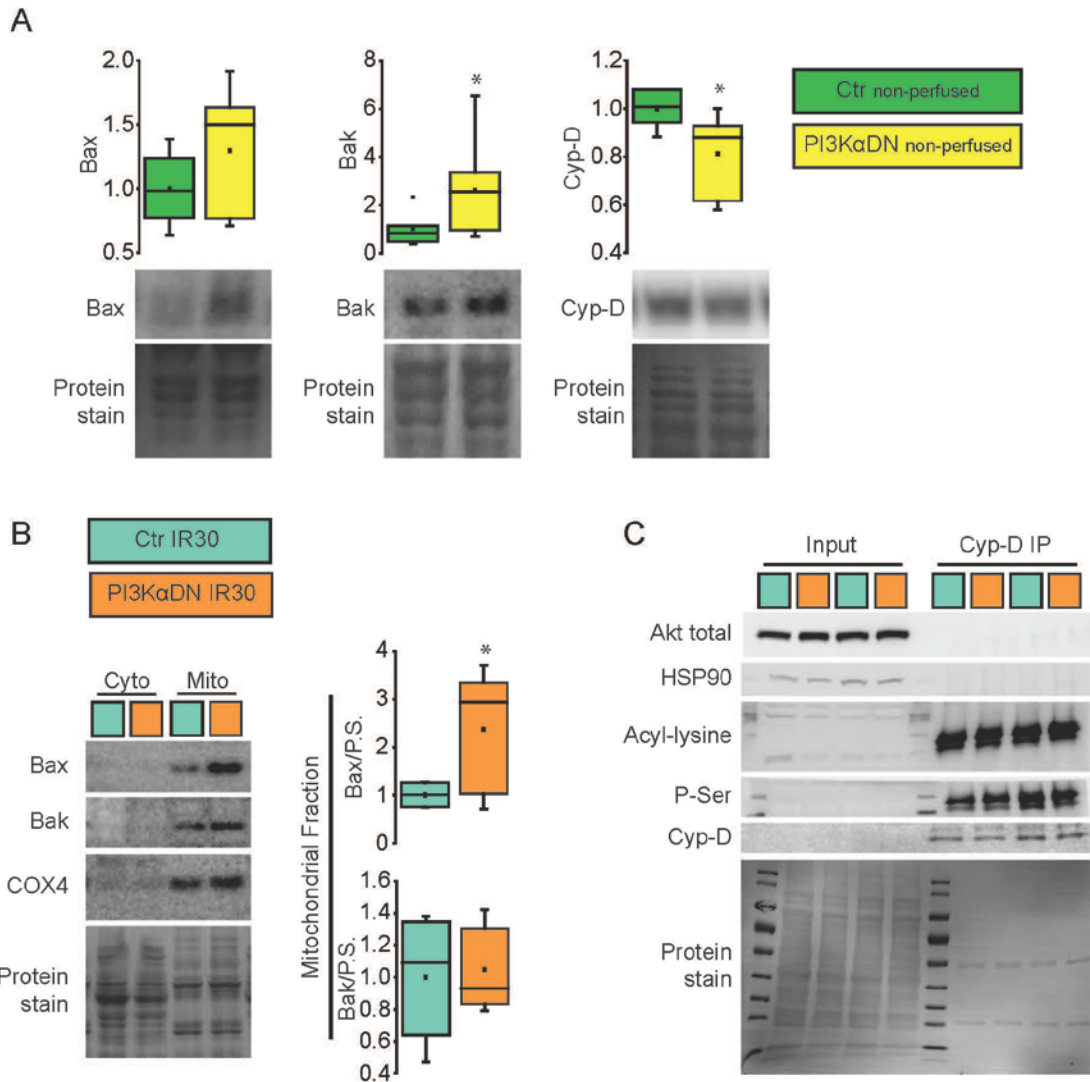


Figure 4.5. Necrosis/apoptosis regulators include Cyp-D and Bcl-2 members Bax and Bak. In baseline, non-perfused hearts Bak was increased and Cyp-D decreased in PI3KαDN hearts (A) (n=6-7). Both Bax and Bak localized to mitochondrial fractions in post IR hearts, with greater levels of Bax in PI3KαDN hearts (B) (n=7). Immunoprecipitation of Cyp-D did not reveal interaction with Akt or HSP90, and similar levels of acyl-lysine and P-Ser at the same molecular weight as Cyp-D (C) (n=2). *P<0.05 in unpaired student t-test.

I conclude from this data that altered regulation of RIPs and P-CaMKII (Thr286) are not likely to be responsible for IR protection in PI3KαDN hearts, and this data also suggests that these regulators may not play a role in acute IR injury, at least in this mouse heart *ex-vivo* model.

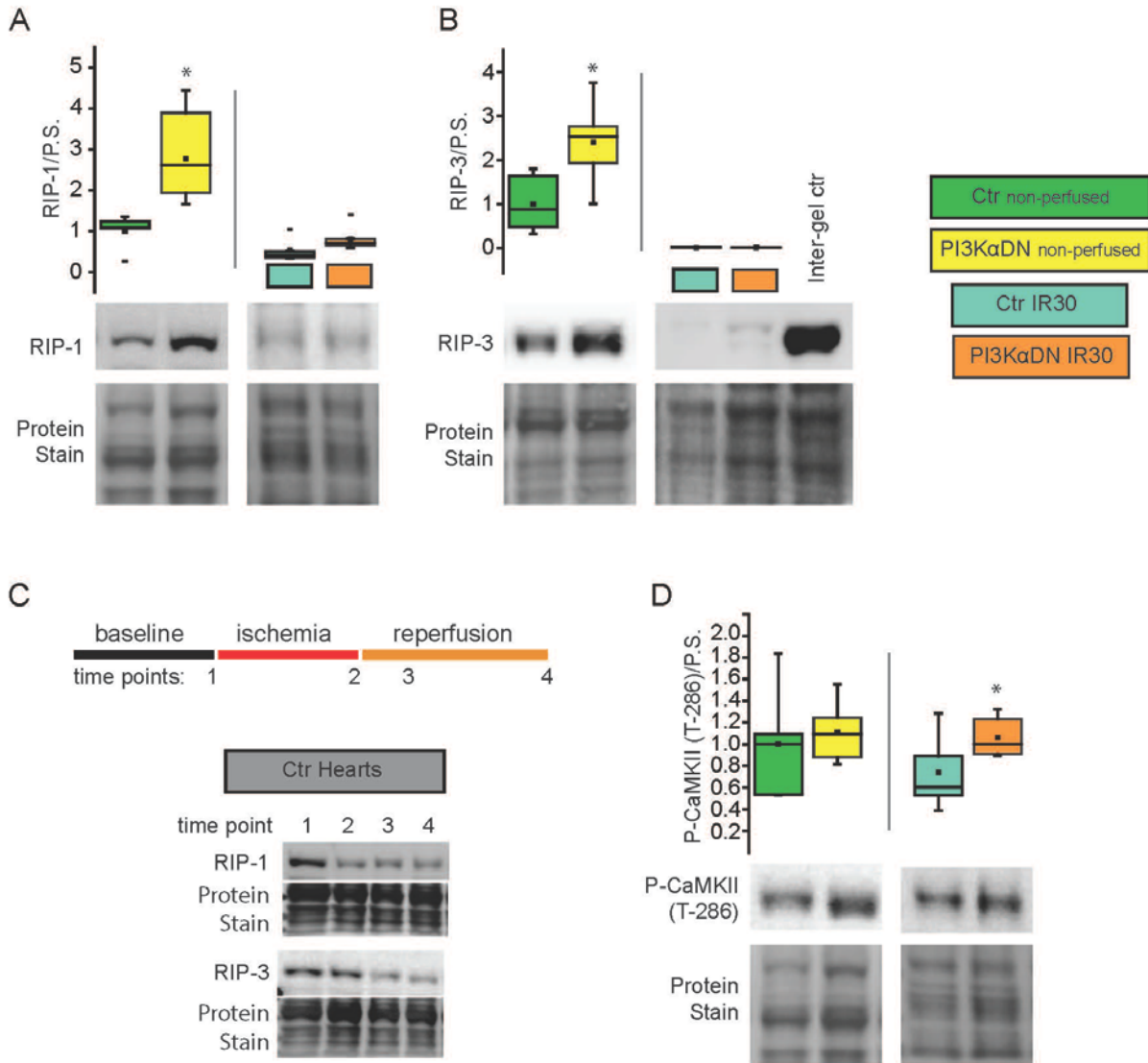


Figure 4.6. Mediators of regulated necrosis RIP-1 and RIP-3 are increased in PI3KαDN hearts compared to Ctr in baseline non-perfused hearts and are minimally detectable in IR hearts (A,B) (n=5-7). Collection of Ctr hearts at 4 different time points (n=3-4) representative Western blots show RIP-1 is predominantly lost by the end of ischemia, and RIP-3 is lost by 10min reperfusion (time point 3) (C). Phosphorylation of CaMKII was increased in PI3KαDN hearts compared to Ctr after IR (D) (n=5-7).

Bcl-2 family members Bak but not Bax protein levels were significantly increased in non-perfused PI3K α DN hearts compared to controls, and Cyp-D levels were moderately reduced (Figure 4.6A). Recruitment of Bax and Bak to mitochondria has been shown as a mechanism of mitochondrial outer membrane permeabilization; this was a different process than Bax/Bak oligomerization and apoptotic pore formation.¹⁸¹ I hypothesized that one or both of these proteins may not be recruited to the mitochondrial membrane upon IR injury in PI3K α DN hearts, however, nuclear fractionation of myocardium from IR hearts showed both Bax and Bak in the mitochondrial fraction, with higher levels of Bax in PI3K α DN hearts (Figure 4.6B). Immunoprecipitation of Cyp-D did not pull out Akt or HSP90, and lysine acylation and serine phosphorylation of Cyp-D appeared similar between PI3K α DN and Ctr hearts (Figure 4.6C).

4.6 Discussion and conclusions regarding PI3K α in IR injury

The search for the underlying mechanism of reduced PI3K α mediated IR protection remains incomplete. The dramatic protection from necrotic cell injury in this model is evidence that a fundamental determinant of necrotic cell death is altered by PI3K α . A fundamental question going forward is to determine if maintained mitochondrial function is due to special properties of the mitochondria that make them resistant to IR stress including calcium overload, or if cellular processes are changed in a way that calcium overload is avoided. My ideas for further experiments are discussed in Chapter 7.

5. PI3K α and Heart Function

Previously published: [PI3K \$\alpha\$ is essential for the recovery from Cre/tamoxifen cardiotoxicity and in myocardial insulin signaling but is not required for normal myocardial contractility in the adult heart.](#) *Cardiovasc Res.* 2015 Mar 1;105(3):292-303.

5.1. Introduction

This chapter shows our work to establish a cardiomyocyte specific, inducible PI3K α deletion model in the lab. We seek to test the claim that the PI3K α DN phenotype, especially concerning regulation of heart function, is limited due to developmental compensatory effects.¹⁰³ We show that insulin signaling in the heart is disrupted, despite normal heart contractile function as a positive control for PI3K α function, while also confirming that this is the dominant insulin mediating PI3K isoform in the heart.

Table 5.1. Echocardiographic measurement of cardiac function in high dose tamoxifen treated mice

	MCM UT	MCM TAM HD 10d	PI3K $\beta^{flx/flx}$ MCM TAM HD 10d	PI3K $\alpha^{flx/flx}$ MCM TAM HD 10d	MCM TAM HD 28d	PI3K $\beta^{flx/flx}$ MCM TAM HD 28d	PI3K $\alpha^{flx/flx}$ MCM TAM HD 28d
n	10	7	7	7	7	9	7
HR (bpm)	432 \pm 10	485 \pm 19	434 \pm 18	484 \pm 18*	451 \pm 10	424 \pm 14	503 \pm 23*#
E/A Ratio	1.50 \pm 0.23	1.92 \pm 0.32	1.8 \pm 0.14	2.07 \pm 0.33	1.67 \pm 0.10	2.09 \pm 0.30	1.62 \pm 0.04
E' (mm/s)	30.4 \pm 1.8	21.2 \pm 1.8*	21.8 \pm 3.7*	17.2 \pm 3.0*	28.7 \pm 2.1	26.1 \pm 1.8	16.1 \pm 1.5*#
E/E' Ratio	21.7 \pm 2.7	33.5 \pm 4.0*	37.4 \pm 8.4*	35.5 \pm 3.6*	26.9 \pm 1.2	30.5 \pm 4.5	42.7 \pm 3.0*#
LA (mm)	1.8 \pm 0.1	2.3 \pm 0.2*	2.5 \pm 0.2*	2.7 \pm 0.2*	1.7 \pm 0.1	1.8 \pm 0.1	2.5 \pm 0.2*#
A' (mm/s)	26.16 \pm 1.92	24.71 \pm 2.06	27.86 \pm 3.83	21.59 \pm 3.66	26.89 \pm 3.20	25.77 \pm 2.01	24.34 \pm 2.36
LVEDD (mm)	4.10 \pm 0.10	4.05 \pm 0.13	4.24 \pm 0.21	4.58 \pm 0.16	4.26 \pm 0.06	4.19 \pm 0.06	4.64 \pm 0.19*#
LVESD (mm)	2.62 \pm 0.17	3.36 \pm 0.16*	3.55 \pm 0.23*	3.85 \pm 0.20*	3.09 \pm 0.09	3.00 \pm 0.08	4.00 \pm 0.20*#
LVFS (%)	36.7 \pm 2.9	17.5 \pm 1.6*	16.6 \pm 2.1	16.2 \pm 1.8*	27.6 \pm 1.5	28.5 \pm 1.1	13.9 \pm 1.3*#
LVEF (%)	65.6 \pm 3.7	36.6 \pm 3.1*	34.6 \pm 4.0*	33.8 \pm 3.5*	53.6 \pm 2.4	55.1 \pm 1.7	29.5 \pm 2.5*#

MCM, mer-cre-mer transgene; UT, untreated with tamoxifen; TAM, tamoxifen; PI3K $\alpha^{flx/flx}$ /PI3K $\beta^{flx/flx}$ denotes flx gene; HD, high dose tamoxifen (60mg/kg*4days); HR, heart rate; E-wave, peak early transmitral inflow velocity; A-wave, transmitral inflow velocity due to atrial contraction; E', early diastolic tissue Doppler velocity; A', late diastolic tissue Doppler velocity due to atrial contraction; LVEDD, left ventricular (LV) end diastolic diameter, LVESD, LV end systolic diameter; LVFS, LV fractional shortening; LVEF, LV ejection fraction; VCEc, Velocity of circumferential shortening corrected for heart rate; LVPWT, LV posterior wall thickness. Values are mean \pm SEM. *p \leq 0.05 using Student t-test compared to the MCM UT group; # p \leq 0.05 one way ANOVA comparing effect of genotype within same tamoxifen treatment time point.

5.2. Results

Oral administration of tamoxifen in food (80mg/kg/day for 7 days) was previously reported to cause effective gene deletion in MCM/[gene]^{flx/flx}.¹⁰⁵ We adopted an oral gavage regimen in order to closely control tamoxifen dosing using MCM transgenic mice without flx sites as controls for Cre/tamoxifen toxicity. We observed considerable morbidity and mortality at higher tamoxifen doses in MCM transgenic mice (80mg/kg/day for 5 days, data not shown) and we found that 4 days of 60mg/kg/day tamoxifen (high dose; HD) was tolerated with no mortality. Heart function, assessed by echocardiography, was significantly reduced in the PI3K α MCM transgenic models at 10 days from the start of treatment (Figure 5.1A-B) (Table 5.1).

We assessed heart function again at 28 days, and observed functional recovery in MCM transgenic controls (no flx targeted genes). However, PI3K α MCM mice had continued severe systolic dysfunction (Figure 5.1C-D), suggesting a critical role for PI3K α in recovering normal heart function after tamoxifen/Cre toxicity.

We reduced the Tamoxifen dose to 4 days of 40mg/kg/day (low dose; LD), and observed normal heart function at 10 days from the start of tamoxifen treatment (Figure 5.2A-B) (Table 5.2), and maintained effective loss of the target protein (Figure 5.2C). Similarly, cardiomyocytes isolated from PI3K α MCM treated with LD tamoxifen had normal function compared to untreated controls (Figure 5.2D). Combined, these results demonstrate a role for PI3K α in recovery from Cre/tamoxifen toxicity, but not a direct role in heart function.

PI3K β MCM mice treated with HD tamoxifen followed the same phenotype as MCM controls, with reduced heart function at 10 days from the start of tamoxifen and recovery to normal function at 28 days (Figure 5.2E-F). PI3K β protein was significantly reduced in this model (Figure 5.2F).

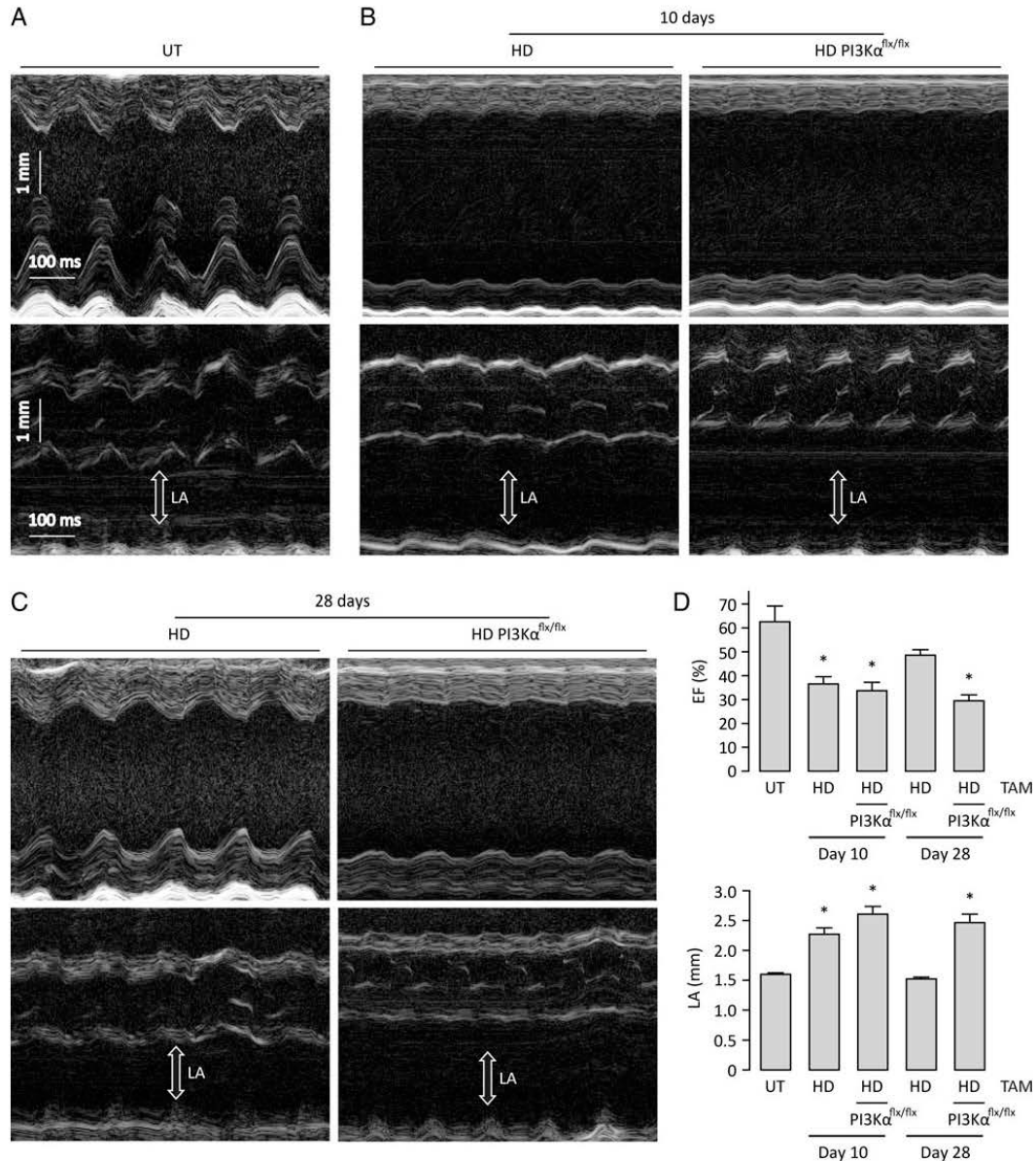


Figure 5.1. Tamoxifen treatment induces transient systolic dysfunction in MCM transgenic mice with PI3Ka dependent recovery. Representative echocardiography M-mode images of left ventricle and left atrium (**A–C**) (UT, untreated; HD, high-dose tamoxifen) showed MCM transgenic mice had normal heart function before tamoxifen treatment (n=10) (**A**). HD tamoxifen caused contractile dysfunction and left atrium dilation at 10 days from start of tamoxifen treatment in MCM controls (n=7) and PI3Ka MCM (n=7) (**B**). MCM transgenic control, but not PI3Ka MCM mice recovered heart function and left atrium dimensions by 28 days after start of tamoxifen treatment (**C**). Summary ejection fraction (EF) and left atrium (LA) measurements are shown for all groups (**D**). All mice are MCM transgenic; *P<0.05 (tamoxifen treated groups at 10 days or 28 days compared with UT by one-way ANOVA; analysis performed according to predefined comparison to normal functioning untreated group).

Table 5.2. Echocardiographic measurement of cardiac function in low dose tamoxifen treated mice

	MCM TAM LD 10d	PI3K α^{MCM} MCM TAM LD 10d
n	4	7
HR (bpm)	450 \pm 13	421 \pm 13
E/A Ratio	1.42 \pm 0.11	1.45 \pm 0.08
E' (mm/s)	32.2 \pm 1.2	30.4 \pm 2.4
E/E' Ratio	24.9 \pm 1.6	22.8 \pm 1.5
LA (mm)	1.7 \pm 0.1	1.7 \pm 0.1
A' (mm/s)	28.96 \pm 1.37	24.54 \pm 1.04
LVEDD (mm)	3.83 \pm 0.15	3.93 \pm 0.09
LVESD (mm)	2.54 \pm 0.10	2.63 \pm 0.12
LVFS (%)	34.0 \pm 0.3	33.2 \pm 1.6
LVEF (%)	63.6 \pm 0.85	64.3 \pm 2.40

MCM, mer-cre-mer transgene; TAM, tamoxifen; PI3K α /PI3K β denotes flx gene; LD, low dose tamoxifen (40mg/kg*4days) HR, heart rate; E-wave, peak early transmitral inflow velocity; A-wave, transmitral inflow velocity due to atrial contraction; E', early diastolic tissue Doppler velocity; A', late diastolic tissue Doppler velocity due to atrial contraction; LVEDD, left ventricular (LV) end diastolic diameter, LVESD, LV end systolic diameter; LVFS, LV fractional shortening; LVEF, LV ejection fraction; VCEc, Velocity of circumferential shortening corrected for heart rate; LVPWT, LV posterior wall thickness. Values are mean \pm SEM.

In addition to reduced function, tamoxifen/Cre toxicity was previously characterized by transient increases in expression of genes associated with heart disease at day 10, but resolved by day 28 from the start of tamoxifen treatment.¹⁰⁵ We observed PI3K α MCM HD mice had elevated expression of markers of heart disease: expression of ANF, BNP and α -skeletal actin, but not β -myosin heavy chain at 28 days (Figure 5.3A), suggesting a continuation of the acute tamoxifen/Cre toxicity phenotype. Tamoxifen/Cre toxicity can also cause increased myocardial fibrosis;¹⁸⁶ we observed elevated transcription of collagen III and increased myocardial fibrosis in PI3K α MCM HD hearts but not LD hearts (Figure 5.3B-C) compared to MCM HD controls. The PI3K α MCM LD did not deviate from controls in disease markers or collagen expression (Figure 5.3A-B) using ANOVA analysis.

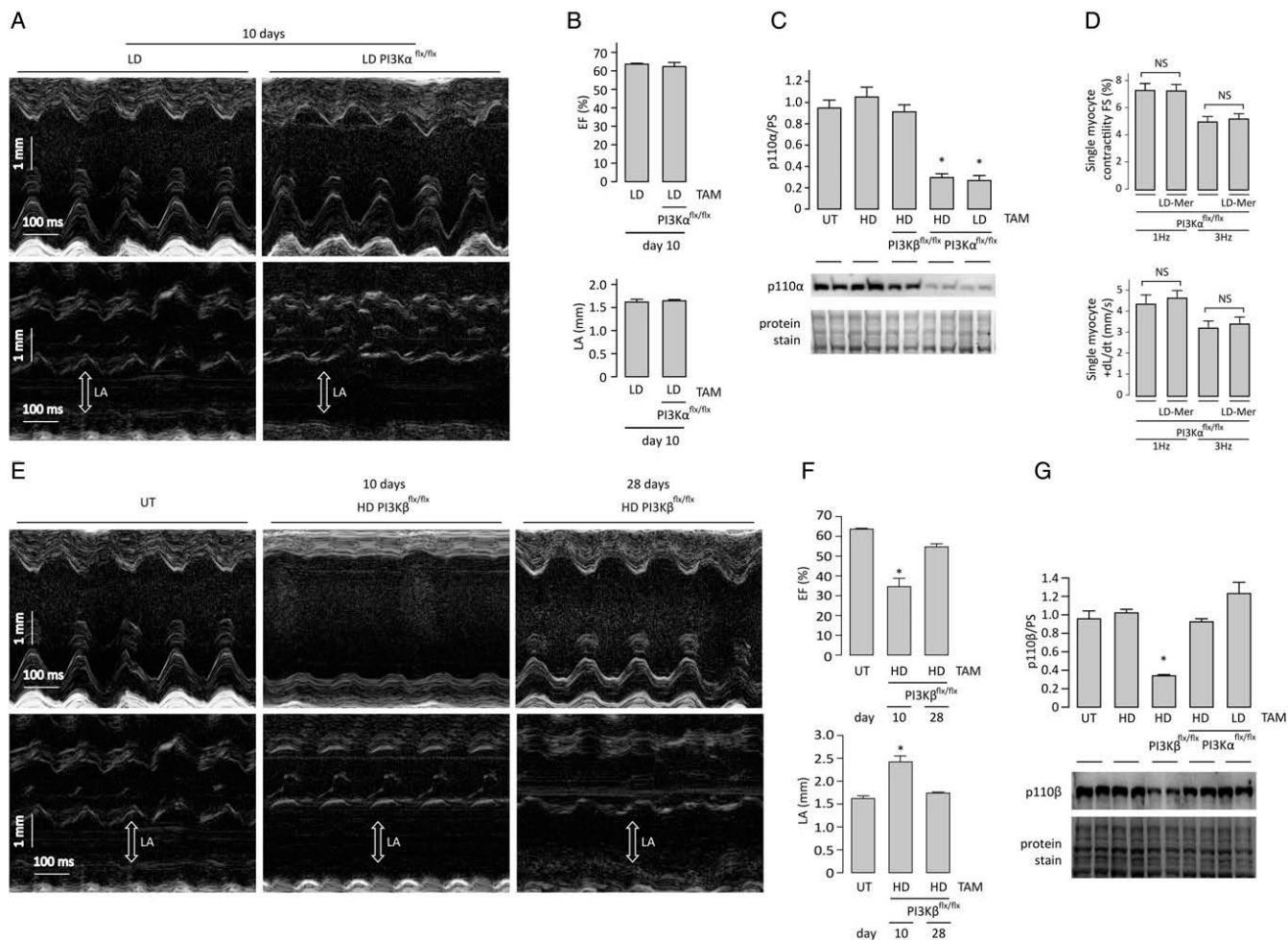


Figure 5.2. Low-dose tamoxifen can remove PI3K α without affecting heart function and PI3K β is not required for recovery from tamoxifen-induced heart dysfunction. Representative echocardiography M-mode images of left ventricle and left atrium showed normal function in LD tamoxifen treated mice 10 days after start of tamoxifen treatment in MCM controls (n=4) and PI3K α MCM (n=7) (A) and summary ejection fraction (EF) and left atrium (LA) measurements (B). Western blot for LV tissue protein levels of PI3K α catalytic subunit p110 α (n=4–6) performed for all MCM transgenic models showed equal reduction of p110 α in HD and LD PI3K α MCM (C). Cardiomyocytes isolated from PI3K α MCM LD and PI3K α non-MCM littermate hearts paced at 1 Hz (n=24,27) and 3 Hz (n=18, 23) from 4 and 3 isolations, respectively (D) (NS, not statistically significant). Targeted deletion of PI3K β with HD tamoxifen causes transient systolic dysfunction and atrial dilation with recovery at 28 days (n=7–9) as shown by representative M-mode images (E) and summary EF and LA measurements compared with untreated (UT) control MCM mice (F). Western blot for LV tissue protein levels of PI3K β showed reduced levels catalytic subunit p110 β (n=4–6) (G). *P \leq 0.05.

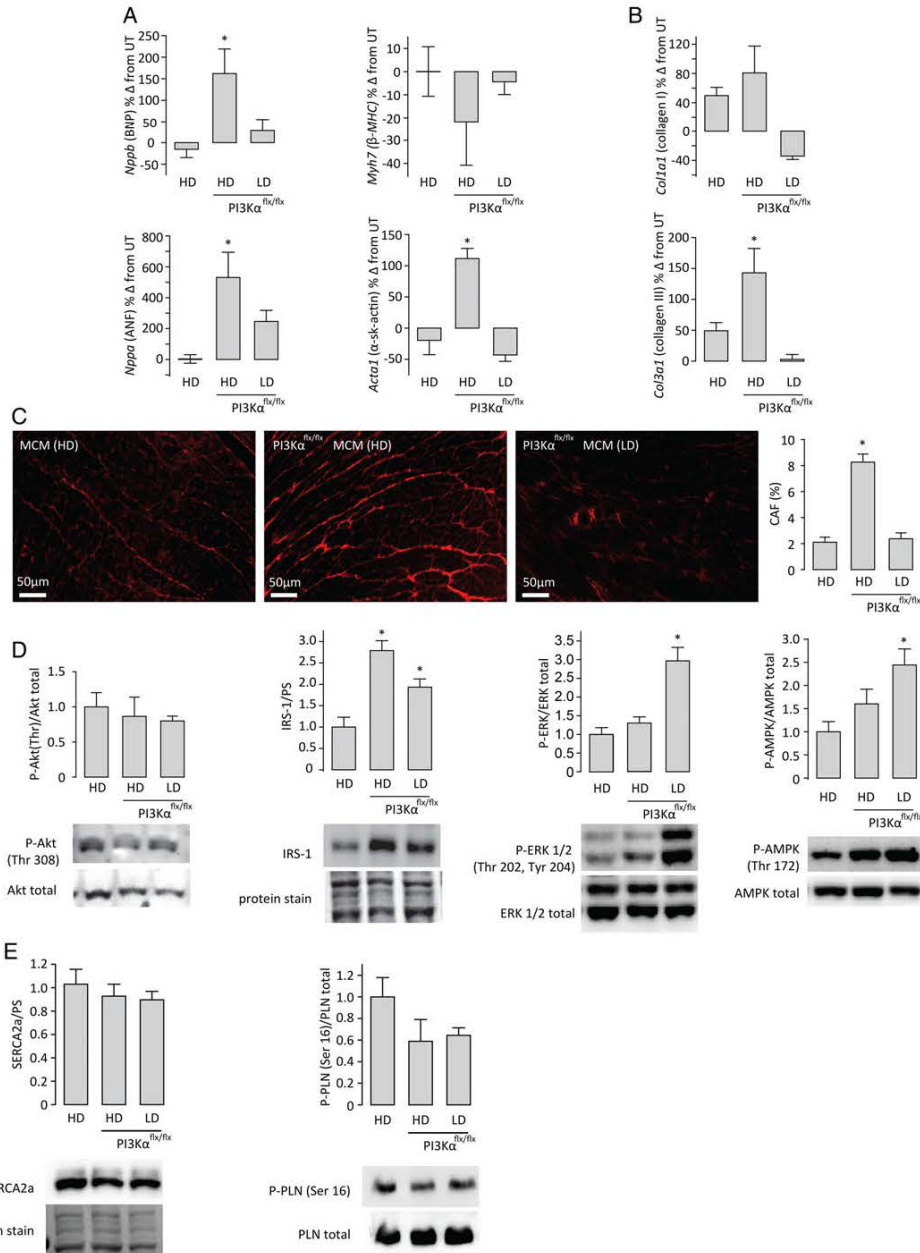


Figure 5.3. Molecular and histological changes in tamoxifen treated PI3Kα MCM at 28 days after start of tamoxifen. Expression of disease markers Nppb (BNP), Nppa (ANF), and Acta1 (α-skeletal actin) but not Myh7 (β-MHC) were increased in HD PI3Kα MCM but not LD PI3Kα MCM or control MCM tamoxifen treated mice at 28 days after start of tamoxifen compared with untreated (UT) controls (n=5) (A). Expression of Col1a1 and Col3a1 (collagen I and III); Col3a1 was increased in HD PI3Kα MCM but not LD PI3Kα MCM or control MCM tamoxifen-treated mice at 28 days after start of tamoxifen compared with UT (n=5) (B). Representative images from histological sections stained for collagen with Picrosirius Red (PSR) and quantification of collagen volume fraction (CVF) (n=3 hearts; averaged from 3 to 4 images/heart) (C). Western blots for changes in activation or protein levels at 28 days after start of tamoxifen for Akt (Thr 308), IRS-1, ERK1/2, and AMPK(Thr 172) (D); and SERCA2a and PLN(phospholamban) (Ser 16) in HD MCM, HD PI3Kα, and LD PI3Kα (n=8) (E). All mice are MCM transgenic; *P<0.05.

However, comparison of only control and PI3K α MCM LD (not shown) did show significant increase ($p=0.034$) in ANF expression which was also previously observed in PI3K α DN hearts,⁴ and may have a beneficial effect due to antihypertrophic and antifibrotic properties.¹⁸⁷

Western blot analysis was performed to investigate changes in signaling pathways related to PI3K α signaling. Akt activation (P-Akt Thr) was consistently low in both HD and LD tamoxifen treated PI3K α MCM models, but Akt activation levels were highly variable in MCM control hearts, so Akt activation was not significantly different between groups (Figure 5.3D). We suspect that this is due to variations in plasma insulin levels because we did not control feeding prior to sacrifice. To better clarify the level of PI3K α activity, we adapted a model of fasting and acute insulin administration in subsequent models. In this way Akt activation can serve as a marker of PI3K α activity. We also wanted to confirm in mouse and human adult cardiomyocytes that PI3K α is a key transducer of insulin signaling.¹⁸⁸

We observed increased MAPK ERK1/2 activation in PI3K α MCM hearts with low dose, but not high dose tamoxifen (Figure 5.3D). We also previously reported increased MAPK ERK1/2 phosphorylation of PI3K α DN hearts in setting of ischemia/reperfusion in a working heart model;¹⁶⁸ others have also shown increased P-ERK activation in PI3K α DN hearts¹⁸⁹ and pharmacological inhibition of PI3K in SkBr3 cells with PI3K inhibitors BEZ235, LY294002 and wortmannin all caused increased ERK1/2 phosphorylation.¹⁹⁰ Activated ERK1/2 can lead to hypertrophy, and has important cardio-protective roles in the setting of cardiac injury and failure.¹⁹¹

Activation of AMPK by phosphorylation was observed in LD PI3K α MCM hearts, and IRS-1, which can be controlled by negative feedback downstream of PI3K,¹⁶⁶ was increased in LD and HD PI3K α MCM hearts. The SERCA2a pump and its regulator phospholamban (PLN) were not changed from control hearts (Figure 5.3E).

In contrast to the MCM model, the constitutively active Cre transgenic model does not allow for a temporally controlled knockout; under the α MHC promoter, Cre is likely active perinatally,¹⁹² with the potential for developmental effects from absent PI3K α signaling and possible toxicity from constitutively active Cre recombinase.¹⁹³ However, no tamoxifen is needed to activate Cre, so there is no chance of tamoxifen/Cre toxicity. With this model, we observed normal heart function (Figure 5.4A-B) (Table 5.3) and normal contractility of isolated cardiomyocytes (Figure 4C).

Table 5.3. Echocardiographic measurements of cardiac function in cardiac-specific PI3K α mutant mice and BYL-719 treated mice

	PI3K $\alpha^{flx/flx}$ No Cre	PI3K $\alpha^{flx/flx}$ Cre	WT Corn Oil	WT BYL-719
n	6	9	9	8
HR (bpm)	454 \pm 15	455 \pm 17	473 \pm 12	482 \pm 19
E/A Ratio	1.96 \pm 0.04	1.59 \pm 0.12*	1.52 \pm 0.09	1.34 \pm 0.14
E' (mm/s)	31.5 \pm 2.3	33.5 \pm 3.7	22.9 \pm 2.0	26 \pm 1.5
E/E' Ratio	24.9 \pm 1.2	22.8 \pm 2.7*	24.4 \pm 1.6	20.2 \pm 4.3
LA (mm)	1.6 \pm 0.1	1.8 \pm 0.1	1.6 \pm 0.1	1.7 \pm 0.1
A' (mm/s)	25.81 \pm 1.79	25.7 \pm 1.93	18.56 \pm 1.56	25.79 \pm 2.30
LVEDD (mm)	3.99 \pm 0.07	3.98 \pm 0.09	3.73 \pm 0.07	3.73 \pm 0.09
LVESD (mm)	2.72 \pm 0.15	2.76 \pm 0.09	2.21 \pm 0.15	2.19 \pm 0.08
LVFS (%)	32.2 \pm 2.8	30.8 \pm 1.2	40.6 \pm 2.5	43.7 \pm 1.4
LVEF (%)	60.4 \pm 3.7	58.8 \pm 1.7	71.5 \pm 2.8	75.6 \pm 1.6

Cre, Cre recombinase transgenic; PI3K $\alpha^{flx/flx}$ denotes flx gene; HD, high dose tamoxifen(60mg/kg*4days); LD, low dose tamoxifen (40mg/kg*4days) HR, heart rate; E-wave, peak early transmitral inflow velocity; A-wave, transmitral inflow velocity due to atrial contraction; E', early diastolic tissue Doppler velocity; A', late diastolic tissue Doppler velocity due to atrial contraction; LVEDD, left ventricular (LV) end diastolic diameter, LVESD, LV end systolic diameter; LVFS, LV fractional shortening; LVEF, LV ejection fraction; VCEc, Velocity of circumferential shortening corrected for heart rate; LVPWT, LV posterior wall thickness. Values are mean \pm SEM; * p <0.05 compared to corresponding control.

To investigate *in-vivo* signaling in PI3K α Cre hearts, mice were fasted overnight and then received an acute injection of insulin 15 min before sacrifice (Figure 5.4E). PI3K α Cre mice had impaired insulin dependent activation of Akt, and constitutively higher activation of ERK1/2 independent of insulin stimulation. IRS-1 levels increased after insulin stimulation consistent with previous findings,¹⁹⁴ but had higher overall levels in PI3K α Cre mice. Activation of AMPK was also increased in PI3K α Cre hearts.

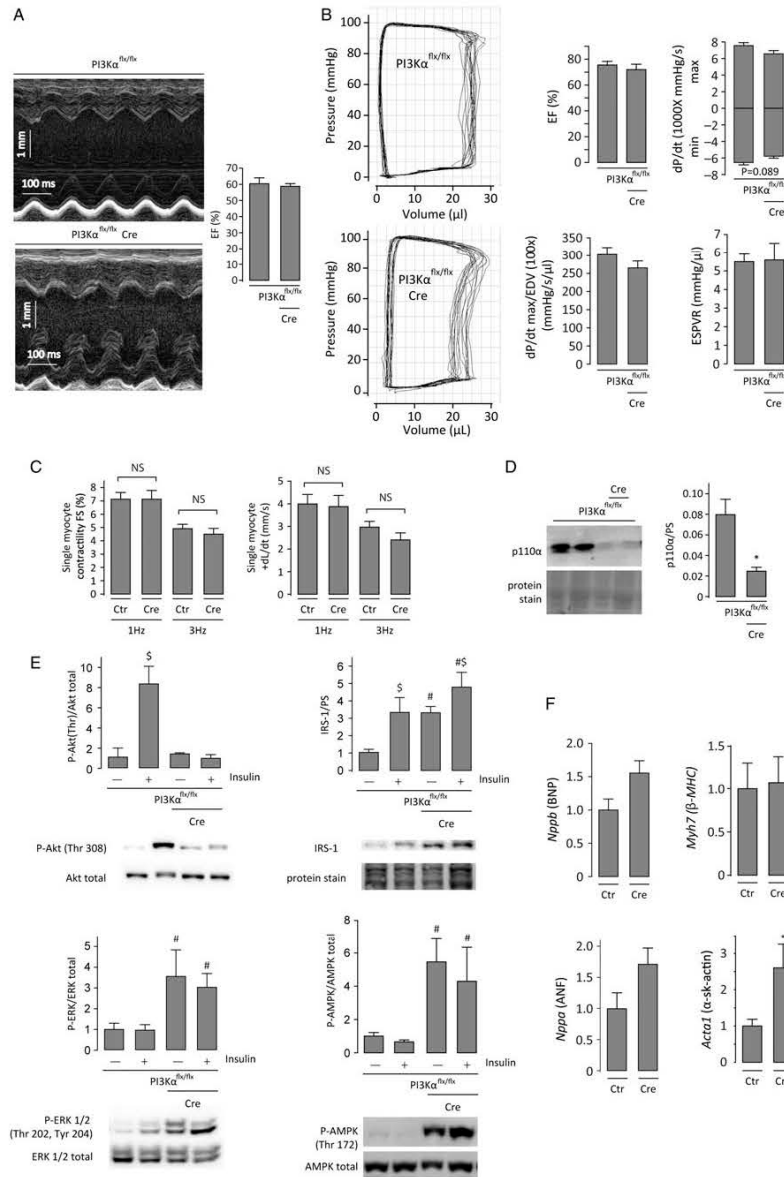


Figure 5.4. Loss of PI3K α in constitutively active Cre model does not significantly affect heart or myocyte function but blocks insulin signalling. Representative echocardiography M-mode images of the left ventricle in PI3K α Cre (n=9) and no Cre (n=6) mice and summary ejection fraction (EF) show normal function (**A**). Representative pressure/volume loops for PI3K α Cre (n=9) and no Cre (n=10) mice and summary haemodynamic parameters from pressure volume loops: ejection fraction, peak maximal, and minimal change in pressure per unit time (dP/dt), maximal change in pressure per unit time divided by end diastolic volume (EDV) and end systolic pressure volume relationship (ESPVR) (**B**). Fractional shortening and maximal change in length per unit time (+dP/dt) of isolated adult cardiomyocytes from PI3K α Cre and control mice paced at 1 Hz (n=11,18) and 3 Hz (n=10, 16) from 2 and 4 isolations, respectively (NS, not statistically significant) (**C**). Representative western blot for PI3K p110 α showing loss of p110 α protein in LV of constitutively active Cre (n=6) (**D**). Western blots from LV tissue of PI3K α Cre and No Cre mice fasted overnight (16 h), with and without acute insulin stimulation by IP injection (1 mg/kg) and hearts collected after 15 min; changes in activation or protein levels of Akt, IRS-1, ERK, and AMPK (significant effect of insulin (\$) and/or genotype (#) (n=6) (**E**). Expression of disease markers: Nppb (BNP), Nppa (ANF) Myh7 (b-MHC) were not changed but Acta1 (α -skeletal actin) was increased (n=11–12) (**F**). *P \leq 0.05.

Alpha skeletal actin expression was significantly increased in PI3K α Cre (Figure 5.4F), but not in LD treated PI3K α MCM (Figure 5.3A), suggesting that this may be a byproduct of the unique characteristics of the Cre model (expressed early in development, constitutively active Cre).

The PI3K α specific inhibitor BYL-719⁶³ blocked insulin mediated activation of Akt *in vivo* in the mouse heart, and *in vitro* in mouse and human adult cardiomyocytes (Figure 5.5A-B). PI3K α inhibition also caused increased activation of ERK1/2 and AMPK signaling, but did not affect protein levels of p110 α or IRS-1 (Figure 5.5B). Treatment of wt mice with BYL-719 did not result in alterations in cardiac function after two weeks of treatment (Figure 5.5C,F). Echocardiography and P/V loop measurements were performed 3 days after the end of drug treatment to avoid any acute drug effects. Consistent with the established role of PI3K α in regulating insulin signaling and glucose metabolism,¹⁹⁵ fasting glucose levels were elevated after the first week of treatment with BYL-719 (Figure 5.5D). Treated mice also had significant weight loss after 2 weeks of treatment (Figure 5.5E). The expression of disease markers did not change between vehicle treated and 4day or 2week BYL-719 treated mice (Figure 5.5G).

5.3. Discussion

The PI3K signaling pathway is a critical regulator of myocardial structure and function in development and pathophysiology.^{5, 140, 141, 196} The MCM and Cre models for PI3K α deletion are an important expansion on research performed with the PI3K α DN model because they offer a true deletion of the gene for either PI3K α or PI3K β , and the MCM model allows for gene deletion in the adult, avoiding complications due to developmental roles for these kinases. Oral administration of tamoxifen sufficient to cause gene deletion was previously shown to cause a transient reduction in cardiac function at 10 days after starting the drug, with full recovery of function at 28 days.¹⁰⁵ This led us to hypothesize that loss of PI3K α may increase susceptibility to tamoxifen/Cre toxicity, but may not be necessary for preserved heart function. Increased

awareness for Cre/tamoxifen toxicity has prompted investigators to now favor a minimal dose of tamoxifen to cause gene deletion.¹⁰⁶ Although we observed functional recovery in our HD tamoxifen control group (Figure 5.1), there may be residual damage present that could not be captured by the methods we used. After observing that PI3K α deletion impaired recovery from tamoxifen/Cre toxicity, our primary aim in this study was not to determine the precise mechanism of the resulting cardiomyopathy, but rather to avoid this compounding variable in our study of PI3K α signaling in relation to heart function, which is why we tested a reduced tamoxifen dose as well as other complementary models of PI3K α deletion/inhibition that do not require tamoxifen.

Numerous genetic models have shown a complex role for PI3K α in diverse cardiovascular pathophysiological processes, with both beneficial and detrimental effects from loss of PI3K α . We observed normal heart function in PI3K α MCM LD and PI3K α Cre models, despite loss of PI3K α , and normal heart function after 2 weeks of PI3K α inhibition with BYL-719. Therefore, we conclude that loss of PI3K α is not inherently pathological to the heart in otherwise healthy mice, and specifically does not directly regulate heart contractility in these models. Our results are consistent with the normal functioning cardiac phenotype observed in PI3K α DN hearts.^{4, 5, 64} We allowed drug washout before functional phenotyping of the BYL-719 treated group to specifically examine persisting effects of PI3K α inhibition on myocardial contractility. We avoided functional phenotyping of acute treatment with BYL-719 to avoid possible off-target effects seen with other PI3K inhibitors,¹⁹⁷ and complicating factors, such as alterations in metabolic substrate utilization, which may alter myocardial efficiency.¹⁹⁸

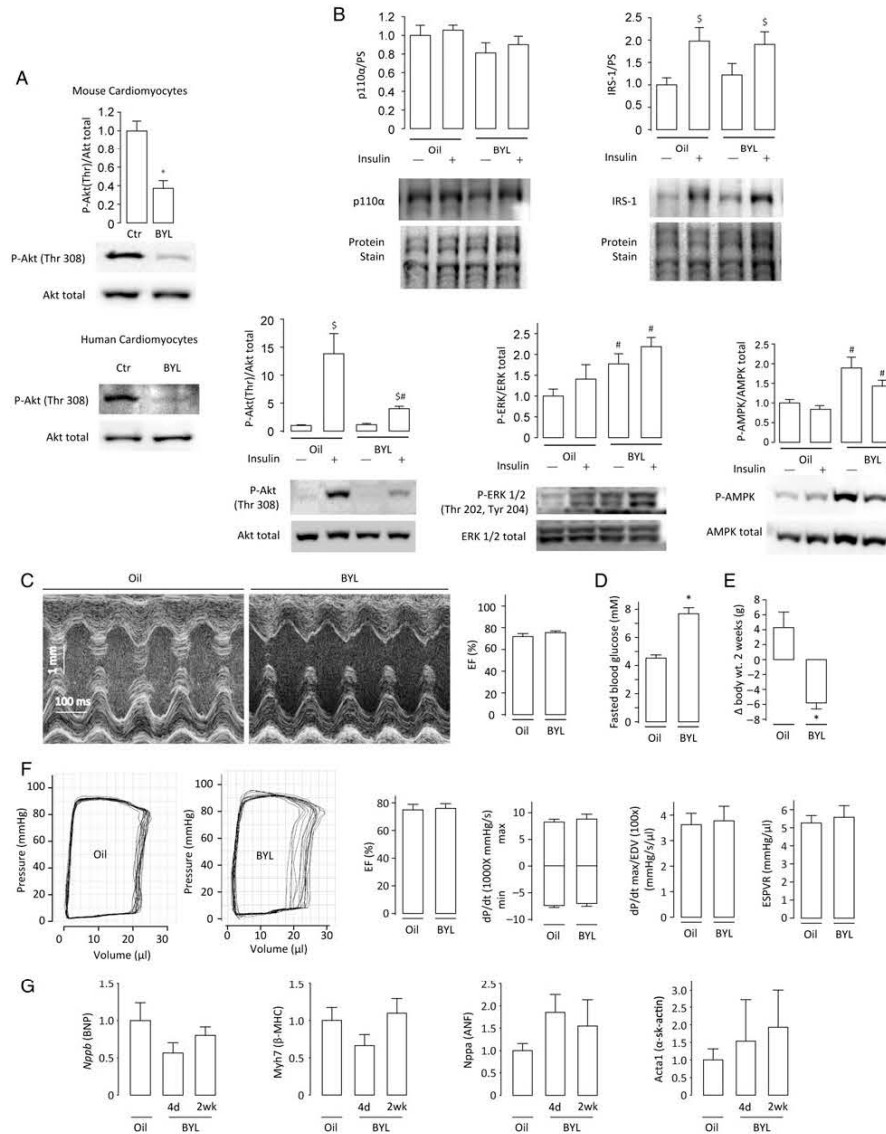


Figure 5.5. Western blot representative image and quantification for Akt activation are shown for wild-type adult mouse cardiomyocytes (average and standard error of change from placebo control to BYL-719 treated myocytes from 3 to 4 replicates obtained independently (n=4) and representative western blot of human non-failing cardiomyocytes (from n=2 donor hearts) cultured with insulin (10 mg/L) supplemented media (12 h) with and without BYL-719 (A). Insulin signalling was tested after a 4-day treatment (30 mg/kg/day BYL-719) with mice fasted 16 h overnight before their final dose of BYL-719. Three hours later, mice were injected with insulin (1 mg/kg) and hearts collected after 15 min (n=4); western blots investigated effect of insulin (\$) and/or BYL-719 (#) on protein levels or activation of p110α, IRS-1, Akt (Thr 308), ERK1/2, and AMPK (Thr 172) (n ¼ 4) (B). Echocardiography M-mode images of left ventricle (LV) of vehicle (oil) or BYL-719 and summary of ejection fraction (EF%) from echocardiography of 2 weeks of vehicle (oil) and BYL-719 treated (n=8–9) (C). Fasted blood glucose measured the day following first 5 days of treatment with BYL-719 (30 mg/kg/day) after fasting overnight for 16 h (n ¼ 6) (D). Change in body weight after 2 week administration of BYL-719 (30 mg/kg/day*5 days/week) for vehicle or BYL-719 treated mice (n ¼ 8–9) (E). Representative pressure/volume loops for vehicle or BYL-719 treated mice and summary haemodynamic parameters from pressure volume loops: ejection fraction, peak maximal and minimal change in pressure per unit time (dP/dt), maximal change in pressure per unit time divided by end diastolic volume (EDV) and end systolic pressure volume relationship (ESPVR) for vehicle (oil) (n=5) and BYL-719 (n=7) treated mice (F). Expression of disease markers in oil treated compared with 4-day and 2 weeks of BYL-719 treatment (n=6–7 each) (G). *P≤0.05.

ERK1/2 activation has been associated with hypertrophy and cell survival effects,¹⁹⁹ and enhanced ERK1/2 signaling in PI3K α MCM and PI3K α Cre hearts may partially compensate for loss of PI3K α due to overlapping roles in cell survival signaling. One possible mechanism of ERK1/2 activation is through reduced negative feedback downstream of PI3K that affects upstream elements common to both PI3K and ERK1/2 signaling pathways. IRS-1 is negatively regulated by the PI3K pathway;¹⁶⁶ PI3K α haploinsufficient mice display increased IRS-1 protein levels and maintained insulin sensitivity with age.²⁰⁰ Increased IRS-1 may partially explain increased ERK1/2 activation,¹⁶⁷ but IRS-1 levels were increased in both HD and LD PI3K α MCM hearts (Fig. 5.3D), despite ERK1/2 activation only being increased in the LD treated mice, so there are likely to be other regulatory factors also influencing ERK1/2 activation. Interestingly, ERK1/2 signaling has an important role in cell survival and proliferation in the setting of PI3K class IA isoform inhibition in hematopoietic progenitor cells and fibroblasts.²⁰¹ Consequently, increased ERK1/2 signaling in PI3K α MCM LD but not HD tamoxifen treated mice may contribute to the disparity in the pathology between these two groups.

AMPK is an energy conserving mechanism activated in the setting of low insulin signaling,²⁰² and is consistent with reduced Akt activation and impaired insulin signaling in the PI3K α MCM hearts.¹⁰³ AMPK activation may have an adaptive role in the setting of mild metabolic stress, due to AMPK mediated inhibition of energy demanding processes such as protein synthesis.²⁰³ Similarly, AMPK may be beneficial for energy homeostasis in PI3K α MCM hearts (Figure 5.3D), but may inhibit cellular stress responses needed to reduce tamoxifen cytotoxicity in HD tamoxifen treated hearts. Our findings showing enhanced AMPK and ERK1/2 signaling in these PI3K α deletion/inhibition models are indicative of the potential for cellular adaptation, and we expect that many more cellular regulatory pathways are also modified in these models. The resulting phenotypes are likely a complex combination of the loss of PI3K α specific signaling, such as insulin and IGF-1,⁶⁸ and adaptations through altered regulation of other signaling pathways.

PI3K α MCM mice with low dose tamoxifen may be an ideal genetic model for further studying the role of PI3K α in the heart, along with the new generation of clinically targeted PI3K inhibitors such as BYL-719. We have observed that PI3K α is critical for insulin mediated activation of Akt in the heart, but further studies are needed to investigate the ramifications for this loss of Akt activation on heart metabolic substrate utilization. We observed marked weight loss in mice treated with the PI3K α inhibitor BYL-719. Future studies looking at the effects of PI3K α inhibitors on food consumption, whole body metabolism and body composition would be useful. Weight loss due to skeletal muscle sarcopenia can have serious negative consequences for cancer patients,²⁰⁴ and it is possible that PI3K α inhibitors may promote this process. Interestingly, human cases with the converse, elevated PI3K activity due to PTEN haploinsufficiency, have increased insulin sensitivity and are more likely to be obese.²⁰⁵ Our data and previous studies have clearly documented that PI3K α is the dominant isoform which controls insulin-mediated signaling in the heart with a secondary regulatory role for PI3K β .^{103, 188} We would also speculate that considering the dramatic difference in PI3K α mediated activation of Akt between fasted and insulin stimulated control mice (Figures 5.4E, 5.5B), it does not seem practical to the organism for this system to also regulate heart function, because the act of eating and insulin release may not closely correlate with times when extra cardiac function is required. This is in contrast to the clear inotropic effect of the sympathetic nervous system, which is rapidly recruited in times of need for increased heart function.

The genetic and pharmacological models of PI3K loss/inhibition are timely models for predicting the effect on the heart of PI3K inhibition considering the current trials for PI3K inhibitors in adults with cancer.^{4, 5, 118} Our observation in this study, that PI3K α loss reduced the ability for recovery from tamoxifen/Cre cardiotoxicity suggests that PI3K α has important cardioprotective properties, and future studies should investigate the impact of PI3K α inhibition in patients with common comorbidities and risk factors such as advanced age, hypertension, coronary artery disease, metabolic syndrome and combinations with other cancer therapies. On

the flipside of PI3K inhibition for cancer patients, activation of PI3K α signaling, such as through exercise⁶⁴ or pharmacological therapies, may be of strategic importance for clinical scenarios where PI3K α signaling is protective. However, the physiological significance of altered PI3K α signaling needs to be established for specific pathological conditions.

6. PI3K α and Doxorubicin Toxicity

Submitted for publication as: Inhibition of PI3K α in a Female Murine Cardiotoxicity Model Causes Heart Atrophy and Distinct Biventricular Remodeling with Pathological p38 MAPK Activation

6.1. Introduction

This chapter follows on our previous findings (Chapter 5) that loss of PI3K α causes increased susceptibility to the cytotoxic effects of tamoxifen combined with Cre recombinase. The tamoxifen/Cre system is a bioengineered tool for pre-clinical researchers to make inducible, tissue specific gene modifications. We next hypothesized that PI3K α may also be important for maintained heart health and function under cytotoxic insults that may be encountered by patients who are also candidates to receive PI3K α inhibitors, such as chemotherapeutic agents (introduced in Chapter 1.10). In fact, increasing evidence shows that additional cytotoxic therapies may be required to be used in combination with PI3K inhibitors to achieve their therapeutic potential.²⁰⁶⁻²⁰⁹ The downside of this scenario is that unintended effects, including adverse effects on the heart, may be increased. Here we test the hypothesis that PI3K α inhibition/deletion will potentiate or exacerbate the cytotoxic effects of the chemotherapeutic drug doxorubicin. We utilized female mice because the majority of cardiotoxic effects of human cancer treatments have been in female patients, particularly combination therapies using Trastuzumab, an antibody based inhibitor of receptor signaling upstream of PI3K, and anthracyclines; however, the majority of animal research done on anthracycline induced heart toxicity has used male mice or not specified the sex of the animal.

6.1. Results

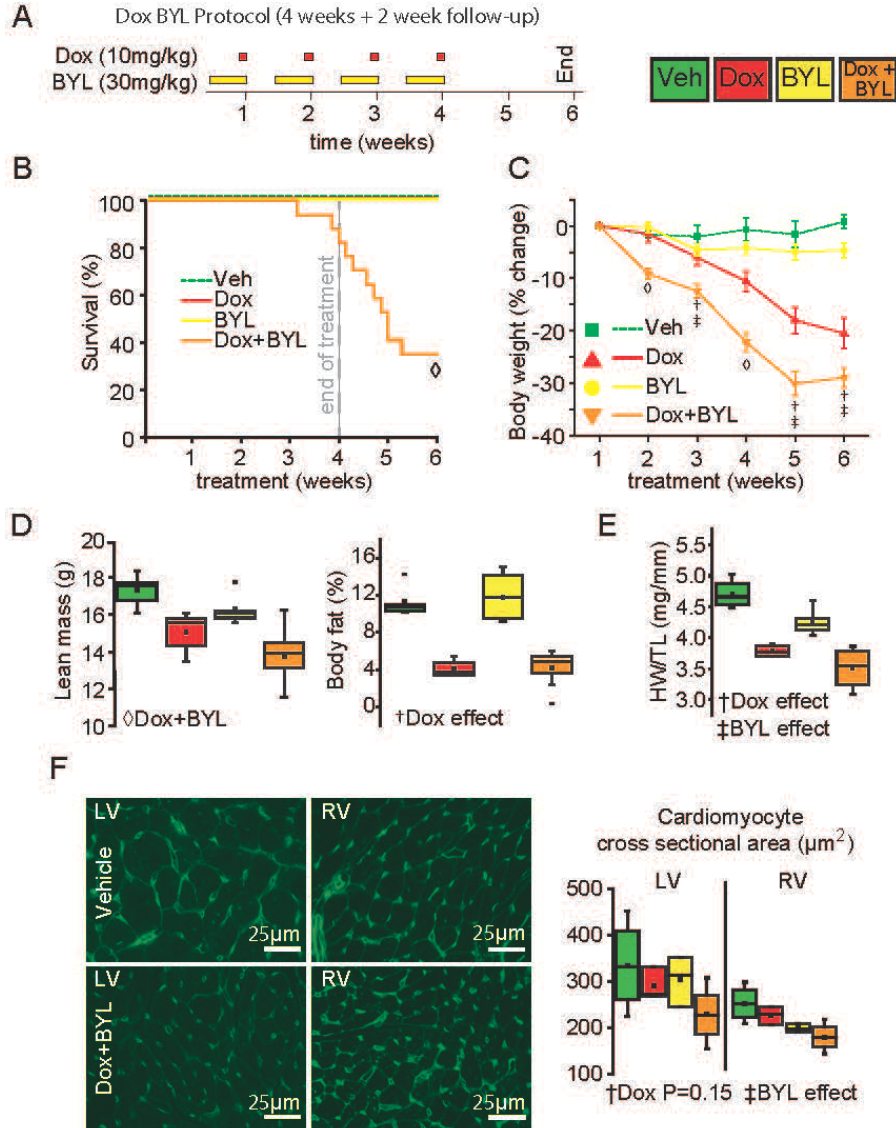


Figure 6.1. Treatment with BYL719 and doxorubicin causes mortality, weight loss and heart atrophy. **A**, Mice were treated 5 days/week with daily BYL719 (30mg/kg) and 1/week with doxorubicin (10mg/kg), along with single drug+vehicle groups and a double vehicle group, for 4 weeks with a 2 week follow-up period (n=8-17). **B**, mice treated with Dox and BYL had mortality which continued after treatment was stopped. **C**, Dox and BYL caused body weight loss. **D**, Whole body lean mass was reduced by Dox and BYL and % body fat was reduced by Dox (body composition measured at end of treatment; n=7-12), **E**, Heart weight (HW) normalized to tibial length (TL) was reduced by Dox and BYL. **F**, Cardiomyocyte cross sectional area outlined by wheat germ agglutinin staining measured in both LV and RV was reduced by BYL in the RV (box graphs and statistics using biological averages, n=4; dot plots show values for individual cardiomyocytes). †Dox effect, ‡BYL effect or ◊Dox+BYL interaction indicates $P \leq 0.05$ in two-way ANOVA.

6.2.1 Co-treatment with PI3K α inhibitor and doxorubicin results in heart atrophy and increased mortality

To simulate the clinical application of anthracycline and PI3K α inhibition, WT female mice were treated 4 weeks with weekly doses of doxorubicin (Dox) and 5/week daily doses of the PI3K α specific inhibitor, BYL (Figure 6.1A).⁶ Phenotyping was performed after 1-2 weeks of follow-up to assess persisting effects. Unexpected mortality was observed in the Dox+BYL group beginning near the end of the 4th week of treatment, and continued over the two-week follow-up period (Figure 6.1B). Dox treatment caused gradual weight loss which was exacerbated in the Dox+BYL group (Figure 6.1C), while body composition analysis showed that Dox caused loss of fat mass and Dox+BYL had an additive negative effect on lean mass (Figure 6.1D).

Both Dox and BYL caused heart atrophy (Figure 6.1E), which was consistent with reduction in myocyte cross sectional area (MCSA), dominated by Dox in the left ventricle (LV; P=0.15) and BYL effect in the right ventricle (RV) (Figure 6.1F). These effects occurred in the absence of significant hyperglycemia (Figure 6.2A), a potential metabolic side effect of PI3K α inhibition. These results demonstrate a striking increase in mortality and heart atrophy in response to combination therapy with a dominant effect of PI3K α inhibition on right ventricular atrophy.

6.2.2 Biventricular remodeling is characterized by reduced stroke volume and RV dilation in the setting of weight loss

Echocardiography showed that Dox treatment caused reduced LV chamber diastolic and systolic dimensions resulting in decreased LV stroke volume, with a further reduction in response to combination therapy with BYL (Figure 6.3A-B; Table 6.1) in the absence of pulmonary congestion (Figure 6.2B).

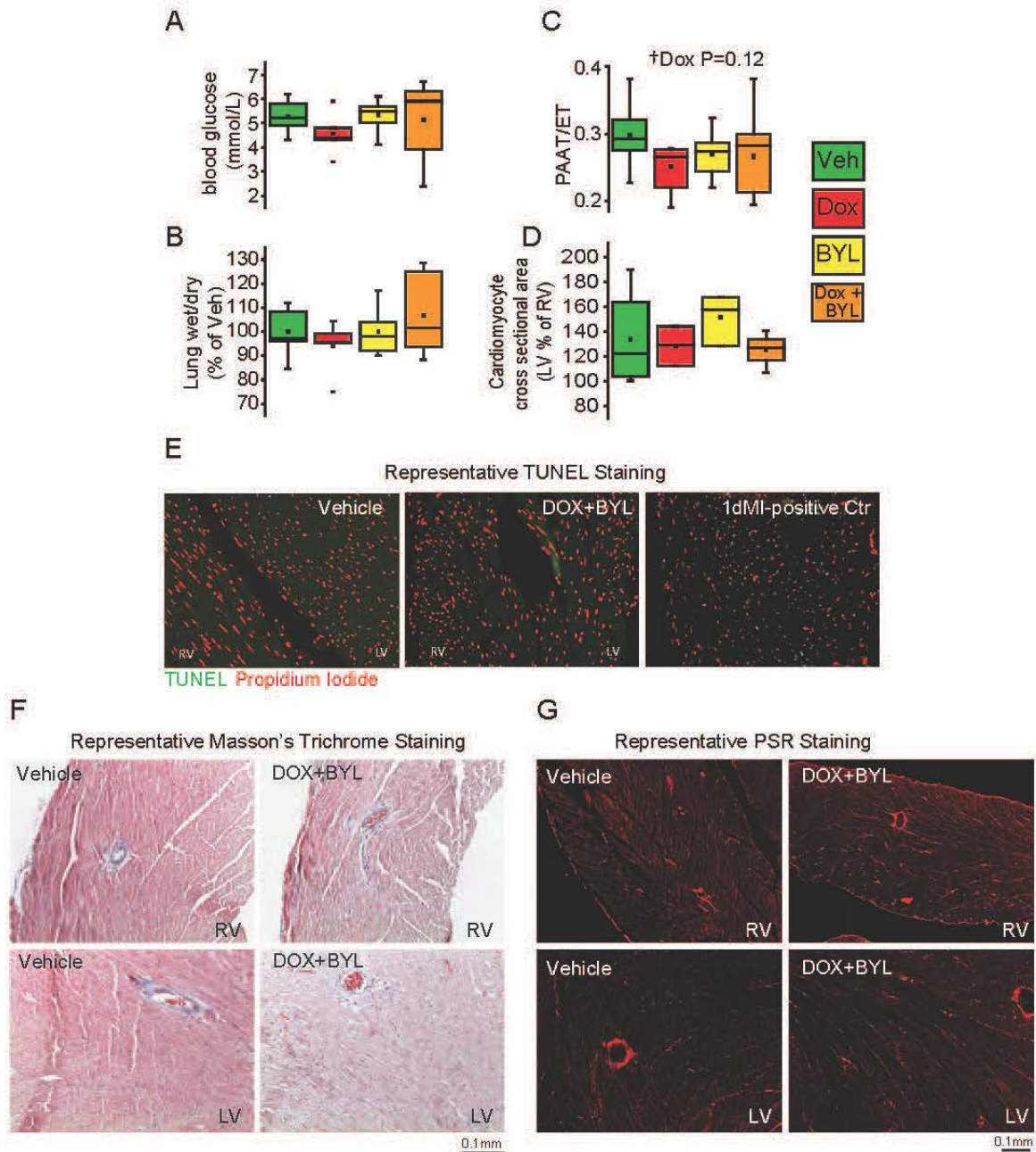


Figure 6.2. Phenotyping of doxorubicin and BYL719 treated mice and hearts

A, Blood glucose levels after 8hrs fasting (n=4-7). **B**, Lung wet to dry weight ratio as a marker of pulmonary edema and **C**, pulmonary artery acceleration time (PAAT) divided by ejection time (PAAT/ET), measured in pulse wave Doppler echocardiography (n=7-12). **D**, Average LV myocyte cross sectional area is shown as a percentage of RV myocyte cross sectional area. **E**, Terminal deoxynucleotidyltransferase-mediated 2'-deoxyuridine-5'-triphosphate nick-end labeling (TUNEL) and nuclear propidium iodide (PI) (n=3); one day post myocardial infarction (MI) was used as a positive control. **F**, Representative Masson's Trichrome staining and **G**, PicroSirius Red (PSR) staining of vehicle and Dox+BYL treated LV and RV sections (n=4). †Dox effect, ‡BYL effect or ◇Dox+BYL interaction indicates $P \leq 0.05$ in two-way ANOVA.

Table 6.1. Left Ventricle Pressure Volume Hemodynamics in Female Hearts with Dox and PI3K α Deletion/Inhibition

	Vehicle	Dox	BYL	Dox+BYL	P
number	(8)	(8)	(8)	(5)	
HR (bpm)	439.3 ±17.4	407.3 ±12.8	430.3 ±12.7	* 399.9 ±12.1	†
ESP, mmHg	92.2 ±1.7	90.4 ±2.8	93.1 ±1.4	* 86.1 ±1.1	†
EDP, mmHg	10.3 ±1.4	5.9 ±0.9	7.4 ±1.0	* 8.7 ±0.9	◇
ESV, μ L	9.7 ±1.6	5.5 ±1.5	6.8 ±0.7	* 5.9 ±1.2	ns; †P=0.079
EDV, μ L	25.4 ±2.0	19.2 ±1.5	25.9 ±2.5	* 19.6 ±2.1	†
SV, μ L	18.1 ±0.7	13.7 ±0.8	19.5 ±2.2	* 13.7 ±1.6	†
CO (mL/min)	7.7 ±0.4	5.7 ±0.5	8.3 ±1.0	* 5.4 ±0.6	†
LVEF, %	72.4 ±5.2	73.5 ±5.6	74.1 ±2.7	* 70.2 ±4.6	ns
ESPVR	6.5 ±0.7	5.6 ±0.7	7.1 ±0.7	* 4.2 ±0.5	†
EDPVR	0.10 ±0.02	0.16 ±0.03	0.08 ±0.01	* 0.21 ±0.05	†

	Flx	Flx+Dox	Cre	Cre+Dox	P
number	(8)	(7)	(6)	(7)	
HR (bpm)	439.3 ±15.4	405.6 ±12.8	438.5 ±10.5	340.7 ±19.2	ns
ESP, mmHg	90.1 ±3.0	87.4 ±2.6	91.1 ±2.2	86.5 ±3.7	ns
EDP, mmHg	7.4 ±1.1	5.9 ±0.8	4.9 ±0.9	6.6 ±1.2	ns
ESV, μ L	12.1 ±3.2	12.5 ±3.5	10.9 ±2.2	7.2 ±1.2	‡
EDV, μ L	34.0 ±4.9	31.1 ±2.7	33.9 ±2.3	24.6 ±2.4	† ‡
SV, μ L	22.6 ±3.2	18.6 ±3.7	24.5 ±2.1	17.4 ±1.5	†
CO (mL/min)	9.2 ±0.7	7.6 ±1.6	10.5 ±0.6	5.9 ±0.6	†
LVEF, %	62.9 ±4.2	62.5 ±10.7	69.9 ±4.8	71.6 ±3.6	ns
ESPVR	5.9 ±0.1	3.8 ±0.7	4.7 ±0.5	3.7 ±0.8	†
EDPVR	0.14 ±0.03	0.13 ±0.02	0.10 ±0.02	0.09 ±0.03	ns

Left ventricle (LV) pressure volume (PV) loops were performed at 4 weeks + 2 weeks of follow-up for Dox and BYL treated groups, and 5 weeks + 2 weeks of follow-up for Dox and Cre groups; HR, heart rate; ESP end systolic pressure; EDP, end diastolic pressure; ESV, end systolic volume; EDV, end diastolic volume; SV, stroke volume; CO, cardiac output; ESPVR, end systolic pressure volume relationship; EDPVR, end diastolic pressure volume relationship. Values are means ±SEM (Two-way ANOVA: ◇P≤0.05 for Dox+BYL or Cre+Dox, if ◇P≥0.05, P values shown for Dox and BYL/Cre individually (†P≤0.05 Dox effect; ‡P≤0.05 BYL/Cre effect; *possible survival bias)

Given the changes in preload, we performed invasive left ventricular pressure-volume analysis to perform load-independent assessment of myocardial contractility, revealing reduced negative dP/dt_{max} upon Dox treatment (Figure 6.3C and Table 6.1). In contrast, the RV of Dox+BYL treated mice were dilated and had reduced fractional shortening (FS); consistent with ventricular interdependence (common stroke volume, shared septum and interdependent contraction forces) and reduction in LV dimensions (Figure 6.3D). Pulmonary artery acceleration time (Figure 6.2C) and the ratio between LV and RV MCSA (Figure 6.2D), indicators of pulmonary arterial hypertension (PAH), were not significantly changed between the experimental groups. Hearts did

not show increased apoptosis (TUNEL staining) or myocardial fibrosis based on Masson's trichrome and picro-sirius red (PSR) staining in response to Dox+BYL (Figure 6.2E-G).

We next treated an additional cohort for only 3.5 weeks (Figure 6.3E) for the following reasons: (1) to avoid survival bias in the Dox-BYL group (the mice that died in this group were likely different from the survivors in several of the key phenotyping indicators that we considered, such as heart function, mass etc, thus potentially skewing this data towards a less severe phenotype), (2) to test for elevated RV afterload pressures while under BYL treatment by invasive, closed chest catheterization, (3) to collect tissues for molecular investigation under conditions in which direct effects of BYL are still present, (4) and to measure food consumption, as a possible confounding cause of weight loss. While both Dox and BYL caused weight loss, daily measurement of food consumption during the third week of treatment showed stable food consumption normalized to body size (Figure 6.3F). Catheterization of the RV was performed 4-6 days after the final dose of Dox and 1-2hrs after the final dose of BYL. Relative RV ejection fraction was reduced in Dox treated hearts with some Dox+BYL hearts declining further in relative ejection fraction and stroke volume at this early time point, but no alteration in RV filling and peak systolic pressures (Figure 6.3H). In contrast, LV demonstrated distinct remodeling: left ventricular chamber dimensions and stroke volume were reduced by BYL at this time point (Figure 6.3I and J), suggesting that the effects of BYL on LV chamber dimensions were partially masked by survival bias and Dox effects in the previous cohort that underwent 4+2 weeks treatment. Electrocardiographic analysis confirmed intact HR, PR interval and QRS duration with significant prolongation of the QTc interval confirming the presence of cardiomyopathy in the absence of conduction disease in the combination treated mice (Figure 6.4). Our results illustrate cardiotoxicity in female mice characterized by RV dilation and decreased LV cardiac output and myocardial contractility, consistent with ventricular interdependence.

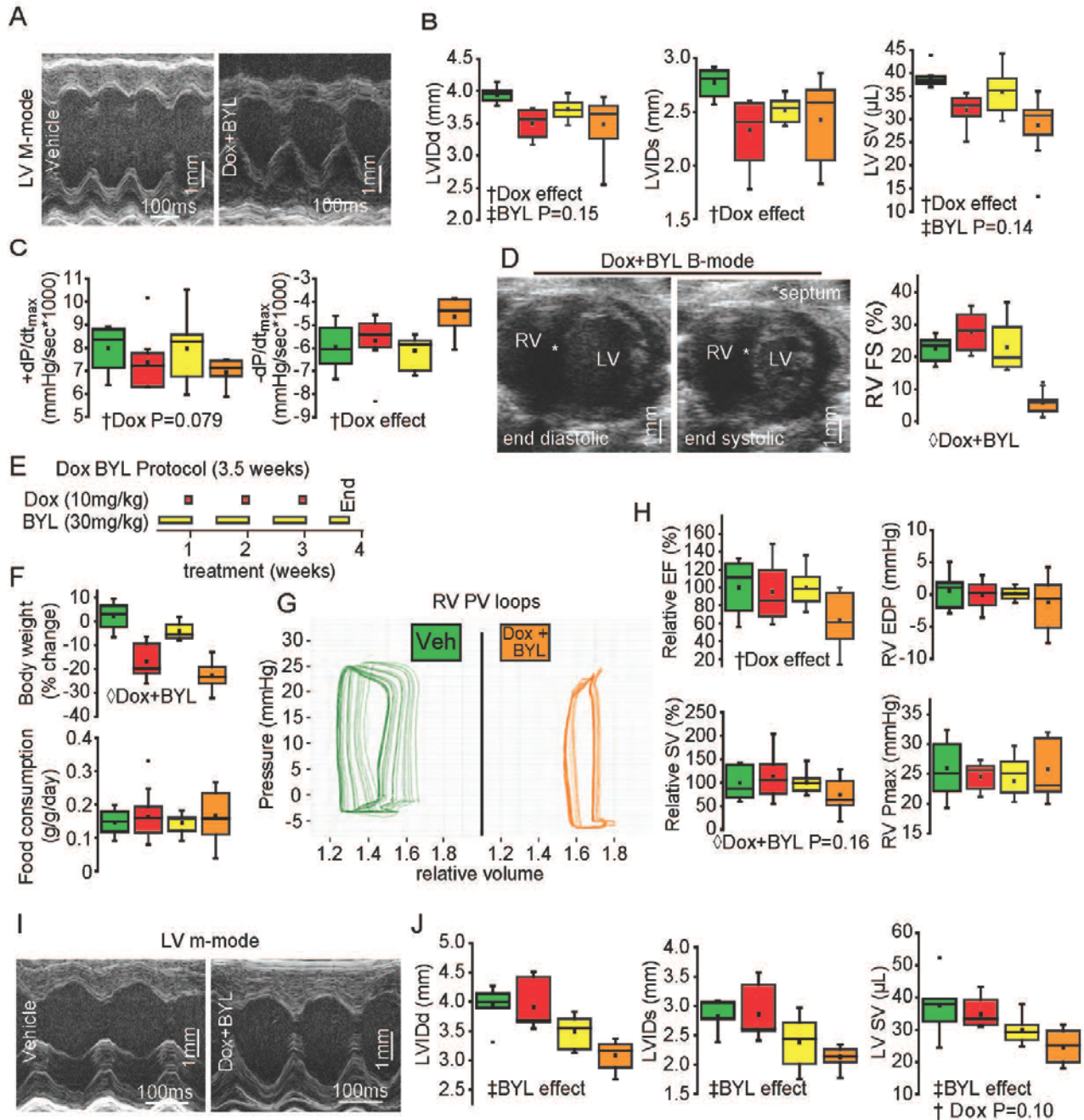
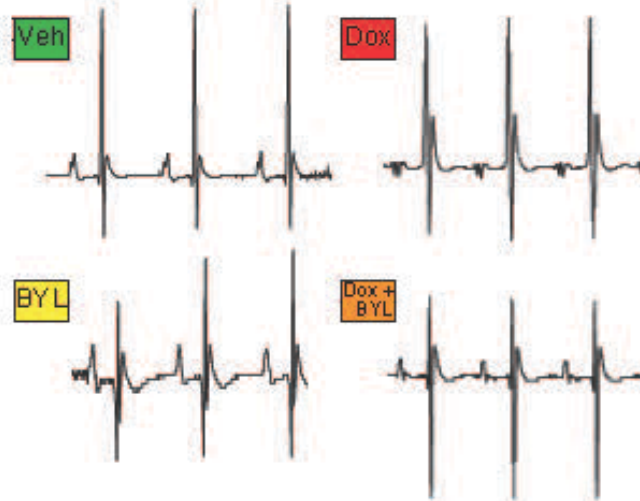


Figure 6.3. Heart function and dimensions in the left and right ventricles in response to cardiotoxicity. **A**, LV M-mode images from control and double treated hearts; **B**, LV chamber dimensions and LV stroke volume were reduced by Dox. **C**, LV positive and negative dP/dt_{max} are indicative of impaired contractility. **D**, Example short axis images from double treated hearts at end diastole and end systole; RV fractional shortening was reduced in double treated hearts. **E**, A new cohort of mice were treated as in figure 1A, but ending at 3.5 weeks (n=7-8). **F**, Body weight was reduced by Dox and BYL treatment despite maintained food consumption (measured for 5 days in week 3). **G**, Invasive, closed chest catheterization of the RV with relative volumes and absolute pressures. **H**, Alterations in ejection fraction (EF), and some Dox+BYL hearts showing decreased RV stroke volume at this time point despite normal filling and peak pressures. **I**, **J**, At this time point, LV chamber dimensions and stroke volume were decreased by a BYL effect. \dagger Dox effect, \ddagger BYL effect or \diamond Dox+BYL interaction indicates $P \leq 0.05$ in two-way ANOVA.



	Vehicle	Dox	BYL	Dox+BYL	P
ECG (n)	(9)	(9)	(9)	(8)	
HR, bpm	449.6±21.7	459.9±17.9	439.3±18.2	421.7±12.9	ns
PR (ms)	41.3±1.4	39.7±1.2	39.9±2.1	40.6±1.4	ns
QRS (ms)	11.7±0.5	10.9±0.3	11.1±0.7	12.0±0.5	♠
QT (ms)	41.3±1.4	53.8±2.6	60.7±2.8	66.2±2.9	‡
QTcB (ms)	43.4±1.9	47.2±2.2	51.6±1.7	55.2±1.9	‡
QTcF (ms)	45.7±2.2	49.3±2.3	54.4±2.0	58.6±2.2	‡
RV PV Loops (n)	(7)	(7)	(8)	(7)	
HR, bpm	463.9±18.9	452.1±35.1	480.4±18.2	435.8±25.2	ns

Figure 6.4. Surface Electrocardiogram

Example electrocardiogram (ECG) traces from WT mice under Dox and BYL treatment in lead 1; ECG, electrocardiogram; HR, heart rate (recorded at ECG and subsequent pressure/volume (PV) catheter insertion); ECG derived PR interval, QRS duration and QT interval with QTc (corrected according to Bazett's (B) and Fridericia's (F) formulas).

6.2.2. Cardiomyocyte-specific loss of PI3K α potentiates the susceptibility to Dox toxicity

We next used a female, cardiomyocyte-specific p110 α deletion mouse strain (α MHC-Cre)¹³ to investigate the direct contribution of the loss of cardiomyocyte p110 α function to biventricular remodeling in response to Dox. The α MHC-Cre/p110 α cohort of Dox treated mice did not sustain the high mortality rates seen in the Dox+BYL group (4+2 week protocol), so a total of 5 weeks of treatment were completed (5+2 week protocol) (Figure 6.5A). While these results indicate that systemic p110 α inhibition did contribute to the increased mortality of Dox+BYL treated mice, Dox treatment caused body weight loss, and cardiac atrophy in the α MHC-Cre/p110 α mice (Figure 6.5B). Transthoracic echocardiography showed dilated RV, reduced fractional shortening with

striking interventricular dependence and D-shaped septum in the Dox+ α MHC-Cre/p110 α group (Figure 6.5C).

A second cohort was treated for 4 weeks and invasive RV catheterization was performed which confirmed RV dilation and reduced relative cardiac output and ejection fraction in the α MHC-Cre/p110 α +Dox group (Figure 6.5D and E). Ventricular functional assessment by invasive catheterization and echocardiography, showed that Dox treatment reduced LV volume and cardiac output coupled with reduced myocardial contractility as illustrated by the decrease in end-systolic pressure-volume relationship (ESPVR) as well as impaired maximal rate of contraction and relaxation (dP/dt_{\max}) (Figure 6.5G and Table 6.1) in female α MHC-Cre/p110 α mice. These results indicate that direct cardiomyocyte PI3K α inhibition is predominantly responsible for the distinct adverse biventricular remodeling and dysfunction we observe in female mice treated with Dox.

6.2.3. Molecular Basis for the Biventricular Cardiomyopathy

We next investigated the molecular pathogenesis of the biventricular myocardial remodeling. We profiled the expression of heart disease markers in the LV and RV from the 3.5-week Dox-BYL protocol, which showed that Dox increased expression of the β -myosin heavy chain isoform and atrial natriuretic factor (ANF) was increased in some hearts of the combination group in both the LV and RV (Figure 6.6A).

We then investigated molecular mechanisms that could account for the biventricular remodeling using tissue from the 3.5-week protocol. We first focused on signaling pathways implicated in muscle atrophy.²¹⁰ Nuclear localization of FOXO1 was reduced by Dox in the RV and FOXO3a and Smad2/3 was detected only in nuclear and non-nuclear fractions, respectively (Figure 6.6B), indicating that these pathways did not have increased activation. Furthermore, expression of atrogin-1, a regulatory target of FOXO1, was not changed (Figure 6.6C).

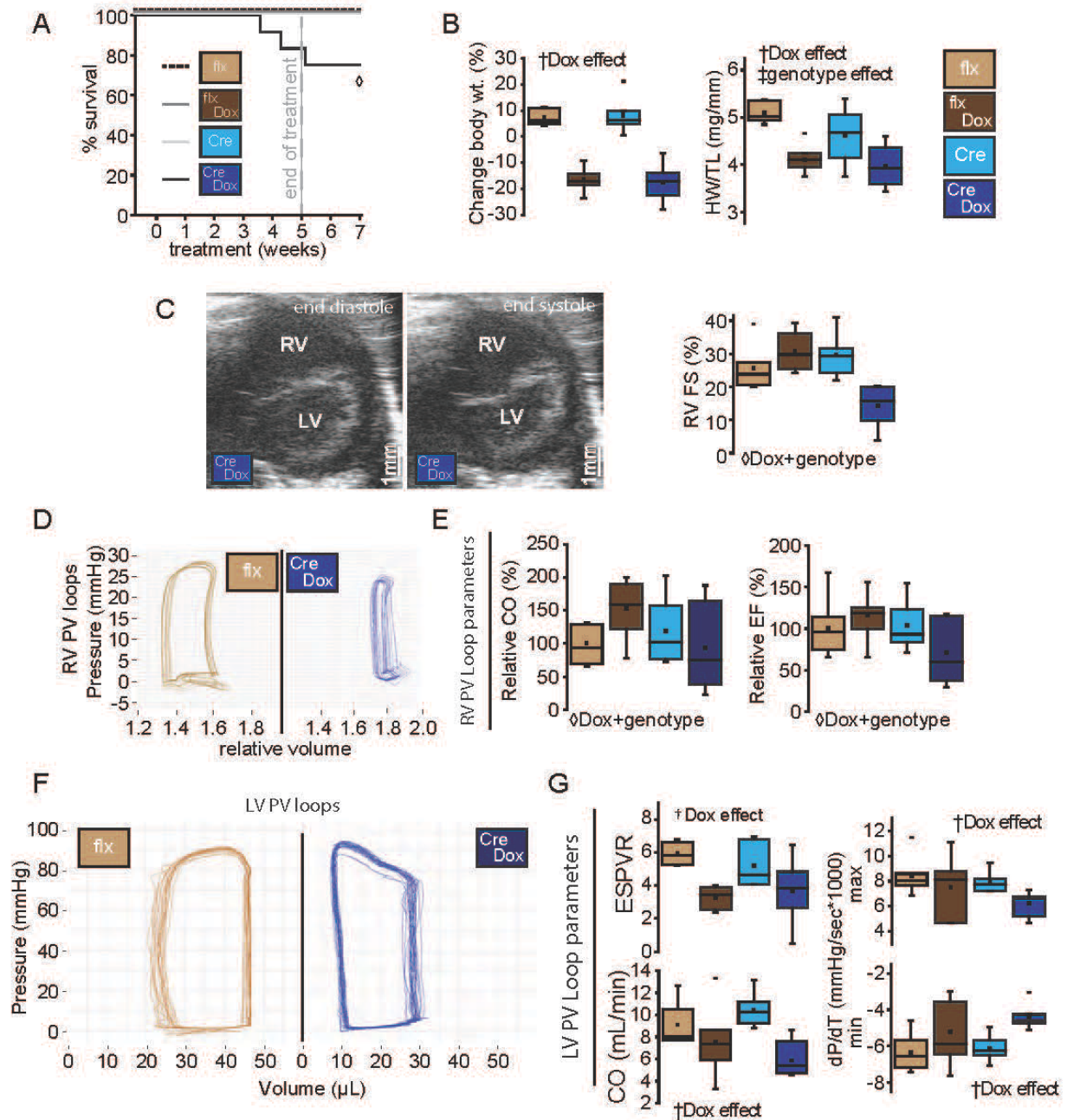


Figure 6.5. Effects of cardiomyocyte-specific deletion of p110 α in response to doxorubicin treatment
A, Mice with α MHC-Cre/p110 α^{flx} (Cre) or only p110 α^{flx} (flx) were treated 1/week with Dox (10mg/kg) or vehicle for 5 weeks with a two week follow-up period; mortality was only seen in Dox treated Cre mice (n=9-12). **B**, Body weight was reduced by Dox, and heart weight (HW) relative to tibial length (TL) was reduced by Dox and genotype. **C**, Right ventricle fractional shortening was reduced in Dox*genotype; B-mode ECHO image shows irregular septal morphology. **D,E**, A second cohort treated for 4 weeks, used for invasive, closed chest catheterization of the RV, had Dox+genotype dependent reductions in relative RV cardiac output (CO) and ejection fraction (EF) (n=7-9). **F**, Example LV PV loops for flx vehicle treated and Cre Dox treated (5+2 week group). **G**, PV loop analysis: end systolic pressure volume relationship (ESPVR), (CO) and peak positive and negative change in pressure relative to time. †Dox effect, ‡genotype effect or ◊Dox+genotype interaction indicates $P \leq 0.05$ in two-way ANOVA.

We next investigated potential molecular mechanisms of RV dysfunction.^{211, 212} Phosphodiesterase-5 (PDE5) was increased in Dox treated LV and with a similar trend in the RV (Figure 6.6D). Pyruvate dehydrogenase (PDH) phosphorylation (inhibitory) was increased in the LV and RV upon BYL treatment with no effect of DOX on LV, but in the RV, Dox suppressed PDH phosphorylation (Figure 6.6E). However, neither of these pathways were specifically altered in Dox+BYL treated hearts and do not correlate with the RV dilation and dysfunction.

Phosphorylation and activation of the p38 MAPK kinase, which is suppressed by the PI3K/Akt pathway²¹³, is linked to the promotion of atrophy.²¹⁴ Activation of the p38MAPK was increased by both Dox and BYL treatment, resulting in even higher activation by additive effects in Dox+BYL treated hearts (Figure 6.8A). In the α MHC-Cre/p110 α mice, Dox treatment also resulted in a similar pattern of increased p38 activation in the heart (Figure 6.8B). Since the activation of p38 is associated with increased redox stress and inflammation,²¹⁴ we then investigated redox stress. Dihydroethidium (DHE) fluorescence imaging indicated increased reactive oxygen species production in Dox+BYL hearts compared to vehicle treated controls (Figure 6.8C). Expression of TNF α , IL6, and IL1 β , pro-inflammatory cytokines, in Dox-BYL treated hearts was not upregulated in either the LV or RV, and plasma TNF α levels were not increased (Figure 6.7).

To understand the translational aspect of these findings, we next investigated p38 MAPK activation and redox stress in female explanted human hearts with dilated cardiomyopathy, a disease which involves both ventricles. Interestingly, while both p38 activation (Figure 6.8D) and DHE fluorescence (Figure 6.8E and F) were increased in dilated cardiomyopathy (DCM) hearts compared to age and sex matched controls (Ctr); the increased p38 kinase activation and redox stress had higher mean values in the RV compared to the LV, although we did not directly compare ventricles.

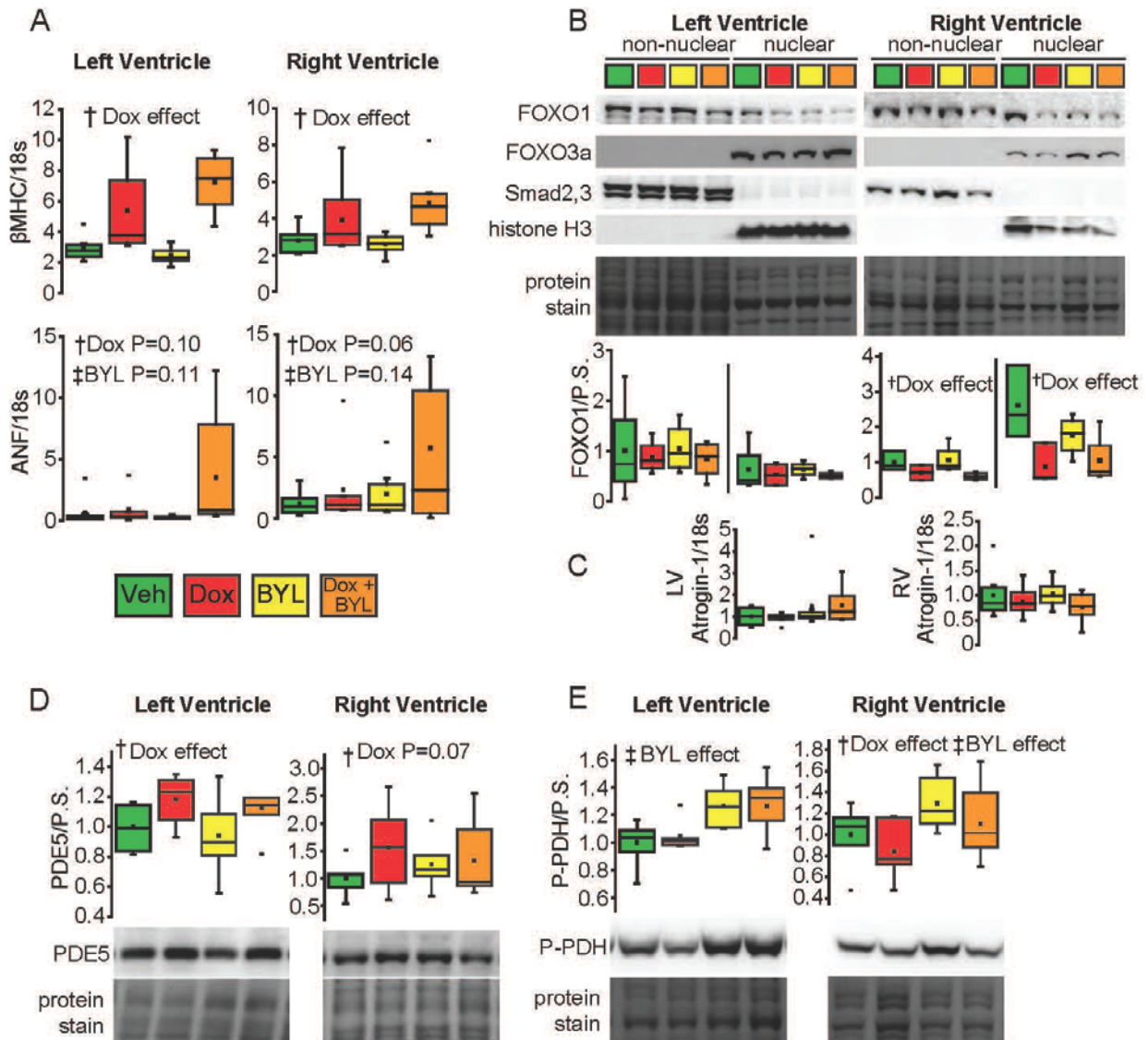


Figure 6.6. Molecular signaling altered in doxorubicin and BYL719 treated hearts

A, Gene expression of disease markers beta myosin heavy chain (β MHC) and **D**, Atrial Natriuretic Factor relative to 18S load control (ANF) (n=7-9). **B**, Representative Western blots of LV and RV heart tissue 3.5 week protocol separated into nuclear and non-nuclear fractions; histone H3 was used as a nuclear marker, localization was assessed for FOXO1, FOXO3a and Smad2,3. Quantification of FOXO1 relative to total protein stain (P.S.) in non-nuclear and nuclear fractions in the LV and RV normalized to vehicle treated non-nuclear fraction (n=4-6). **C**, Expression of atrogin-1 (Fbxo32) in the LV and RV. **D,E**, Western blots in whole LV and RV tissue lysates show a Dox dependent increase in PDE5 in the LV, and a BYL dependent increase in phosphorylated Pyruvate Dehydrogenase (PDH) that is reduced by Dox in the RV (n=6). †Dox effect, ‡BYL effect or ◊Dox+BYL interaction indicates $P \leq 0.05$ in two-way ANOVA.

These results support the relevance of p38 activation, correlating with increase redox stress as an important mechanism driving the biventricular cardiomyopathy in response to PI3K α inhibition and Dox treatment.

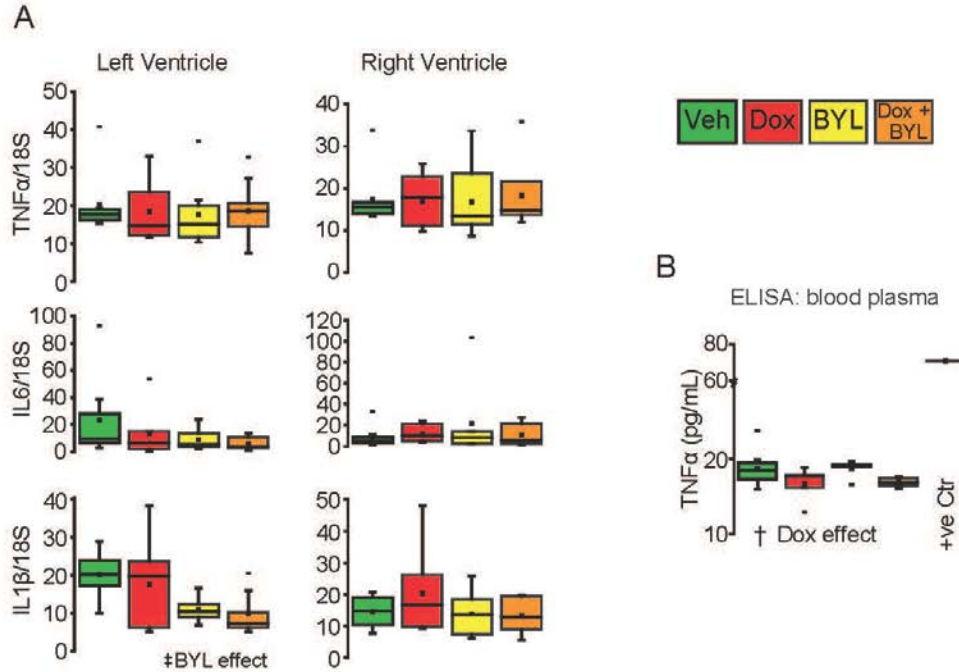


Figure 6.7 Inflammatory cytokines in the LV, RV and plasma

A, Gene expression of inflammatory cytokines TNF α , IL-6 and IL-1 β in heart LV and RV tissue (n=7-9). **B**, TNF α protein levels in blood plasma measured by ELISA (n=5-9) with positive control supplied by manufacturer. †Dox effect, ‡BYL effect or ◊Dox+BYL interaction indicates $P \leq 0.05$ in two-way ANOVA.

6.2.4. Inhibition of p38 signaling partially reversed the biventricular cardiomyopathy

Inhibition of p38 has been linked with skeletal muscle atrophy in cancer cachexia²¹⁵ as well as heart dysfunction and remodeling.²¹⁶ Since p38 MAPK inhibitors are currently in clinical trials,²¹⁷ we tested a rescue strategy using a p38 MAPK inhibitor in our Dox+BYL model. Inhibition of p38 MAPK with SB202190 in the Dox+BYL group attenuated weight loss and heart atrophy with a trend toward retained whole body fat and lean mass (Figure 6A). Cardiomyocyte cross-sectional area was increased in the LV and RV with p38 inhibition (Figure 6B). Invasive pressure-volume analysis of the RV showed reduced ventricular volume associated with increased relative ejection fraction and cardiac output (Figure 6C and Table 2) in response to p38 kinase inhibition. The LV stroke volume and fractional shortening increased, which was consistent with improved RV parameters and interventricular interdependence (Figure 6D and Table 2). Dihydroethidium fluorescence, as a marker of redox stress, showed a non-significant reduction (Figure 6E),

consistent with p38 activation being primarily a down-stream effect rather than upstream cause of redox stress. Electrocardiographic analysis showed normalization of the QT interval with p38 inhibition (Figure 6F). These results support a mechanistic role for p38 activation in mediating the adverse Dox+BYL effects on the heart and the potential for p38 inhibition as a therapeutic strategy.

6.3. Discussion

The emergence of targeted cancer therapies may contribute to the cumulative risk for heart disease since they are often used in combination with chemotherapeutic agents such as anthracyclines and in patients with risk factors for heart disease.¹⁰⁸⁻¹¹³ A striking example of this is the growing list of tyrosine kinase inhibitors indirectly blocking upstream or downstream PI3K α signaling and direct PI3K α inhibitors that have the potential to be broadly used both in patients with identified PI3K pathway mutations as well as general adjuvant therapies.^{118, 218, 219} The compounded CV risk of PI3K α inhibitor use in vulnerable groups such as women with breast cancer is particularly relevant given the high prevalence of p110 α gain-of-function mutations and the large number of clinical trials currently in progress.^{115, 220} Breast cancer survivors have an increased risk of CV death compared to a cancer free comparison cohort²²¹ which could be compounded if therapies that increase cancer survival also increase CV risk when coupled with comorbidities.¹²² Preclinical studies can be used to understand the type and mechanism of the cardiac risk of PI3K α inhibition in combination with other perturbations or comorbidities.

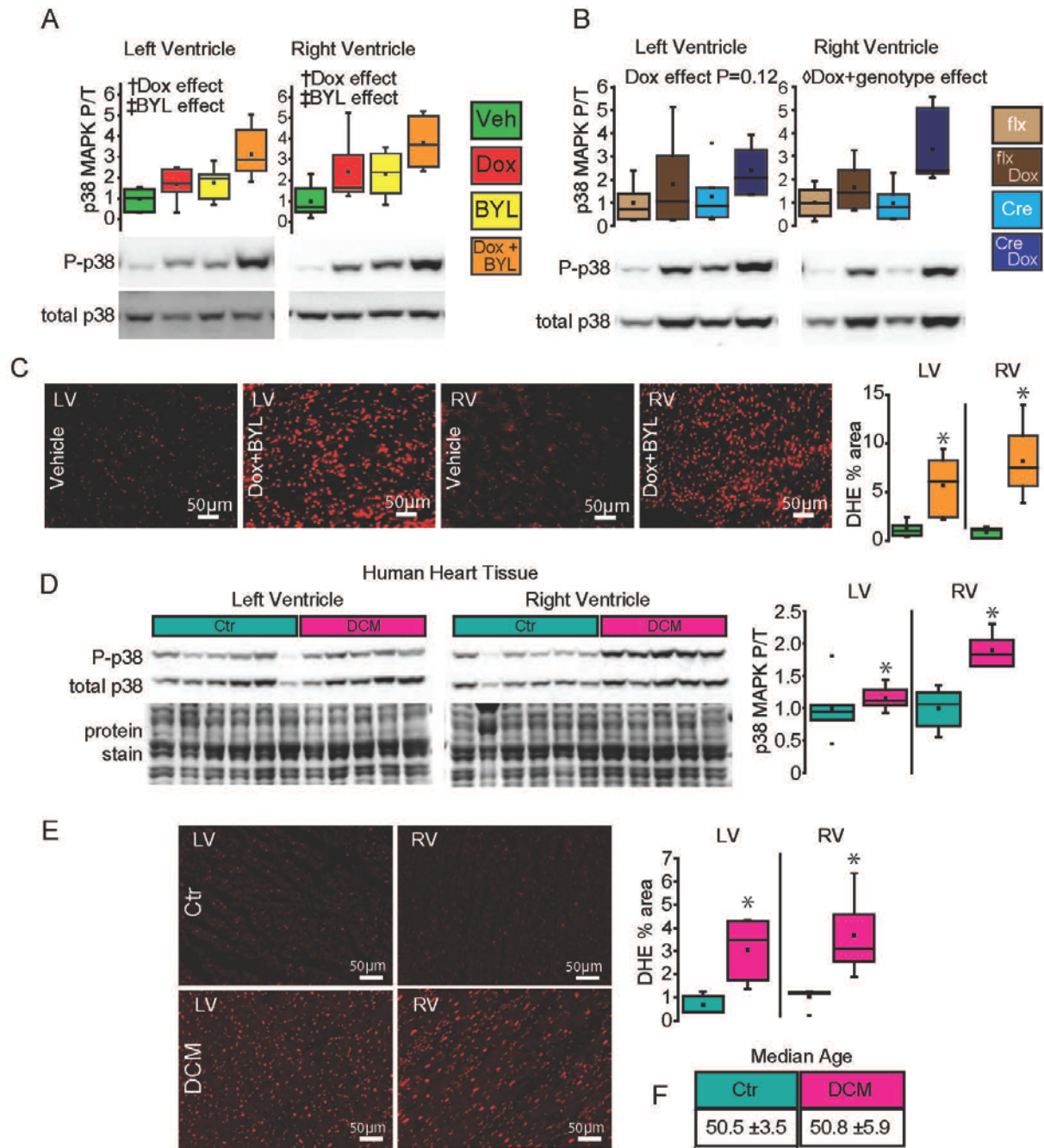


Figure 6.8. Activation of p38 MAPK with increased redox stress in diseased murine and human hearts
A, Representative Western blots from LV and RV heart tissue, 3.5 week protocol, show Dox and BYL dependent increases in phosphorylated p38 in both ventricles (n=6). **B**, Western blot showed Dox+genotype had increased p38 phosphorylation in the RV (n=6). **C**, Dihydroethidium (DHE) staining with quantification of DHE positive area in vehicle treated and Dox+BYL treated sections (n=4). **D**, Human myocardium from age and sex matched non-diseased donor hearts (Ctr; n=6) and non-ischemic, ex-transplanted dilated cardiomyopathy (DCM; n=5) hearts show increased p-38 activation in DCM LV and RVs. **E**, DHE staining with quantification of positive area showed increases in LV and RVs in DCM hearts compared to age matched, female Ctr (n=5). †Dox effect, ‡BYL/genotype effect or ΔDox+BYL/genotype interaction indicates P≤0.05 in two-way ANOVA; *indicates P≤0.05 in two tailed, unpaired T-test between two groups.

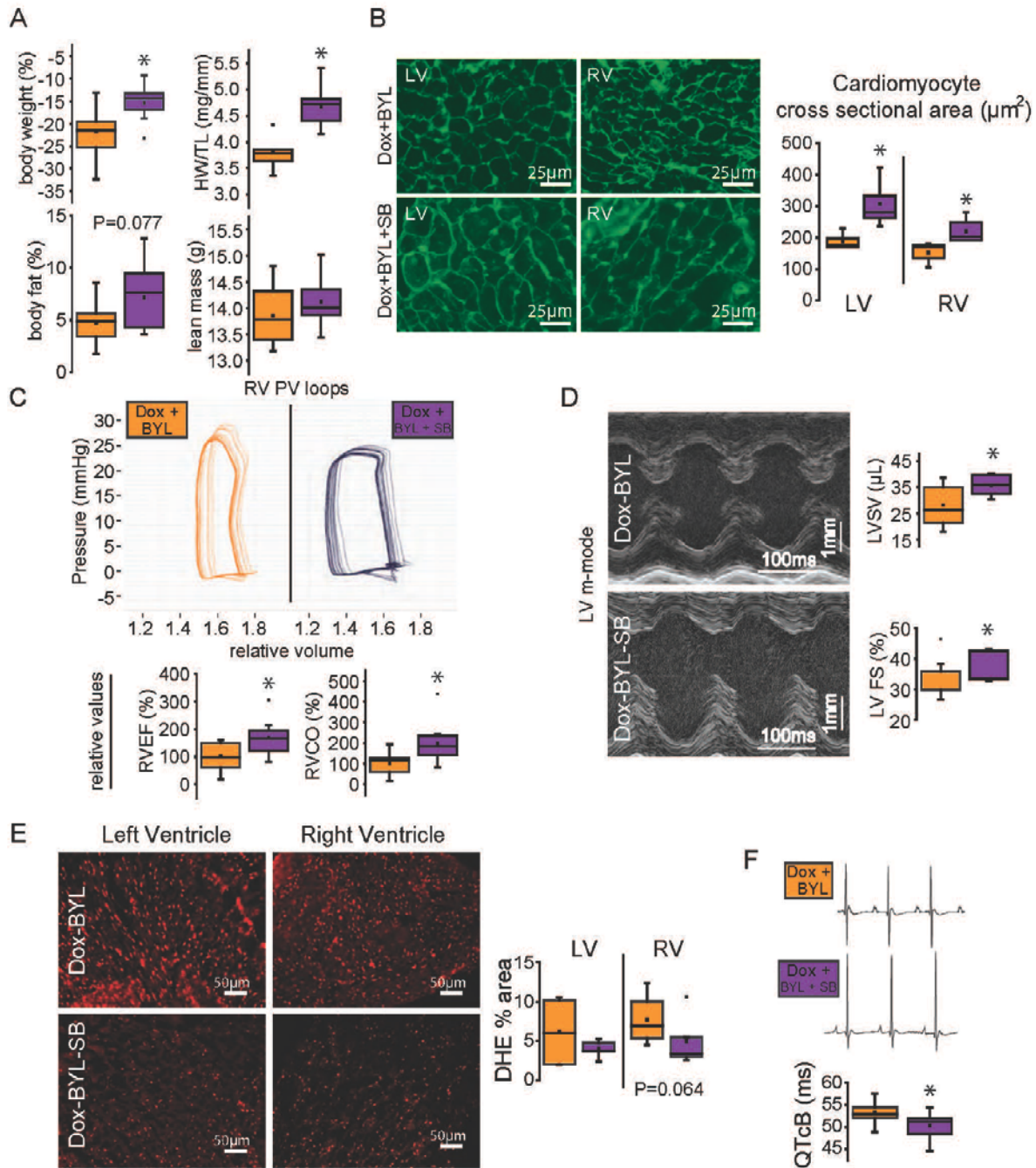


Figure 6.9. Therapeutic inhibition of p38 MAPK in doxorubicin and BYL719 treated mice
 Mice were treated with Dox+BYL for 3.5 weeks as in Figures 3-4 but randomized to receive a daily dose (5 days/week) of the p38 inhibitor SB202190 (5mg/kg). **A**, With p38 inhibition, body and heart weight reduction was attenuated, with trends towards retained body fat and total lean mass (n=9). **B**, Cardiomyocyte cross sectional area reduction was attenuated with p38 inhibition (n=5). **C**, Invasive, closed chest catheterization of the RV showed p38 inhibition increased relative right ventricle ejection fraction (RVEF) and relative cardiac output (CO) (n=9). **D**, Echocardiography showed an increase in left ventricle stroke volume (LVSV) with p38 inhibition (n=9). **E**, DHE positive area was not significantly changed by p38 inhibition (n=4-5). **F**, Surface ECG recordings showed that p38 inhibition reduced QT interval duration (Bazett correction) (n=9). *Indicates P≤0.05 in two tailed, unpaired T-test.

Using female murine models, we demonstrated that combined doxorubicin and PI3K α inhibition resulted in increased mortality and a distinct biventricular remodeling (Figure 6.10) documented by echocardiography and invasive pressure-volume analysis. Right ventricular dilation and reduced fractional shortening resulted in ventricular interdependence and reduced cardiac output. Invasive, closed chest measurement of RV showed normal peak and filling pressures in the presence of PI3K α inhibition indicated that pulmonary artery hypertension was not present in our model, consistent with the lack of cardiomyocyte hypertrophy in the RV and normal lung morphology. Rodent models of doxorubicin toxicity often report dilated LV end diastolic dimensions²²²⁻²²⁴ whereas we observed reduced LV dimensions in our chronic treatment using female mice, possibly due to sex dimorphic responses to these therapies or differences in dosage protocols. Our chemotherapy regimen also resulted in significant weight loss and reduced heart mass and LV chamber dimensions; heart mass is normally closely correlated with body mass, and anorexia also causes reduced heart mass.²²⁵ The LV may be partially protected from atrophy due to its higher systolic pressures, which activate pro-hypertrophy/mass maintaining signaling in comparison to the RV; consistent with this, in a rat, tumor driven cachexia model, RV mass was preferentially decreased.²²⁶ In patients with advanced heart failure, cachexia correlated with reduced RV function, and worse outcomes compared to patients without cachexia.²²⁷

The RV has a number of inherent differences from the LV, which may contribute to the distinct ventricular remodeling in response to chemotherapy. The RV has reduced defense against redox stress,²²⁸ and molecular changes underpinning ventricular remodeling vary by type and magnitude between the LV and RV.^{229, 230} Genetic variation in estradiol metabolism and androgen signaling was associated with RV morphology in a sex-specific manner.²³¹ Right ventricular cardiomyocytes are predominantly longitudinal in orientation, whereas LV myocytes are more radially orientated.²³²

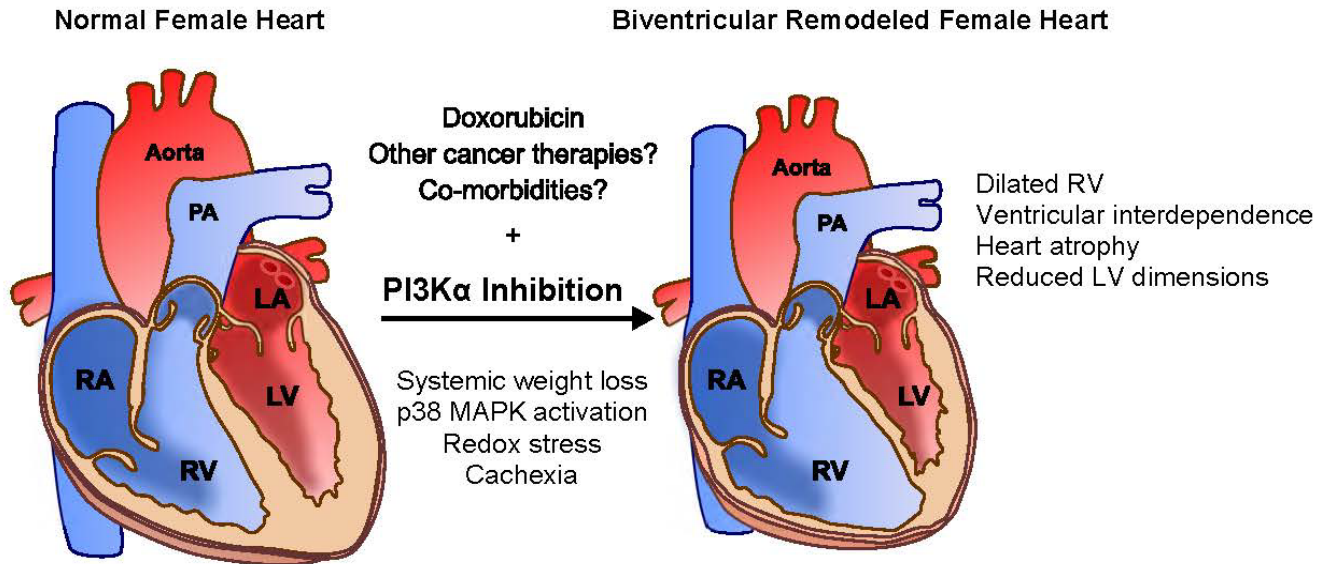


Figure 6.10. Illustration of biventricular cardiotoxicity and remodeling in female mice
 These effects were seen with PI3K α inhibition and doxorubicin therapy, but may apply broadly to PI3K pathway inhibition; other cancer therapies and co-morbidities may also precipitate similar adverse effects when combined with PI3K inhibition. PA, pulmonary artery; RA, right atrium; RV, right ventricle; LA, left atrium; LV, left ventricle.

Sex differences in RV remodeling is also seen in obese women who exhibit right ventricle remodeling with increased end diastolic dimension, which is not present in obese men.²³³ Our findings that PI3K α inhibition contributes to RV dysfunction in a female mouse model should raise concern considering the profile of advanced heart disease cancer patients/survivors as indicated by the INTERMACS registry for patients with LVAD where patients with chemotherapy related cardiomyopathy receiving LVAD were predominantly female and were more likely to require right ventricle assistance.²³⁴ Indeed, in cancer patients, female sex is an independent risk factor for cardiac abnormalities after treatment with doxorubicin in association with a greater decrease in LV mass.²³⁵

We identified that the activation of the p38 MAPK signaling pathway in both LV and RV may underlie our observed phenotype in female hearts with cardiotoxicity. Dox can activate p38 activation in cardiomyocytes through negative modulation of the PI3K pathway and promotion of an atrophy gene program²¹³ and p38 MAPK activation can have a direct negative inotropic effect

at the level of myofilament Ca^{2+} sensitivity.²³⁶ Activation of p38 promotes increased energy expenditure and mitochondrial uncoupling in muscle,²¹⁴ and p38 inhibition has beneficial effects in models of muscle atrophy in tumor bearing cancer cachexia models.^{131, 215} Importantly, in female human hearts with DCM we found that both p38 MAPK activation and redox stress as assessed by DHE staining was increased. To our surprise, FOXO1 signaling, which is implicated in skeletal muscle atrophy and regulated by PI3K signaling,¹²⁰ was not activated in the heart in this study. In cancer patients with tumor types and therapies that place them at a high risk for cachexia, PI3K inhibition may exacerbate and possibly potentiate pathological weight loss, potentially through increased p38 signaling. Importantly, p38 MAPK inhibition may be beneficial for both heart^{216, 217} and cancer treatment.²³⁷

Our study shows that in female preclinical models, PI3K α inhibition and Dox resulted in marked RV dilation and dysfunction in the setting of weight loss and heart atrophy. These changes were linked to increased pathological p38 MAPK activation coupled with redox stress. We suspect that weight loss and adverse heart remodeling will be key safety indicators once PI3K inhibitors are used for extended periods. PI3K inhibition may soon become a mainstay in multi-drug combination cancer therapy; a search for “PI3K” on clinicaltrials.gov yielded 411 studies, and “PI3K+cancer gives” 377 studies, most of which utilize a PI3K inhibitor, often in combination with other therapies. Our current animal study focuses on the PI3K α isoform, although many PI3K inhibitors target multiple PI3K isoforms which are broadly expressed, creating the potential for additional adverse effects. More studies are needed to fully characterize the significance of different PI3K isoform inhibition in combination with other cancer therapies and comorbidities.

7. Final discussion, research impact and future directions

7.1 General comments

As much as we might talk about PI3K signaling as pro-growth or pro-survival, the physiological impact of PI3K signaling in a complex organ system like the heart is highly context dependent. Just as heart disease itself is of heterogeneous origin and presentation, my graduate research has impressed me with the view that alterations in PI3K signaling can be neutral, beneficial or detrimental depending on the context.

7.2 Discussion and impact: ischemia/reperfusion project

I began with the IR project (chapter 3), which we expected to confirm that PI3K α DN expression was dependent on enhanced PI3K γ signaling, which I thought would lead into further studies of the crosstalk between these different PI3K isoforms. However, cross breeding of PI3K α DN and PI3K γ ^{-/-} mice did not abrogate IR protection, forcing us to reject this hypothesis. The large effect size and consistent IR protection now seen in multiple models of reduced myocardial PI3K α has motivated me to continue the search for the underlying mechanism of this phenomenon. A downstream target, rather than PI3K α itself, may be the ideal target for therapeutic intervention that harnesses these protective effects, which is why an understanding of the underlying mechanism is critical.

The most immediate impact of these IR studies may be to challenge the idea of PI3K and Akt signaling as inherently beneficial in the setting of IR. Akt activation is often reported as mechanistic proof of a beneficial effect, even without inhibiting Akt to see if Akt activation is a side effect and not a cause of the process in question. PI3K signaling research may also be affected by the many studies using non-specific inhibitors such as LY294002, which has many off-target effects outside of PI3K.²³⁸ There are over 500 citations in Pubmed for this drug in 2016 alone, despite many highly specific new generation PI3K inhibitors being available to

researchers.¹¹⁸ Focused PI3K research will likely continue to contend with the prevalent conception that PI3K activation is a panacea that ameliorates almost any pathological process.

7.3 Suggestions for future work

Looking again to fundamental mechanisms of IR injury, it is still not clear in PI3K α deficient hearts if damaging processes, such as cytosolic calcium overload, never reach the high levels found in control hearts, or if the cardiomyocyte is better able to withstand and ameliorate these processes. For example, high cytosolic calcium in the first few minutes of reperfusion may cause loss of mitochondrial membrane potential, leading to poor ATP production, which further impairs the removal of cytosolic calcium via ATP dependent pumps (such as SERCA2A). Do PI3K α deficient hearts never sustain sufficiently high cytosolic calcium to cause this vicious cycle, or is there something different about their mitochondria that causes them to remain functional long enough to clear the high cytosolic calcium? This question could be addressed using optical mapping and a calcium sensitive dye such as Fura-2²³⁹ loaded into the heart followed by an IR protocol.

If high cytosolic calcium levels are recorded in PI3K α deficient hearts at the initial moments around reperfusion, it would support the theory that mitochondria are resistant to high cytosolic calcium. I would try to confirm this theory using experiments with isolated mitochondria. The Molkentin lab has shown that Cyp-D knockout mitochondria can sustain repeated calcium challenges before mitochondria integrity is impaired, whereas control mitochondria are quickly compromised.²⁴⁰ I would do similar experiment using mitochondria from PI3K α deficient hearts.

If calcium overload is avoided altogether in PI3K α deficient hearts, then I would trace back the steps that lead to calcium overload, looking for differences compared to control hearts. One hypothesis is that reduced PI3K α affects glycogen metabolism through its role in glucose uptake and regulation of glycogen synthesis/degradation. Upon induction of no-flow ischemia,

glucose is no longer delivered to the heart, and oxygen is no longer available for mitochondrial respiration. Stored glycogen is the available fuel source for uncoupled glycolysis, which is metabolized to lactate.²⁴¹ This acidifying process can then lead to intracellular calcium overload via ion exchange, and intracellular calcium overload then results in loss of mitochondrial membrane potential and necrotic cell death.⁹⁸ This hypothesis would be tested first by measuring glycogen and lactate levels in hearts after baseline aerobic perfusion and then after no-flow ischemia. If glycogen flux and lactate production is reduced, we would then probe for protein levels and activation of key glycogen regulators, including GSK3 β , glycogen synthase and glycogen phosphorylase. This information could then inform how we approached interventions that promoted glycogen flux in PI3K α reduced hearts (expecting loss of IR protection) or reduce glycogen flux in wildtype hearts (expecting improved IR recovery).

Looking further ahead, if a mechanistic understanding of our model is established using perfused hearts, the same processes could be tested in an *in vivo* IR model. If a therapeutic target is identified that recapitulates the reduced PI3K α protection phenotype, and a strategy is found to achieve these effects in wildtype hearts, experiments could be pursued in large animals models of IR and *ex vivo* human heart perfusions such as donor hearts that are found to be unsuitable for transplant. The potential for new therapies to emerge from this work will become clearer when a mechanistic understanding of this IR protection phenotype is better understood. Specifically, if the unknown mechanism can be harnessed at a reperfusion or post reperfusion time point, since many of the IR scenarios found in real-world clinical scenarios do not allow for preconditioning treatment. This would include patients with occluded coronary arteries who will be receiving angioplasty, or donor hearts which have stopped beating and have sustained an ischemic period before being reperfused and transplanted. If a suitable drug target is found based on this research, maybe anyone at risk of an ischemic event could be given medications to keep with them at home, and be told to take a pill anytime they have symptoms of angina and also see a doctor.

7.4 Discussion and impact: heart function project

This project arose as we worked out the protocol for inducible deletion of PI3K α using the tamoxifen/Cre system. The 2009 Circulation paper from Lin¹⁰³ seemed to be ignored by pharmaceutical companies who continued with PI3K inhibitor development as cancer therapies. If PI3K α inhibition really did cause depletion of membrane calcium channels and heart dysfunction, I would expect that this finding would disqualify PI3K α as a safe therapeutic target. The heart phenotype could also be potentially affected by the long exposure to tamoxifen, and indeed, I found that heart dysfunction could be uncoupled from PI3K α deletion with a reduced tamoxifen administration regimen.

I initially submitted these findings for publication at Circulation Research, but was rejected; however, soon after this Circulation Research published an article reporting cardiomyocyte specific deletion of myostatin causing acute heart dysfunction and mortality, again using a very high dose of tamoxifen. Myostatin inhibitors are being tested in clinical trials to reduce pathological muscle wasting. It was hard for me to imagine how this circulating signaling protein could be deleted only in cardiomyocytes, a relatively minor contributor to myostatin expression, with such severe consequences for the heart. Meanwhile, whole body inhibition of myostatin had beneficial effects,²⁴² and genetic deletion of myostatin in cardiomyocytes reduced heart failure associated skeletal muscle loss.²⁴³ I expressed my concern that tamoxifen/Cre toxicity may be contributing to this newly reported myostatin phenotype in a letter to the editor.¹⁰⁷

Despite our findings that PI3K α was dispensable in the hearts of otherwise healthy mice, we know that the target population for PI3K α inhibition, cancer patients, is not a healthy population. We had seen that PI3K α caused increased vulnerability to tamoxifen/Cre toxicity, so we hypothesized that PI3K α inhibition may also predispose the heart to cytotoxic cancer therapies. We investigated the commonly used anthracycline drug doxorubicin. In this context,

we found that PI3K α inhibition promoted loss of heart and body mass. Promotion of atrophy may be the most important adverse effect of PI3K α inhibition in cancer patients, including whole body loss of lean mass and reduced heart mass, to which the RV may be especially vulnerable. Cancer cachexia causes a significant burden for cancer survival as well as quality of life. If PI3K inhibition promotes cachexia symptoms, this is likely to be a significant factor that will limit the application of these drugs in clinical use. I was surprised that I did not detect activation of the FOXO1 or Smad2/3 transcription factors from PI3K α inhibition. These pathways have been closely connected with PI3K α signaling in skeletal muscle models of sarcopenia.²⁴⁴

7.5 Suggestions for future work

There are many directions to pursue for subsequent studies into the effects of PI3K inhibition on the heart. First, electrophysiology effects of PI3K inhibition needs to be better understood. This is being pursued in the Oudit Lab. Second, PI3K inhibition, including isoform specific and pan inhibition, should be applied to numerous models of comorbidities to further establish the risk profile of these drugs in the heart and the body. This would include experiments in tumor bearing animals, obesity, and aged animals.

Considering that numerous PI3K inhibitors are being tested in clinical trials, an ideal scenario for ongoing preclinical investigation would be to design animal experiments that use the strengths of animal work, such as deductive and invasive mechanistic experiments, to explain and predict clinical effects of PI3K inhibition. I would search for clinical groups using the PI3K inhibitors and doing extensive heart imaging, ideally MRI to get reliable heart mass and biventricular volumes. If heart changes were observed, such as reduced heart mass or RV dysfunction, I would try to replicate these conditions in an animal model to investigate the underlying molecular mechanisms. A challenge in this type of clinical research is that heart tissue will not likely be available from these cancer patients, because they are not likely to receive heart surgery or get a heart transplant; therefore, preclinical models will be essential for

understanding molecular mechanisms. Noninvasive assessment of heart and body mass and composition will likely continue to be an important tool to assess atrophy in the heart and body for cancer patients. Also, surgeries that have incidental access and removal of muscle or adipose tissue from these patients will likely be an important source of tissue for research, although molecular mechanisms of atrophy may differ between the heart and skeletal muscle.

References

1. Andjelkovic M, Alessi DR, Meier R, Fernandez A, Lamb NJ, Frech M, Cron P, Cohen P, Lucocq JM and Hemmings BA. Role of translocation in the activation and function of protein kinase B. *The Journal of biological chemistry*. 1997;272:31515-24.
2. Lemmon MA. Membrane recognition by phospholipid-binding domains. *Nature reviews Molecular cell biology*. 2008;9:99-111.
3. Vanhaesebroeck B, Guillermet-Guibert J, Graupera M and Bilanges B. The emerging mechanisms of isoform-specific PI3K signalling. *Nat Rev Mol Cell Biol*. 2010;11:329-41.
4. Shioi T, Kang PM, Douglas PS, Hampe J, Yballe CM, Lawitts J, Cantley LC and Izumo S. The conserved phosphoinositide 3-kinase pathway determines heart size in mice. *EMBO J*. 2000;19:2537-48.
5. Crackower MA, Oudit GY, Kozieradzki I, Sarao R, Sun H, Sasaki T, Hirsch E, Suzuki A, Shioi T, Irie-Sasaki J, Sah R, Cheng HY, Rybin VO, Lembo G, Fratta L, Oliveira-dos-Santos AJ, Benovic JL, Kahn CR, Izumo S, Steinberg SF, Wymann MP, Backx PH and Penninger JM. Regulation of myocardial contractility and cell size by distinct PI3K-PTEN signaling pathways. *Cell*. 2002;110:737-49.
6. McLean BA, Zhabyeyev P, Patel VB, Basu R, Parajuli N, DesAulniers J, Murray AG, Kassiri Z, Vanhaesebroeck B and Oudit GY. PI3Kalpha is essential for the recovery from Cre/tamoxifen cardiotoxicity and in myocardial insulin signalling but is not required for normal myocardial contractility in the adult heart. *Cardiovasc Res*. 2015;105:292-303.
7. Voigt P, Dorner MB and Schaefer M. Characterization of p87PIKAP, a novel regulatory subunit of phosphoinositide 3-kinase gamma that is highly expressed in heart and interacts with PDE3B. *The Journal of biological chemistry*. 2006;281:9977-86.
8. Brock C, Schaefer M, Reusch HP, Czupalla C, Michalke M, Spicher K, Schultz G and Nurnberg B. Roles of G beta gamma in membrane recruitment and activation of p110 gamma/p101 phosphoinositide 3-kinase gamma. *The Journal of cell biology*. 2003;160:89-99.
9. Guillermet-Guibert J, Bjorklof K, Salpekar A, Gonella C, Ramadani F, Bilancio A, Meek S, Smith AJ, Okkenhaug K and Vanhaesebroeck B. The p110beta isoform of phosphoinositide 3-kinase signals downstream of G protein-coupled receptors and is functionally redundant with p110gamma. *Proc Natl Acad Sci U S A*. 2008;105:8292-7.
10. Suire S, Condliffe AM, Ferguson GJ, Ellson CD, Guillou H, Davidson K, Welch H, Coadwell J, Turner M, Chilvers ER, Hawkins PT and Stephens L. Gbetagammias and the Ras binding domain of p110gamma are both important regulators of PI(3)Kgamma signalling in neutrophils. *Nature cell biology*. 2006;8:1303-9.
11. Gupta S, Ramjaun AR, Haiko P, Wang Y, Warne PH, Nicke B, Nye E, Stamp G, Alitalo K and Downward J. Binding of ras to phosphoinositide 3-kinase p110alpha is required for ras-driven tumorigenesis in mice. *Cell*. 2007;129:957-68.

12. Alessi DR, Deak M, Casamayor A, Caudwell FB, Morrice N, Norman DG, Gaffney P, Reese CB, MacDougall CN, Harbison D, Ashworth A and Bownes M. 3-Phosphoinositide-dependent protein kinase-1 (PDK1): structural and functional homology with the Drosophila DSTPK61 kinase. *Current biology : CB*. 1997;7:776-89.
13. Alessi DR, James SR, Downes CP, Holmes AB, Gaffney PR, Reese CB and Cohen P. Characterization of a 3-phosphoinositide-dependent protein kinase which phosphorylates and activates protein kinase Balpha. *Current biology : CB*. 1997;7:261-9.
14. Sarbassov DD, Guertin DA, Ali SM and Sabatini DM. Phosphorylation and regulation of Akt/PKB by the rictor-mTOR complex. *Science*. 2005;307:1098-101.
15. Gan X, Wang J, Su B and Wu D. Evidence for direct activation of mTORC2 kinase activity by phosphatidylinositol 3,4,5-trisphosphate. *The Journal of biological chemistry*. 2011;286:10998-1002.
16. Sano H, Kane S, Sano E, Miinea CP, Asara JM, Lane WS, Garner CW and Lienhard GE. Insulin-stimulated phosphorylation of a Rab GTPase-activating protein regulates GLUT4 translocation. *The Journal of biological chemistry*. 2003;278:14599-602.
17. Rayasam GV, Tulasi VK, Sodhi R, Davis JA and Ray A. Glycogen synthase kinase 3: more than a namesake. *British journal of pharmacology*. 2009;156:885-98.
18. Sugden PH, Fuller SJ, Weiss SC and Clerk A. Glycogen synthase kinase 3 (GSK3) in the heart: a point of integration in hypertrophic signalling and a therapeutic target? A critical analysis. *Br J Pharmacol*. 2008;153 Suppl 1:S137-53.
19. Zhang D, Contu R, Latronico MV, Zhang J, Rizzi R, Catalucci D, Miyamoto S, Huang K, Ceci M, Gu Y, Dalton ND, Peterson KL, Guan KL, Brown JH, Chen J, Sonenberg N and Condorelli G. mTORC1 regulates cardiac function and myocyte survival through 4E-BP1 inhibition in mice. *The Journal of clinical investigation*. 2010;120:2805-16.
20. Sugimoto Y, Whitman M, Cantley LC and Erikson RL. Evidence that the Rous sarcoma virus transforming gene product phosphorylates phosphatidylinositol and diacylglycerol. *Proc Natl Acad Sci U S A*. 1984;81:2117-21.
21. Macara IG, Marinetti GV and Balduzzi PC. Transforming protein of avian sarcoma virus UR2 is associated with phosphatidylinositol kinase activity: possible role in tumorigenesis. *Proc Natl Acad Sci U S A*. 1984;81:2728-32.
22. Ruderman NB, Kapeller R, White MF and Cantley LC. Activation of phosphatidylinositol 3-kinase by insulin. *Proc Natl Acad Sci U S A*. 1990;87:1411-5.
23. Zito CR, Jilaveanu LB, Anagnostou V, Rimm D, Bepler G, Maira SM, Hackl W, Camp R, Kluger HM and Chao HH. Multi-level targeting of the phosphatidylinositol-3-kinase pathway in non-small cell lung cancer cells. *PLoS one*. 2012;7:e31331.
24. Salmena L, Carracedo A and Pandolfi PP. Tenets of PTEN tumor suppression. *Cell*. 2008;133:403-14.

25. Leslie NR and Foti M. Non-genomic loss of PTEN function in cancer: not in my genes. *Trends in pharmacological sciences*. 2011;32:131-40.
26. Zhao L and Vogt PK. Class I PI3K in oncogenic cellular transformation. *Oncogene*. 2008;27:5486-96.
27. Shi J, Yao D, Liu W, Wang N, Lv H, Zhang G, Ji M, Xu L, He N, Shi B and Hou P. Highly frequent PIK3CA amplification is associated with poor prognosis in gastric cancer. *BMC cancer*. 2012;12:50.
28. Philp AJ, Campbell IG, Leet C, Vincan E, Rockman SP, Whitehead RH, Thomas RJ and Phillips WA. The phosphatidylinositol 3'-kinase p85alpha gene is an oncogene in human ovarian and colon tumors. *Cancer research*. 2001;61:7426-9.
29. Courtney KD, Corcoran RB and Engelman JA. The PI3K pathway as drug target in human cancer. *Journal of clinical oncology : official journal of the American Society of Clinical Oncology*. 2010;28:1075-83.
30. Foukas LC, Claret M, Pearce W, Okkenhaug K, Meek S, Peskett E, Sancho S, Smith AJ, Withers DJ and Vanhaesebroeck B. Critical role for the p110alpha phosphoinositide-3-OH kinase in growth and metabolic regulation. *Nature*. 2006;441:366-70.
31. Liu P, Cheng H, Roberts TM and Zhao JJ. Targeting the phosphoinositide 3-kinase pathway in cancer. *Nature reviews Drug discovery*. 2009;8:627-44.
32. Baselga J. Targeting the phosphoinositide-3 (PI3) kinase pathway in breast cancer. *The oncologist*. 2011;16 Suppl 1:12-9.
33. Whelan RS, Kaplinskiy V and Kitsis RN. Cell death in the pathogenesis of heart disease: mechanisms and significance. *Annual review of physiology*. 2010;72:19-44.
34. Miled N, Yan Y, Hon WC, Perisic O, Zvebil M, Inbar Y, Schneidman-Duhovny D, Wolfson HJ, Backer JM and Williams RL. Mechanism of two classes of cancer mutations in the phosphoinositide 3-kinase catalytic subunit. *Science*. 2007;317:239-42.
35. Mandelker D, Gabelli SB, Schmidt-Kittler O, Zhu J, Cheong I, Huang CH, Kinzler KW, Vogelstein B and Amzel LM. A frequent kinase domain mutation that changes the interaction between PI3Kalpha and the membrane. *Proceedings of the National Academy of Sciences of the United States of America*. 2009;106:16996-7001.
36. Vadas O, Burke JE, Zhang X, Berndt A and Williams RL. Structural basis for activation and inhibition of class I phosphoinositide 3-kinases. *Science signaling*. 2011;4:re2.
37. Kalinsky K, Jacks LM, Heguy A, Patil S, Drobnjak M, Bhanot UK, Hedvat CV, Traina TA, Solit D, Gerald W and Moynahan ME. PIK3CA mutation associates with improved outcome in breast cancer. *Clinical cancer research : an official journal of the American Association for Cancer Research*. 2009;15:5049-59.
38. Wang L, Zhang Q, Zhang J, Sun S, Guo H, Jia Z, Wang B, Shao Z, Wang Z and Hu X. PI3K pathway activation results in low efficacy of both trastuzumab and lapatinib. *BMC cancer*. 2011;11:11:248.

39. Ciruolo E, Iezzi M, Marone R, Marengo S, Curcio C, Costa C, Azzolino O, Gonella C, Rubinetto C, Wu H, Dastru W, Martin EL, Silengo L, Altruda F, Turco E, Lanzetti L, Musiani P, Ruckle T, Rommel C, Backer JM, Forni G, Wymann MP and Hirsch E. Phosphoinositide 3-kinase p110beta activity: key role in metabolism and mammary gland cancer but not development. *Science signaling*. 2008;1:ra3.
40. Jia S, Liu Z, Zhang S, Liu P, Zhang L, Lee SH, Zhang J, Signoretti S, Loda M, Roberts TM and Zhao JJ. Essential roles of PI(3)K-p110beta in cell growth, metabolism and tumorigenesis. *Nature*. 2008;454:776-9.
41. Jiang X, Chen S, Asara JM and Balk SP. Phosphoinositide 3-kinase pathway activation in phosphate and tensin homolog (PTEN)-deficient prostate cancer cells is independent of receptor tyrosine kinases and mediated by the p110beta and p110delta catalytic subunits. *The Journal of biological chemistry*. 2010;285:14980-9.
42. Genetech. A Dose Escalation Study Evaluating the Safety and Tolerability of GDC-0032 in Patients With Locally Advanced or Metastatic Solid Tumors And in Combination With Endocrine Therapy in Patients With Locally Advanced or Metastatic Hormone Receptor-Positive Breast Cancer. 2011:NCT01296555.
43. Pharmaceuticals N. A Study of BYL719 in Adult Patients With Advanced Solid Malignancies. 2011:NCT01387321.
44. Folkes AJ, Ahmadi K, Alderton WK, Alix S, Baker SJ, Box G, Chuckowree IS, Clarke PA, Depledge P, Eccles SA, Friedman LS, Hayes A, Hancox TC, Kugendradas A, Lensun L, Moore P, Olivero AG, Pang J, Patel S, Pergl-Wilson GH, Raynaud FI, Robson A, Saghir N, Salphati L, Sohal S, Ultsch MH, Valenti M, Wallweber HJ, Wan NC, Wiesmann C, Workman P, Zhyvoloup A, Zvelebil MJ and Shuttleworth SJ. The identification of 2-(1H-indazol-4-yl)-6-(4-methanesulfonyl-piperazin-1-ylmethyl)-4-morpholin-4-yl-thieno[3,2-d]pyrimidine (GDC-0941) as a potent, selective, orally bioavailable inhibitor of class I PI3 kinase for the treatment of cancer. *Journal of medicinal chemistry*. 2008;51:5522-32.
45. Raynaud FI, Eccles SA, Patel S, Alix S, Box G, Chuckowree I, Folkes A, Gowan S, De Haven Brandon A, Di Stefano F, Hayes A, Henley AT, Lensun L, Pergl-Wilson G, Robson A, Saghir N, Zhyvoloup A, McDonald E, Sheldrake P, Shuttleworth S, Valenti M, Wan NC, Clarke PA and Workman P. Biological properties of potent inhibitors of class I phosphatidylinositide 3-kinases: from PI-103 through PI-540, PI-620 to the oral agent GDC-0941. *Molecular cancer therapeutics*. 2009;8:1725-38.
46. Maira SM, Pecchi S, Huang A, Burger M, Knapp M, Sterker D, Schnell C, Guthy D, Nagel T, Wiesmann M, Brachmann SM, Fritsch C, Dorsch M, Chene P, Shoemaker K, De Pover A, Menezes D, Martiny-Baron G, Fabbro D, Wilson C, Schlegel R, Hofmann F, Garcia-Echeverria C, Sellers WR and Voliva CF. Identification and characterization of NVP-BKM120, an orally available pan class I PI3-Kinase inhibitor. *Molecular cancer therapeutics*. 2011.
47. Koul D, Fu J, Shen R, Lafortune TA, Wang S, Tiao N, Kim YW, Liu JL, Ramnarian D, Yuan Y, Garcia-Echeverria C, Maira SM and Yung WK. Antitumor Activity of NVP-BKM120--A Selective Pan Class I PI3 Kinase Inhibitor Showed Differential Forms of Cell Death Based on p53 Status of Glioma Cells. *Clinical cancer research : an official journal of the American Association for Cancer Research*. 2011.

48. Ihle NT, Williams R, Chow S, Chew W, Berggren MI, Paine-Murrieta G, Minion DJ, Halter RJ, Wipf P, Abraham R, Kirkpatrick L and Powis G. Molecular pharmacology and antitumor activity of PX-866, a novel inhibitor of phosphoinositide-3-kinase signaling. *Molecular cancer therapeutics*. 2004;3:763-72.
49. Chakrabarty A, Sanchez V, Kuba MG, Rinehart C and Arteaga CL. Feedback upregulation of HER3 (ErbB3) expression and activity attenuates antitumor effect of PI3K inhibitors. *Proceedings of the National Academy of Sciences of the United States of America*. 2011.
50. Kong D and Yamori T. ZSTK474 is an ATP-competitive inhibitor of class I phosphatidylinositol 3 kinase isoforms. *Cancer science*. 2007;98:1638-42.
51. Maira SM, Stauffer F, Brueggen J, Furet P, Schnell C, Fritsch C, Brachmann S, Chene P, De Pover A, Schoemaker K, Fabbro D, Gabriel D, Simonen M, Murphy L, Finan P, Sellers W and Garcia-Echeverria C. Identification and characterization of NVP-BE2235, a new orally available dual phosphatidylinositol 3-kinase/mammalian target of rapamycin inhibitor with potent in vivo antitumor activity. *Molecular cancer therapeutics*. 2008;7:1851-63.
52. Roulin D, Waselle L, Dormond-Meuwly A, Dufour M, Demartines N and Dormond O. Targeting renal cell carcinoma with NVP-BE2235, a dual PI3K/mTOR inhibitor, in combination with sorafenib. *Molecular cancer*. 2011;10:90.
53. Prasad G, Sottero T, Yang X, Mueller S, James CD, Weiss WA, Polley MY, Ozawa T, Berger MS, Aftab DT, Prados MD and Haas-Kogan DA. Inhibition of PI3K/mTOR pathways in glioblastoma and implications for combination therapy with temozolomide. *Neuro-oncology*. 2011;13:384-92.
54. Mirzoeva OK, Hann B, Hom YK, Debnath J, Aftab D, Shokat K and Korn WM. Autophagy suppression promotes apoptotic cell death in response to inhibition of the PI3K-mTOR pathway in pancreatic adenocarcinoma. *J Mol Med (Berl)*. 2011;89:877-89.
55. Ozbay T, Durden DL, Liu T, O'Regan RM and Nahta R. In vitro evaluation of pan-PI3-kinase inhibitor SF1126 in trastuzumab-sensitive and trastuzumab-resistant HER2-over-expressing breast cancer cells. *Cancer chemotherapy and pharmacology*. 2010;65:697-706.
56. Garlich JR, De P, Dey N, Su JD, Peng X, Miller A, Murali R, Lu Y, Mills GB, Kundra V, Shu HK, Peng Q and Durden DL. A vascular targeted pan phosphoinositide 3-kinase inhibitor prodrug, SF1126, with antitumor and antiangiogenic activity. *Cancer research*. 2008;68:206-15.
57. Sutherlin DP, Bao L, Berry M, Castanedo G, Chuckowree I, Dotson J, Folks A, Friedman L, Goldsmith R, Gunzner J, Heffron T, Lesnick J, Lewis C, Mathieu S, Murray J, Nonomiya J, Pang J, Pegg N, Prior WW, Rouge L, Salphati L, Sampath D, Tian Q, Tsui V, Wan NC, Wang S, Wei B, Wiesmann C, Wu P, Zhu BY and Olivero A. Discovery of a potent, selective, and orally available class I phosphatidylinositol 3-kinase (PI3K)/mammalian target of rapamycin (mTOR) kinase inhibitor (GDC-0980) for the treatment of cancer. *Journal of medicinal chemistry*. 2011;54:7579-87.
58. Wallin JJ, Edgar KA, Guan J, Berry M, Prior WW, Lee L, Lesnick JD, Lewis C, Nonomiya J, Pang J, Salphati L, Olivero AG, Sutherlin DP, O'Brien C, Spoerke JM, Patel S, Lensun L, Kassees R, Ross L, Lackner MR, Sampath D, Belvin M and Friedman LS. GDC-0980 is a novel

class I PI3K/mTOR kinase inhibitor with robust activity in cancer models driven by the PI3K pathway. *Molecular cancer therapeutics*. 2011;10:2426-36.

59. Chang KY, Tsai SY, Wu CM, Yen CJ, Chuang BF and Chang JY. Novel phosphoinositide 3-kinase/mTOR dual inhibitor, NVP-BGT226, displays potent growth-inhibitory activity against human head and neck cancer cells in vitro and in vivo. *Clinical cancer research : an official journal of the American Association for Cancer Research*. 2011;17:7116-26.

60. Venkatesan AM, Dehnhardt CM, Delos Santos E, Chen Z, Dos Santos O, Ayrál-Kaloustian S, Khafizova G, Brooijmans N, Mallon R, Hollander I, Feldberg L, Lucas J, Yu K, Gibbons J, Abraham RT, Chaudhary I and Mansour TS. Bis(morpholino-1,3,5-triazine) derivatives: potent adenosine 5'-triphosphate competitive phosphatidylinositol-3-kinase/mammalian target of rapamycin inhibitors: discovery of compound 26 (PKI-587), a highly efficacious dual inhibitor. *Journal of medicinal chemistry*. 2010;53:2636-45.

61. Noble ME, Endicott JA and Johnson LN. Protein kinase inhibitors: insights into drug design from structure. *Science*. 2004;303:1800-5.

62. Folkes AJ, Ahmadi K, Alderton WK, Alix S, Baker SJ, Box G, Chuckowree IS, Clarke PA, Depledge P, Eccles SA, Friedman LS, Hayes A, Hancox TC, Kugendradas A, Lensun L, Moore P, Olivero AG, Pang J, Patel S, Pergl-Wilson GH, Raynaud FI, Robson A, Saghir N, Salphati L, Sohal S, Ultsch MH, Valenti M, Wallweber HJ, Wan NC, Wiesmann C, Workman P, Zhyvoloup A, Zvelebil MJ and Shuttleworth SJ. The identification of 2-(1H-indazol-4-yl)-6-(4-methanesulfonyl-piperazin-1-ylmethyl)-4-morpholin-4-yl-t hieno[3,2-d]pyrimidine (GDC-0941) as a potent, selective, orally bioavailable inhibitor of class I PI3 kinase for the treatment of cancer. *Journal of medicinal chemistry*. 2008;51:5522-32.

63. Furet P, Guagnano V, Fairhurst RA, Imbach-Weese P, Bruce I, Knapp M, Fritsch C, Blasco F, Blanz J, Aichholz R, Hamon J, Fabbro D and Caravatti G. Discovery of NVP-BYL719 a potent and selective phosphatidylinositol-3 kinase alpha inhibitor selected for clinical evaluation. *Bioorg Med Chem Lett*. 2013;23:3741-8.

64. Weeks KL, Gao X, Du XJ, Boey EJ, Matsumoto A, Bernardo BC, Kiriazis H, Cemerlang N, Tan JW, Tham YK, Franke TF, Qian H, Bogoyevitch MA, Woodcock EA, Febbraio MA, Gregorevic P and McMullen JR. Phosphoinositide 3-kinase p110alpha is a master regulator of exercise-induced cardioprotection and PI3K gene therapy rescues cardiac dysfunction. *Circ Heart Fail*. 2012;5:523-34.

65. McMullen JR, Shioi T, Zhang L, Tarnavski O, Sherwood MC, Kang PM and Izumo S. Phosphoinositide 3-kinase(p110alpha) plays a critical role for the induction of physiological, but not pathological, cardiac hypertrophy. *Proc Natl Acad Sci U S A*. 2003;100:12355-60.

66. Kehat I and Molkentin JD. Molecular pathways underlying cardiac remodeling during pathophysiological stimulation. *Circulation*. 2010;122:2727-35.

67. Shah S, Nelson CP, Gaunt TR, van der Harst P, Barnes T, Braund PS, Lawlor DA, Casas JP, Padmanabhan S, Drenos F, Kivimaki M, Talmud PJ, Humphries SE, Whittaker J, Morris RW, Whincup PH, Dominiczak A, Munroe PB, Johnson T, Goodall AH, Cambien F, Diemert P, Hengstenberg C, Ouwehand WH, Felix JF, Glazer NL, Tomaszewski M, Burton PR, Tobin MD, van Veldhuisen DJ, de Boer RA, Navis G, van Gilst WH, Mayosi BM, Thompson JR, Kumari M, MacFarlane PW, Day IN, Hingorani AD and Samani NJ. Four genetic loci influencing

electrocardiographic indices of left ventricular hypertrophy. *Circulation Cardiovascular genetics*. 2011;4:626-35.

68. McMullen JR, Shioi T, Huang WY, Zhang L, Tarnavski O, Bisping E, Schinke M, Kong S, Sherwood MC, Brown J, Riggi L, Kang PM and Izumo S. The insulin-like growth factor 1 receptor induces physiological heart growth via the phosphoinositide 3-kinase(p110alpha) pathway. *The Journal of biological chemistry*. 2004;279:4782-93.

69. Jankowska EA, Biel B, Majda J, Szklarska A, Lopuszanska M, Medras M, Anker SD, Banasiak W, Poole-Wilson PA and Ponikowski P. Anabolic deficiency in men with chronic heart failure: prevalence and detrimental impact on survival. *Circulation*. 2006;114:1829-37.

70. McMullen JR and Izumo S. Role of the insulin-like growth factor 1 (IGF1)/phosphoinositide-3-kinase (PI3K) pathway mediating physiological cardiac hypertrophy. *Novartis Foundation symposium*. 2006;274:90-111; discussion 111-7, 152-5, 272-6.

71. Luo J, McMullen JR, Sobkiw CL, Zhang L, Dorfman AL, Sherwood MC, Logsdon MN, Horner JW, DePinho RA, Izumo S and Cantley LC. Class IA phosphoinositide 3-kinase regulates heart size and physiological cardiac hypertrophy. *Molecular and cellular biology*. 2005;25:9491-502.

72. Tseng YT, Yano N, Rojan A, Stabila JP, McGonnigal BG, Ianus V, Wadhawan R and Padbury JF. Ontogeny of phosphoinositide 3-kinase signaling in developing heart: effect of acute beta-adrenergic stimulation. *American journal of physiology Heart and circulatory physiology*. 2005;289:H1834-42.

73. Yang KC, Jay PY, McMullen JR and Nerbonne JM. Enhanced cardiac PI3Kalpha signalling mitigates arrhythmogenic electrical remodelling in pathological hypertrophy and heart failure. *Cardiovascular research*. 2011.

74. Inuzuka Y, Okuda J, Kawashima T, Kato T, Niizuma S, Tamaki Y, Iwanaga Y, Yoshida Y, Kosugi R, Watanabe-Maeda K, Machida Y, Tsuji S, Aburatani H, Izumi T, Kita T and Shioi T. Suppression of phosphoinositide 3-kinase prevents cardiac aging in mice. *Circulation*. 2009;120:1695-703.

75. O'Neill BT, Kim J, Wende AR, Theobald HA, Tuinei J, Buchanan J, Guo A, Zaha VG, Davis DK, Schell JC, Boudina S, Wayment B, Litwin SE, Shioi T, Izumo S, Birnbaum MJ and Abel ED. A conserved role for phosphatidylinositol 3-kinase but not Akt signaling in mitochondrial adaptations that accompany physiological cardiac hypertrophy. *Cell Metab*. 2007;6:294-306.

76. Salazar NC, Chen J and Rockman HA. Cardiac GPCRs: GPCR signaling in healthy and failing hearts. *Biochimica et biophysica acta*. 2007;1768:1006-18.

77. Das S, Aiba T, Rosenberg M, Hessler K, Xiao C, Quintero PA, Ottaviano FG, Knight AC, Graham EL, Bostrom P, Morissette MR, Del Monte F, Begley MJ, Cantley LC, Ellinor PT, Tomaselli GF and Rosenzweig A. Pathological role of serum- and glucocorticoid-regulated kinase 1 in adverse ventricular remodeling. *Circulation*. 2012;126:2208-19.

78. Oudit GY, Crackower MA, Eriksson U, Sarao R, Kozieradzki I, Sasaki T, Irie-Sasaki J, Gidrewicz D, Rybin VO, Wada T, Steinberg SF, Backx PH and Penninger JM. Phosphoinositide

3-kinase gamma-deficient mice are protected from isoproterenol-induced heart failure. *Circulation*. 2003;108:2147-52.

79. Hirsch E, Katanaev VL, Garlanda C, Azzolino O, Pirola L, Silengo L, Sozzani S, Mantovani A, Altruda F and Wymann MP. Central role for G protein-coupled phosphoinositide 3-kinase gamma in inflammation. *Science*. 2000;287:1049-53.

80. Chang JD, Sukhova GK, Libby P, Schwartz E, Lichtenstein AH, Field SJ, Kennedy C, Madhavarapu S, Luo J, Wu D and Cantley LC. Deletion of the phosphoinositide 3-kinase p110gamma gene attenuates murine atherosclerosis. *Proceedings of the National Academy of Sciences of the United States of America*. 2007;104:8077-82.

81. Perino A, Ghigo A, Ferrero E, Morello F, Santulli G, Baillie GS, Damilano F, Dunlop AJ, Pawson C, Walser R, Levi R, Altruda F, Silengo L, Langeberg LK, Neubauer G, Heymans S, Lembo G, Wymann MP, Wetzker R, Houslay MD, Iaccarino G, Scott JD and Hirsch E. Integrating cardiac PIP3 and cAMP signaling through a PKA anchoring function of p110gamma. *Molecular cell*. 2011;42:84-95.

82. Kerfant BG, Zhao D, Lorenzen-Schmidt I, Wilson LS, Cai S, Chen SR, Maurice DH and Backx PH. PI3Kgamma is required for PDE4, not PDE3, activity in subcellular microdomains containing the sarcoplasmic reticular calcium ATPase in cardiomyocytes. *Circ Res*. 2007;101:400-8.

83. Siragusa M, Katare R, Meloni M, Damilano F, Hirsch E, Emanuelli C and Madeddu P. Involvement of phosphoinositide 3-kinase gamma in angiogenesis and healing of experimental myocardial infarction in mice. *Circulation research*. 2010;106:757-68.

84. Guo D, Kassiri Z, Basu R, Chow FL, Kandalam V, Damilano F, Liang W, Izumo S, Hirsch E, Penninger JM, Backx PH and Oudit GY. Loss of PI3Kgamma enhances cAMP-dependent MMP remodeling of the myocardial N-cadherin adhesion complexes and extracellular matrix in response to early biomechanical stress. *Circ Res*. 2010;107:1275-89.

85. Haubner BJ, Neely GG, Voelkl JG, Damilano F, Kuba K, Imai Y, Komnenovic V, Mayr A, Pachinger O, Hirsch E, Penninger JM and Metzler B. PI3Kgamma protects from myocardial ischemia and reperfusion injury through a kinase-independent pathway. *PLoS One*. 2010;5:e9350.

86. Hollander MC, Blumenthal GM and Dennis PA. PTEN loss in the continuum of common cancers, rare syndromes and mouse models. *Nature reviews Cancer*. 2011;11:289-301.

87. Oudit GY, Kassiri Z, Zhou J, Liu QC, Liu PP, Backx PH, Dawood F, Crackower MA, Scholey JW and Penninger JM. Loss of PTEN attenuates the development of pathological hypertrophy and heart failure in response to biomechanical stress. *Cardiovasc Res*. 2008;78:505-14.

88. Ruan H, Li J, Ren S, Gao J, Li G, Kim R, Wu H and Wang Y. Inducible and cardiac specific PTEN inactivation protects ischemia/reperfusion injury. *Journal of molecular and cellular cardiology*. 2009;46:193-200.

89. Dyson JM, Fedele CG, Davies EM, Becanovic J and Mitchell CA. Phosphoinositide phosphatases: just as important as the kinases. *Sub-cellular biochemistry*. 2012;58:215-79.

90. Yellon DM and Hausenloy DJ. Myocardial reperfusion injury. *N Engl J Med*. 2007;357:1121-35.
91. Sutton MG and Sharpe N. Left ventricular remodeling after myocardial infarction: pathophysiology and therapy. *Circulation*. 2000;101:2981-8.
92. Heusch G. Molecular basis of cardioprotection: signal transduction in ischemic pre-, post-, and remote conditioning. *Circ Res*. 2015;116:674-99.
93. Hausenloy DJ, Tsang A and Yellon DM. The reperfusion injury salvage kinase pathway: a common target for both ischemic preconditioning and postconditioning. *Trends Cardiovasc Med*. 2005;15:69-75.
94. Mehta SR, Yusuf S, Diaz R, Zhu J, Pais P, Xavier D, Paolasso E, Ahmed R, Xie C, Kazmi K, Tai J, Orlandini A, Pogue J, Liu L and Investigators C-ETG. Effect of glucose-insulin-potassium infusion on mortality in patients with acute ST-segment elevation myocardial infarction: the CREATE-ECLA randomized controlled trial. *JAMA*. 2005;293:437-46.
95. Cung TT, Morel O, Cayla G, Rioufol G, Garcia-Dorado D, Angoulvant D, Bonnefoy-Cudraz E, Guerin P, Elbaz M, Delarche N, Coste P, Vanzetto G, Metge M, Aupetit JF, Jouve B, Motreff P, Tron C, Labeque JN, Steg PG, Cottin Y, Range G, Clerc J, Claeys MJ, Coussement P, Prunier F, Moulin F, Roth O, Belle L, Dubois P, Barragan P, Gilard M, Piot C, Colin P, De Poli F, Morice MC, Ider O, Dubois-Rande JL, Untersee T, Le Breton H, Beard T, Blanchard D, Grollier G, Malquarti V, Staat P, Sudre A, Elmer E, Hansson MJ, Bergerot C, Boussaha I, Jossan C, Derumeaux G, Mewton N and Ovize M. Cyclosporine before PCI in Patients with Acute Myocardial Infarction. *N Engl J Med*. 2015;373:1021-31.
96. Ban K, Cooper AJ, Samuel S, Bhatti A, Patel M, Izumo S, Penninger JM, Backx PH, Oudit GY and Tsushima RG. Phosphatidylinositol 3-kinase gamma is a critical mediator of myocardial ischemic and adenosine-mediated preconditioning. *Circ Res*. 2008;103:643-53.
97. Vanden Berghe T, Linkermann A, Jouan-Lanhouet S, Walczak H and Vandenabeele P. Regulated necrosis: the expanding network of non-apoptotic cell death pathways. *Nat Rev Mol Cell Biol*. 2014;15:135-47.
98. Karch J and Molkentin JD. Regulated necrotic cell death: the passive aggressive side of Bax and Bak. *Circ Res*. 2015;116:1800-9.
99. Wang JX, Zhang XJ, Li Q, Wang K, Wang Y, Jiao JQ, Feng C, Teng S, Zhou LY, Gong Y, Zhou ZX, Liu J, Wang JL and Li PF. MicroRNA-103/107 Regulate Programmed Necrosis and Myocardial Ischemia/Reperfusion Injury Through Targeting FADD. *Circ Res*. 2015;117:352-63.
100. Oerlemans MI, Liu J, Arslan F, den Ouden K, van Middelaar BJ, Doevendans PA and Sluijter JP. Inhibition of RIP1-dependent necrosis prevents adverse cardiac remodeling after myocardial ischemia-reperfusion in vivo. *Basic Res Cardiol*. 2012;107:270.
101. Zhang T, Zhang Y, Cui M, Jin L, Wang Y, Lv F, Liu Y, Zheng W, Shang H, Zhang J, Zhang M, Wu H, Guo J, Zhang X, Hu X, Cao CM and Xiao RP. CaMKII is a RIP3 substrate mediating ischemia- and oxidative stress-induced myocardial necroptosis. *Nat Med*. 2016;22:175-82.

102. Luedde M, Lutz M, Carter N, Sosna J, Jacoby C, Vucur M, Gautheron J, Roderburg C, Borg N, Reisinger F, Hippe HJ, Linkermann A, Wolf MJ, Rose-John S, Lullmann-Rauch R, Adam D, Fogel U, Heikenwalder M, Luedde T and Frey N. RIP3, a kinase promoting necroptotic cell death, mediates adverse remodelling after myocardial infarction. *Cardiovasc Res.* 2014;103:206-16.
103. Lu Z, Jiang YP, Wang W, Xu XH, Mathias RT, Entcheva E, Ballou LM, Cohen IS and Lin RZ. Loss of cardiac phosphoinositide 3-kinase p110 alpha results in contractile dysfunction. *Circulation.* 2009;120:318-25.
104. Bersell K, Choudhury S, Mollova M, Polizzotti BD, Ganapathy B, Walsh S, Wadugu B, Arab S and Kuhn B. Moderate and high amounts of tamoxifen in alphaMHC-MerCreMer mice induce a DNA damage response, leading to heart failure and death. *Disease models & mechanisms.* 2013;6:1459-69.
105. Koitabashi N, Bedja D, Zaiman AL, Pinto YM, Zhang M, Gabrielson KL, Takimoto E and Kass DA. Avoidance of transient cardiomyopathy in cardiomyocyte-targeted tamoxifen-induced MerCreMer gene deletion models. *Circ Res.* 2009;105:12-5.
106. Hougen K, Aronsen JM, Stokke MK, Enger U, Nygard S, Andersson KB, Christensen G, Sejersted OM and Sjaastad I. Cre-loxP DNA recombination is possible with only minimal unspecific transcriptional changes and without cardiomyopathy in Tg(alphaMHC-MerCreMer) mice. *American journal of physiology Heart and circulatory physiology.* 2010;299:H1671-8.
107. McLean BA and Oudit GY. Letter by McLean and Oudit regarding article, "myostatin regulates energy homeostasis in the heart and prevents heart failure". *Circ Res.* 2015;116:e51-2.
108. Romond EH, Perez EA, Bryant J, Suman VJ, Geyer CE, Jr., Davidson NE, Tan-Chiu E, Martino S, Paik S, Kaufman PA, Swain SM, Pisansky TM, Fehrenbacher L, Kutteh LA, Vogel VG, Visscher DW, Yothers G, Jenkins RB, Brown AM, Dakhil SR, Mamounas EP, Lingle WL, Klein PM, Ingle JN and Wolmark N. Trastuzumab plus adjuvant chemotherapy for operable HER2-positive breast cancer. *N Engl J Med.* 2005;353:1673-84.
109. Yeh ET, Tong AT, Lenihan DJ, Yusuf SW, Swafford J, Champion C, Durand JB, Gibbs H, Zafarmand AA and Ewer MS. Cardiovascular complications of cancer therapy: diagnosis, pathogenesis, and management. *Circulation.* 2004;109:3122-31.
110. Cardinale D, Colombo A, Bacchiani G, Tedeschi I, Meroni CA, Veglia F, Civelli M, Lamantia G, Colombo N, Curigliano G, Fiorentini C and Cipolla CM. Early detection of anthracycline cardiotoxicity and improvement with heart failure therapy. *Circulation.* 2015;131:1981-8.
111. Ky B, Vejpongsa P, Yeh ET, Force T and Moslehi JJ. Emerging paradigms in cardiomyopathies associated with cancer therapies. *Circulation research.* 2013;113:754-64.
112. Piccart-Gebhart MJ, Procter M, Leyland-Jones B, Goldhirsch A, Untch M, Smith I, Gianni L, Baselga J, Bell R, Jackisch C, Cameron D, Dowsett M, Barrios CH, Steger G, Huang CS, Andersson M, Inbar M, Lichinitser M, Lang I, Nitz U, Iwata H, Thomssen C, Lohrisch C, Suter TM, Ruschoff J, Suto T, Greatorex V, Ward C, Straehle C, McFadden E, Dolci MS, Gelber RD

and Herceptin Adjuvant Trial Study T. Trastuzumab after adjuvant chemotherapy in HER2-positive breast cancer. *N Engl J Med*. 2005;353:1659-72.

113. Bellinger AM, Arteaga CL, Force T, Humphreys BD, Demetri GD, Druker BJ and Moslehi JJ. Cardio-Oncology: How New Targeted Cancer Therapies and Precision Medicine Can Inform Cardiovascular Discovery. *Circulation*. 2015;132:2248-58.

114. Lui VW, Hedberg ML, Li H, Vangara BS, Pendleton K, Zeng Y, Lu Y, Zhang Q, Du Y, Gilbert BR, Freilino M, Sauerwein S, Peyser ND, Xiao D, Diergaarde B, Wang L, Chiosea S, Seethala R, Johnson JT, Kim S, Duvvuri U, Ferris RL, Romkes M, Nukui T, Kwok-Shing Ng P, Garraway LA, Hammerman PS, Mills GB and Grandis JR. Frequent mutation of the PI3K pathway in head and neck cancer defines predictive biomarkers. *Cancer Discov*. 2013;3:761-9.

115. Cancer Genome Atlas N. Comprehensive molecular portraits of human breast tumours. *Nature*. 2012;490:61-70.

116. Rexer BN and Arteaga CL. Optimal targeting of HER2-PI3K signaling in breast cancer: mechanistic insights and clinical implications. *Cancer Res*. 2013;73:3817-20.

117. Mayer IA, Abramson V, Formisano L, Balko JM, Estrada MV, Sanders M, Juric D, Solit D, Berger MF, Won H, Li Y, Cantley LC, Winer EP and Arteaga CL. A Phase Ib Study of Alpelisib (BYL719), a PI3K α -specific Inhibitor, with Letrozole in ER+/HER2-Negative Metastatic Breast Cancer. *Clin Cancer Res*. 2016.

118. McLean BA, Zhabyeyev P, Pituskin E, Paterson I, Haykowsky MJ and Oudit GY. PI3K inhibitors as novel cancer therapies: implications for cardiovascular medicine. *J Card Fail*. 2013;19:268-82.

119. Okkenhaug K, Graupera M and Vanhaesebroeck B. Targeting PI3K in Cancer: Impact on Tumor Cells, Their Protective Stroma, Angiogenesis, and Immunotherapy. *Cancer Discov*. 2016;6:1090-1105.

120. Glass DJ. PI3 kinase regulation of skeletal muscle hypertrophy and atrophy. *Curr Top Microbiol Immunol*. 2010;346:267-78.

121. Kumar NT, Liestol K, Loberg EM, Reims HM and Maehlen J. Postmortem heart weight: relation to body size and effects of cardiovascular disease and cancer. *Cardiovasc Pathol*. 2014;23:5-11.

122. Groarke JD, Cheng S and Moslehi J. Cancer-drug discovery and cardiovascular surveillance. *N Engl J Med*. 2013;369:1779-81.

123. Wenger NK. Women and coronary heart disease: a century after Herrick: understudied, underdiagnosed, and undertreated. *Circulation*. 2012;126:604-11.

124. Mosca L, Barrett-Connor E and Wenger NK. Sex/gender differences in cardiovascular disease prevention: what a difference a decade makes. *Circulation*. 2011;124:2145-54.

125. Middleman E, Luce J and Frei E, 3rd. Clinical trials with adriamycin. *Cancer*. 1971;28:844-50.

126. Sasaki T, Irie-Sasaki J, Jones RG, Oliveira-dos-Santos AJ, Stanford WL, Bolon B, Wakeham A, Itie A, Bouchard D, Kozieradzki I, Joza N, Mak TW, Ohashi PS, Suzuki A and Penninger JM. Function of PI3Kgamma in thymocyte development, T cell activation, and neutrophil migration. *Science*. 2000;287:1040-6.
127. Graupera M, Guillermet-Guibert J, Foukas LC, Phng LK, Cain RJ, Salpekar A, Pearce W, Meek S, Millan J, Cutillas PR, Smith AJ, Ridley AJ, Ruhrberg C, Gerhardt H and Vanhaesebroeck B. Angiogenesis selectively requires the p110alpha isoform of PI3K to control endothelial cell migration. *Nature*. 2008;453:662-6.
128. Young CD, Pfefferle AD, Owens P, Kuba MG, Rexer BN, Balko JM, Sanchez V, Cheng H, Perou CM, Zhao JJ, Cook RS and Arteaga CL. Conditional loss of ErbB3 delays mammary gland hyperplasia induced by mutant PIK3CA without affecting mammary tumor latency, gene expression, or signaling. *Cancer Res*. 2013;73:4075-85.
129. Pei Y, Moore CE, Wang J, Tewari AK, Eroshkin A, Cho YJ, Witt H, Korshunov A, Read TA, Sun JL, Schmitt EM, Miller CR, Buckley AF, McLendon RE, Westbrook TF, Northcott PA, Taylor MD, Pfister SM, Febbo PG and Wechsler-Reya RJ. An animal model of MYC-driven medulloblastoma. *Cancer cell*. 2012;21:155-67.
130. Juvekar A, Hu H, Yadegarynia S, Lyssiotis CA, Ullas S, Lien EC, Bellinger G, Son J, Hok RC, Seth P, Daly MB, Kim B, Scully R, Asara JM, Cantley LC and Wulf GM. Phosphoinositide 3-kinase inhibitors induce DNA damage through nucleoside depletion. *Proc Natl Acad Sci U S A*. 2016;113:E4338-47.
131. Zhang G, Jin B and Li YP. C/EBPbeta mediates tumour-induced ubiquitin ligase atrogin1/MAFbx upregulation and muscle wasting. *EMBO J*. 2011;30:4323-35.
132. Patel VB, Bodiga S, Basu R, Das SK, Wang W, Wang Z, Lo J, Grant MB, Zhong J, Kassiri Z and Oudit GY. Loss of angiotensin-converting enzyme-2 exacerbates diabetic cardiovascular complications and leads to systolic and vascular dysfunction: a critical role of the angiotensin II/AT1 receptor axis. *Circulation research*. 2012;110:1322-35.
133. Zhong J, Basu R, Guo D, Chow FL, Byrns S, Schuster M, Loibner H, Wang XH, Penninger JM, Kassiri Z and Oudit GY. Angiotensin-converting enzyme 2 suppresses pathological hypertrophy, myocardial fibrosis, and cardiac dysfunction. *Circulation*. 2010;122:717-28, 18 p following 728.
134. Wang W, McKinnie SM, Patel VB, Haddad G, Wang Z, Zhabyeyev P, Das SK, Basu R, McLean B, Kandalam V, Penninger JM, Kassiri Z, Vederas JC, Murray AG and Oudit GY. Loss of Apelin exacerbates myocardial infarction adverse remodeling and ischemia-reperfusion injury: therapeutic potential of synthetic Apelin analogues. *Journal of the American Heart Association*. 2013;2:e000249.
135. Kuang M, Febbraio M, Wagg C, Lopaschuk GD and Dyck JR. Fatty acid translocase/CD36 deficiency does not energetically or functionally compromise hearts before or after ischemia. *Circulation*. 2004;109:1550-7.
136. Dyck JR, Hopkins TA, Bonnet S, Michelakis ED, Young ME, Watanabe M, Kawase Y, Jishage K and Lopaschuk GD. Absence of malonyl coenzyme A decarboxylase in mice

- increases cardiac glucose oxidation and protects the heart from ischemic injury. *Circulation*. 2006;114:1721-8.
137. O'Connell TD, Rodrigo MC and Simpson PC. Isolation and culture of adult mouse cardiac myocytes. *Methods Mol Biol*. 2007;357:271-96.
138. Patel VB, Wang Z, Fan D, Zhabyeyev P, Basu R, Das SK, Wang W, Desaulniers J, Holland SM, Kassiri Z and Oudit GY. Loss of p47phox subunit enhances susceptibility to biomechanical stress and heart failure because of dysregulation of cortactin and actin filaments. *Circ Res*. 2013;112:1542-56.
139. Dimauro I, Pearson T, Caporossi D and Jackson MJ. A simple protocol for the subcellular fractionation of skeletal muscle cells and tissue. *BMC Res Notes*. 2012;5:513.
140. Oudit GY and Penninger JM. Cardiac regulation by phosphoinositide 3-kinases and PTEN. *Cardiovasc Res*. 2009;82:250-60.
141. Oudit GY, Sun H, Kerfant BG, Crackower MA, Penninger JM and Backx PH. The role of phosphoinositide-3 kinase and PTEN in cardiovascular physiology and disease. *J Mol Cell Cardiol*. 2004;37:449-71.
142. Juhaszova M, Zorov DB, Yaniv Y, Nuss HB, Wang S and Sollott SJ. Role of glycogen synthase kinase-3beta in cardioprotection. *Circ Res*. 2009;104:1240-52.
143. Wu CY, Jia Z, Wang W, Ballou LM, Jiang YP, Chen B, Mathias RT, Cohen IS, Song LS, Entcheva E and Lin RZ. PI3Ks maintain the structural integrity of T-tubules in cardiac myocytes. *PLoS One*. 2011;6:e24404.
144. Kunuthur SP, Mocanu MM, Hemmings BA, Hausenloy DJ and Yellon DM. The Akt1 isoform is an essential mediator of ischaemic preconditioning. *J Cell Mol Med*. 2012;16:1739-49.
145. Liu Q, Docherty JC, Rendell JC, Clanachan AS and Lopaschuk GD. High levels of fatty acids delay the recovery of intracellular pH and cardiac efficiency in post-ischemic hearts by inhibiting glucose oxidation. *Journal of the American College of Cardiology*. 2002;39:718-25.
146. Lopaschuk GD, Ussher JR, Folmes CD, Jaswal JS and Stanley WC. Myocardial fatty acid metabolism in health and disease. *Physiol Rev*. 2010;90:207-58.
147. Ussher JR, Wang W, Gandhi M, Keung W, Samokhvalov V, Oka T, Wagg CS, Jaswal JS, Harris RA, Clanachan AS, Dyck JR and Lopaschuk GD. Stimulation of glucose oxidation protects against acute myocardial infarction and reperfusion injury. *Cardiovasc Res*. 2012;94:359-69.
148. Matsui T, Nagoshi T, Hong EG, Luptak I, Hartil K, Li L, Gorovits N, Charron MJ, Kim JK, Tian R and Rosenzweig A. Effects of chronic Akt activation on glucose uptake in the heart. *Am J Physiol Endocrinol Metab*. 2006;290:E789-97.
149. Randle PJ, Garland PB, Hales CN and Newsholme EA. The glucose fatty-acid cycle. Its role in insulin sensitivity and the metabolic disturbances of diabetes mellitus. *Lancet*. 1963;1:785-9.

150. Dyck JR and Lopaschuk GD. AMPK alterations in cardiac physiology and pathology: enemy or ally? *J Physiol*. 2006;574:95-112.
151. Beauloye C, Bertrand L, Horman S and Hue L. AMPK activation, a preventive therapeutic target in the transition from cardiac injury to heart failure. *Cardiovascular research*. 2011;90:224-33.
152. Kudo N, Barr AJ, Barr RL, Desai S and Lopaschuk GD. High rates of fatty acid oxidation during reperfusion of ischemic hearts are associated with a decrease in malonyl-CoA levels due to an increase in 5'-AMP-activated protein kinase inhibition of acetyl-CoA carboxylase. *The Journal of biological chemistry*. 1995;270:17513-20.
153. Dyck JR, Kudo N, Barr AJ, Davies SP, Hardie DG and Lopaschuk GD. Phosphorylation control of cardiac acetyl-CoA carboxylase by cAMP-dependent protein kinase and 5'-AMP activated protein kinase. *Eur J Biochem*. 1999;262:184-90.
154. Treebak JT, Glund S, Deshmukh A, Klein DK, Long YC, Jensen TE, Jorgensen SB, Viollet B, Andersson L, Neumann D, Wallimann T, Richter EA, Chibalin AV, Zierath JR and Wojtaszewski JF. AMPK-mediated AS160 phosphorylation in skeletal muscle is dependent on AMPK catalytic and regulatory subunits. *Diabetes*. 2006;55:2051-8.
155. Neubauer S. The failing heart--an engine out of fuel. *The New England journal of medicine*. 2007;356:1140-51.
156. Amin DN, Sergina N, Ahuja D, McMahon M, Blair JA, Wang D, Hann B, Koch KM, Shokat KM and Moasser MM. Resiliency and vulnerability in the HER2-HER3 tumorigenic driver. *Science translational medicine*. 2010;2:16ra7.
157. Lips DJ, Bueno OF, Wilkins BJ, Purcell NH, Kaiser RA, Lorenz JN, Voisin L, Saba-EI-Leil MK, Meloche S, Pouyssegur J, Pages G, De Windt LJ, Doevendans PA and Molkentin JD. MEK1-ERK2 signaling pathway protects myocardium from ischemic injury in vivo. *Circulation*. 2004;109:1938-41.
158. Bueno OF and Molkentin JD. Involvement of extracellular signal-regulated kinases 1/2 in cardiac hypertrophy and cell death. *Circ Res*. 2002;91:776-81.
159. Vassalli G, Milano G and Moccetti T. Role of Mitogen-Activated Protein Kinases in Myocardial Ischemia-Reperfusion Injury during Heart Transplantation. *Journal of transplantation*. 2012;2012:928954.
160. Chai W, Wu Y, Li G, Cao W, Yang Z and Liu Z. Activation of p38 mitogen-activated protein kinase abolishes insulin-mediated myocardial protection against ischemia-reperfusion injury. *Am J Physiol Endocrinol Metab*. 2008;294:E183-9.
161. Tong H, Imahashi K, Steenbergen C and Murphy E. Phosphorylation of glycogen synthase kinase-3beta during preconditioning through a phosphatidylinositol-3-kinase--dependent pathway is cardioprotective. *Circ Res*. 2002;90:377-9.
162. Ferby IM, Waga I, Sakanaka C, Kume K and Shimizu T. Wortmannin inhibits mitogen-activated protein kinase activation induced by platelet-activating factor in guinea pig neutrophils. *J Biol Chem*. 1994;269:30485-8.

163. Chandarlapaty S, Sawai A, Scaltriti M, Rodrik-Outmezguine V, Grbovic-Huezo O, Serra V, Majumder PK, Baselga J and Rosen N. AKT inhibition relieves feedback suppression of receptor tyrosine kinase expression and activity. *Cancer cell*. 2011;19:58-71.
164. Carver BS, Chapinski C, Wongvipat J, Hieronymus H, Chen Y, Chandarlapaty S, Arora VK, Le C, Koutcher J, Scher H, Scardino PT, Rosen N and Sawyers CL. Reciprocal feedback regulation of PI3K and androgen receptor signaling in PTEN-deficient prostate cancer. *Cancer cell*. 2011;19:575-86.
165. Garrett JT, Chakrabarty A and Arteaga CL. Will PI3K pathway inhibitors be effective as single agents in patients with cancer? *Oncotarget*. 2011;2:1314-21.
166. Harrington LS, Findlay GM, Gray A, Tolkacheva T, Wigfield S, Rebholz H, Barnett J, Leslie NR, Cheng S, Shepherd PR, Gout I, Downes CP and Lamb RF. The TSC1-2 tumor suppressor controls insulin-PI3K signaling via regulation of IRS proteins. *The Journal of cell biology*. 2004;166:213-23.
167. Carracedo A, Ma L, Teruya-Feldstein J, Rojo F, Salmena L, Alimonti A, Egia A, Sasaki AT, Thomas G, Kozma SC, Papa A, Nardella C, Cantley LC, Baselga J and Pandolfi PP. Inhibition of mTORC1 leads to MAPK pathway activation through a PI3K-dependent feedback loop in human cancer. *The Journal of clinical investigation*. 2008;118:3065-74.
168. McLean BA, Kienesberger PC, Wang W, Masson G, Zhabyeyev P, Dyck JR and Oudit GY. Enhanced recovery from ischemia-reperfusion injury in PI3K α dominant negative hearts: investigating the role of alternate PI3K isoforms, increased glucose oxidation and MAPK signaling. *Journal of molecular and cellular cardiology*. 2013;54:9-18.
169. Hausenloy DJ, Tsang A, Mocanu MM and Yellon DM. Ischemic preconditioning protects by activating prosurvival kinases at reperfusion. *Am J Physiol Heart Circ Physiol*. 2005;288:H971-6.
170. Hirai H, Sootome H, Nakatsuru Y, Miyama K, Taguchi S, Tsujioka K, Ueno Y, Hatch H, Majumder PK, Pan BS and Kotani H. MK-2206, an allosteric Akt inhibitor, enhances antitumor efficacy by standard chemotherapeutic agents or molecular targeted drugs in vitro and in vivo. *Mol Cancer Ther*. 2010;9:1956-67.
171. Vila-Petroff M, Salas MA, Said M, Valverde CA, Sapia L, Portiansky E, Hajjar RJ, Kranias EG, Mundina-Weilenmann C and Mattiazzi A. CaMKII inhibition protects against necrosis and apoptosis in irreversible ischemia-reperfusion injury. *Cardiovasc Res*. 2007;73:689-98.
172. Malhotra R, Valuckaite V, Staron ML, Theccanat T, D'Souza KM, Alverdy JC and Akhter SA. High-molecular-weight polyethylene glycol protects cardiac myocytes from hypoxia- and reoxygenation-induced cell death and preserves ventricular function. *Am J Physiol Heart Circ Physiol*. 2011;300:H1733-42.
173. Ikeno F, Inagaki K, Rezaee M and Mochly-Rosen D. Impaired perfusion after myocardial infarction is due to reperfusion-induced deltaPKC-mediated myocardial damage. *Cardiovasc Res*. 2007;73:699-709.
174. Green DR. Apoptotic pathways: ten minutes to dead. *Cell*. 2005;121:671-4.

175. Zamaraeva MV, Sabirov RZ, Maeno E, Ando-Akatsuka Y, Bessonova SV and Okada Y. Cells die with increased cytosolic ATP during apoptosis: a bioluminescence study with intracellular luciferase. *Cell Death Differ.* 2005;12:1390-7.
176. Kung G, Konstantinidis K and Kitsis RN. Programmed necrosis, not apoptosis, in the heart. *Circ Res.* 2011;108:1017-36.
177. Adameova A, Goncalvesova E, Szobi A and Dhalla NS. Necroptotic cell death in failing heart: relevance and proposed mechanisms. *Heart Fail Rev.* 2016;21:213-21.
178. Koudstaal S, Oerlemans MI, Van der Spoel TI, Janssen AW, Hoefler IE, Doevendans PA, Sluijter JP and Chamuleau SA. Necrostatin-1 alleviates reperfusion injury following acute myocardial infarction in pigs. *Eur J Clin Invest.* 2015;45:150-9.
179. Smith CC, Davidson SM, Lim SY, Simpkin JC, Hothersall JS and Yellon DM. Necrostatin: a potentially novel cardioprotective agent? *Cardiovasc Drugs Ther.* 2007;21:227-33.
180. Whelan RS, Konstantinidis K, Wei AC, Chen Y, Reyna DE, Jha S, Yang Y, Calvert JW, Lindsten T, Thompson CB, Crow MT, Gavathiotis E, Dorn GW, 2nd, O'Rourke B and Kitsis RN. Bax regulates primary necrosis through mitochondrial dynamics. *Proc Natl Acad Sci U S A.* 2012;109:6566-71.
181. Karch J, Kwong JQ, Burr AR, Sargent MA, Elrod JW, Peixoto PM, Martinez-Caballero S, Osinska H, Cheng EH, Robbins J, Kinnally KW and Molkentin JD. Bax and Bak function as the outer membrane component of the mitochondrial permeability pore in regulating necrotic cell death in mice. *Elife.* 2013;2:e00772.
182. Tsuruta F, Masuyama N and Gotoh Y. The phosphatidylinositol 3-kinase (PI3K)-Akt pathway suppresses Bax translocation to mitochondria. *J Biol Chem.* 2002;277:14040-7.
183. Shulga N, Wilson-Smith R and Pastorino JG. Sirtuin-3 deacetylation of cyclophilin D induces dissociation of hexokinase II from the mitochondria. *J Cell Sci.* 2010;123:894-902.
184. Ghosh JC, Siegelin MD, Vaira V, Favarsani A, Tavecchio M, Chae YC, Lisanti S, Rampini P, Giroda M, Caino MC, Seo JH, Kossenkov AV, Michalek RD, Schultz DC, Bosari S, Languino LR and Altieri DC. Adaptive mitochondrial reprogramming and resistance to PI3K therapy. *J Natl Cancer Inst.* 2015;107.
185. Lam CK, Zhao W, Liu GS, Cai WF, Gardner G, Adly G and Kranias EG. HAX-1 regulates cyclophilin-D levels and mitochondria permeability transition pore in the heart. *Proc Natl Acad Sci U S A.* 2015;112:E6466-75.
186. Lexow J, Poggioli T, Sarathchandra P, Santini MP and Rosenthal N. Cardiac fibrosis in mice expressing an inducible myocardial-specific Cre driver. *Dis Model Mech.* 2013;6:1470-6.
187. Calvieri C, Rubattu S and Volpe M. Molecular mechanisms underlying cardiac antihypertrophic and antifibrotic effects of natriuretic peptides. *J Mol Med (Berl).* 2012;90:5-13.
188. Knight ZA, Gonzalez B, Feldman ME, Zunder ER, Goldenberg DD, Williams O, Loewith R, Stokoe D, Balla A, Toth B, Balla T, Weiss WA, Williams RL and Shokat KM. A

pharmacological map of the PI3-K family defines a role for p110alpha in insulin signaling. *Cell*. 2006;125:733-47.

189. McMullen JR, Amirahmadi F, Woodcock EA, Schinke-Braun M, Bouwman RD, Hewitt KA, Mollica JP, Zhang L, Zhang Y, Shioi T, Buerger A, Izumo S, Jay PY and Jennings GL. Protective effects of exercise and phosphoinositide 3-kinase(p110alpha) signaling in dilated and hypertrophic cardiomyopathy. *Proc Natl Acad Sci U S A*. 2007;104:612-7.

190. Amin DN, Sergina N, Ahuja D, McMahon M, Blair JA, Wang D, Hann B, Koch KM, Shokat KM and Moasser MM. Resiliency and vulnerability in the HER2-HER3 tumorigenic driver. *Sci Transl Med*. 2010;2:3000389.

191. Kehat I and Molkentin JD. Extracellular signal-regulated kinase 1/2 (ERK1/2) signaling in cardiac hypertrophy. *Ann N Y Acad Sci*. 2010.

192. Ng WA, Grupp IL, Subramaniam A and Robbins J. Cardiac myosin heavy chain mRNA expression and myocardial function in the mouse heart. *Circulation research*. 1991;68:1742-50.

193. Buerger A, Rozhitskaya O, Sherwood MC, Dorfman AL, Bisping E, Abel ED, Pu WT, Izumo S and Jay PY. Dilated cardiomyopathy resulting from high-level myocardial expression of Cre-recombinase. *Journal of cardiac failure*. 2006;12:392-8.

194. Ruiz-Alcaraz AJ, Liu HK, Cuthbertson DJ, McManus EJ, Akhtar S, Lipina C, Morris AD, Petrie JR, Hundal HS and Sutherland C. A novel regulation of IRS1 (insulin receptor substrate-1) expression following short term insulin administration. *The Biochemical journal*. 2005;392:345-52.

195. Smith GC, Ong WK, Rewcastle GW, Kendall JD, Han W and Shepherd PR. Effects of acutely inhibiting PI3K isoforms and mTOR on regulation of glucose metabolism in vivo. *The Biochemical journal*. 2012;442:161-9.

196. Patrucco E, Notte A, Barberis L, Selvetella G, Maffei A, Brancaccio M, Marengo S, Russo G, Azzolino O, Rybalkin SD, Silengo L, Altruda F, Wetzker R, Wymann MP, Lembo G and Hirsch E. PI3Kgamma modulates the cardiac response to chronic pressure overload by distinct kinase-dependent and -independent effects. *Cell*. 2004;118:375-87.

197. Sun H, Oudit GY, Ramirez RJ, Costantini D and Backx PH. The phosphoinositide 3-kinase inhibitor LY294002 enhances cardiac myocyte contractility via a direct inhibition of I_k,slow currents. *Cardiovascular research*. 2004;62:509-20.

198. Sasso FC, Carbonara O, Cozzolino D, Rambaldi P, Mansi L, Torella D, Gentile S, Turco S, Torella R and Salvatore T. Effects of insulin-glucose infusion on left ventricular function at rest and during dynamic exercise in healthy subjects and noninsulin dependent diabetic patients: a radionuclide ventriculographic study. *Journal of the American College of Cardiology*. 2000;36:219-26.

199. Lorenz K, Schmitt JP, Vidal M and Lohse MJ. Cardiac hypertrophy: targeting Raf/MEK/ERK1/2-signaling. *The international journal of biochemistry & cell biology*. 2009;41:2351-5.

200. Foukas LC, Bilanges B, Betti L, Pearce W, Ali K, Sancho S, Withers DJ and Vanhaesebroeck B. Long-term p110alpha PI3K inactivation exerts a beneficial effect on metabolism. *EMBO Mol Med*. 2013;5:563-71.
201. Foukas LC, Berenjeno IM, Gray A, Khwaja A and Vanhaesebroeck B. Activity of any class IA PI3K isoform can sustain cell proliferation and survival. *Proceedings of the National Academy of Sciences of the United States of America*. 2010;107:11381-6.
202. Hardie DG. AMP-activated/SNF1 protein kinases: conserved guardians of cellular energy. *Nature reviews Molecular cell biology*. 2007;8:774-85.
203. Dolinsky VW and Dyck JR. Role of AMP-activated protein kinase in healthy and diseased hearts. *American journal of physiology Heart and circulatory physiology*. 2006;291:14.
204. Fearon K, Strasser F, Anker SD, Bosaeus I, Bruera E, Fainsinger RL, Jatoi A, Loprinzi C, MacDonald N, Mantovani G, Davis M, Muscaritoli M, Ottery F, Radbruch L, Ravasco P, Walsh D, Wilcock A, Kaasa S and Baracos VE. Definition and classification of cancer cachexia: an international consensus. *The lancet oncology*. 2011;12:489-95.
205. Pal A, Barber TM, Van de Bunt M, Rudge SA, Zhang Q, Lachlan KL, Cooper NS, Linden H, Levy JC, Wakelam MJ, Walker L, Karpe F and Gloyn AL. PTEN mutations as a cause of constitutive insulin sensitivity and obesity. *N Engl J Med*. 2012;367:1002-11.
206. Bezler M, Hengstler JG and Ullrich A. Inhibition of doxorubicin-induced HER3-PI3K-AKT signalling enhances apoptosis of ovarian cancer cells. *Mol Oncol*. 2012;6:516-29.
207. Wallin JJ, Guan J, Prior WW, Edgar KA, Kassees R, Sampath D, Belvin M and Friedman LS. Nuclear phospho-Akt increase predicts synergy of PI3K inhibition and doxorubicin in breast and ovarian cancer. *Sci Transl Med*. 2010;2:48ra66.
208. Fruman DA and Rommel C. PI3K and cancer: lessons, challenges and opportunities. *Nat Rev Drug Discov*. 2014;13:140-56.
209. Babichev Y, Kabaroff L, Datti A, Uehling D, Isaac M, Al-Awar R, Prakesch M, Sun RX, Boutros PC, Venier R, Dickson BC and Gladly RA. PI3K/AKT/mTOR inhibition in combination with doxorubicin is an effective therapy for leiomyosarcoma. *J Transl Med*. 2016;14:67.
210. Cohen S, Nathan JA and Goldberg AL. Muscle wasting in disease: molecular mechanisms and promising therapies. *Nat Rev Drug Discov*. 2015;14:58-74.
211. Archer SL, Fang YH, Ryan JJ and Piao L. Metabolism and bioenergetics in the right ventricle and pulmonary vasculature in pulmonary hypertension. *Pulm Circ*. 2013;3:144-52.
212. Nagendran J, Archer SL, Soliman D, Gurtu V, Moudgil R, Haromy A, St Aubin C, Webster L, Rebeyka IM, Ross DB, Light PE, Dyck JR and Michelakis ED. Phosphodiesterase type 5 is highly expressed in the hypertrophied human right ventricle, and acute inhibition of phosphodiesterase type 5 improves contractility. *Circulation*. 2007;116:238-48.
213. Yamamoto Y, Hoshino Y, Ito T, Nariai T, Mohri T, Obana M, Hayata N, Uozumi Y, Maeda M, Fujio Y and Azuma J. Atrogin-1 ubiquitin ligase is upregulated by doxorubicin via p38-MAP kinase in cardiac myocytes. *Cardiovasc Res*. 2008;79:89-96.

214. Puigserver P, Rhee J, Lin J, Wu Z, Yoon JC, Zhang CY, Krauss S, Mootha VK, Lowell BB and Spiegelman BM. Cytokine stimulation of energy expenditure through p38 MAP kinase activation of PPARgamma coactivator-1. *Mol Cell*. 2001;8:971-82.
215. Fukawa T, Yan-Jiang BC, Min-Wen JC, Jun-Hao ET, Huang D, Qian CN, Ong P, Li Z, Chen S, Mak SY, Lim WJ, Kanayama HO, Mohan RE, Wang RR, Lai JH, Chua C, Ong HS, Tan KK, Ho YS, Tan IB, Teh BT and Shyh-Chang N. Excessive fatty acid oxidation induces muscle atrophy in cancer cachexia. *Nat Med*. 2016;22:666-71.
216. Arabacilar P and Marber M. The case for inhibiting p38 mitogen-activated protein kinase in heart failure. *Front Pharmacol*. 2015;6:102.
217. Muchir A, Wu W, Choi JC, Iwata S, Morrow J, Homma S and Worman HJ. Abnormal p38alpha mitogen-activated protein kinase signaling in dilated cardiomyopathy caused by lamin A/C gene mutation. *Hum Mol Genet*. 2012;21:4325-33.
218. Wang Q, Liu P, Spangle JM, Von T, Roberts TM, Lin NU, Krop IE, Winer EP and Zhao JJ. PI3K-p110alpha mediates resistance to HER2-targeted therapy in HER2+, PTEN-deficient breast cancers. *Oncogene*. 2016;35:3607-12.
219. Zhang C, Xu B and Liu P. Addition of the p110alpha inhibitor BYL719 overcomes targeted therapy resistance in cells from Her2-positive-PTEN-loss breast cancer. *Tumour Biol*. 2016.
220. Pappalardo E and O'Regan R. The PI3K/AKT/mTOR pathway in breast cancer: targets, trials and biomarkers. *Ther Adv Med Oncol*. 2014;6:154-66.
221. Bradshaw PT, Stevens J, Khankari N, Teitelbaum SL, Neugut AI and Gammon MD. Cardiovascular Disease Mortality Among Breast Cancer Survivors. *Epidemiology*. 2016;27:6-13.
222. Zhang S, Liu X, Bawa-Khalife T, Lu LS, Lyu YL, Liu LF and Yeh ET. Identification of the molecular basis of doxorubicin-induced cardiotoxicity. *Nature medicine*. 2012;18:1639-42.
223. Kim KH, Oudit GY and Backx PH. Erythropoietin protects against doxorubicin-induced cardiomyopathy via a phosphatidylinositol 3-kinase-dependent pathway. *The Journal of pharmacology and experimental therapeutics*. 2008;324:160-9.
224. Moulin M, Piquereau J, Mateo P, Fortin D, Rucker-Martin C, Gressette M, Lefebvre F, Gresikova M, Solgadi A, Veksler V, Garnier A and Ventura-Clapier R. Sexual dimorphism of doxorubicin-mediated cardiotoxicity: potential role of energy metabolism remodeling. *Circ Heart Fail*. 2015;8:98-108.
225. Oflaz S, Yucel B, Oz F, Sahin D, Ozturk N, Yaci O, Polat N, Gurdal A, Cizgici AY, Dursun M and Oflaz H. Assessment of myocardial damage by cardiac MRI in patients with anorexia nervosa. *Int J Eat Disord*. 2013;46:862-6.
226. Borges FH, Marinello PC, Cecchini AL, Blegniski FP, Guarnier FA and Cecchini R. Oxidative and proteolytic profiles of the right and left heart in a model of cancer-induced cardiac cachexia. *Pathophysiology*. 2014;21:257-65.

227. Melenovsky V, Kotrc M, Borlaug BA, Marek T, Kovar J, Malek I and Kautzner J. Relationships between right ventricular function, body composition, and prognosis in advanced heart failure. *J Am Coll Cardiol*. 2013;62:1660-70.
228. Reddy S and Bernstein D. Molecular Mechanisms of Right Ventricular Failure. *Circulation*. 2015;132:1734-42.
229. Kaufman BD, Desai M, Reddy S, Osorio JC, Chen JM, Mosca RS, Ferrante AW and Mital S. Genomic profiling of left and right ventricular hypertrophy in congenital heart disease. *J Card Fail*. 2008;14:760-7.
230. Rouleau JL, Paradis P, Shenasa H and Juneau C. Faster time to peak tension and velocity of shortening in right versus left ventricular trabeculae and papillary muscles of dogs. *Circ Res*. 1986;59:556-61.
231. Ventetuolo CE, Mitra N, Wan F, Manichaikul A, Barr RG, Johnson C, Bluemke DA, Lima JA, Tandri H, Ouyang P and Kawut SM. Oestradiol metabolism and androgen receptor genotypes are associated with right ventricular function. *Eur Respir J*. 2016;47:553-63.
232. Friedberg MK and Redington AN. Right versus left ventricular failure: differences, similarities, and interactions. *Circulation*. 2014;129:1033-44.
233. Rider OJ, Lewis AJ, Lewandowski AJ, Ntusi N, Nethononda R, Petersen SE, Francis JM, Pitcher A, Banerjee R, Leeson P and Neubauer S. Obese subjects show sex-specific differences in right ventricular hypertrophy. *Circ Cardiovasc Imaging*. 2015;8.
234. Oliveira GH, Dupont M, Naftel D, Myers SL, Yuan Y, Tang WH, Gonzalez-Stawinski G, Young JB, Taylor DO and Starling RC. Increased need for right ventricular support in patients with chemotherapy-induced cardiomyopathy undergoing mechanical circulatory support: outcomes from the INTERMACS Registry (Interagency Registry for Mechanically Assisted Circulatory Support). *J Am Coll Cardiol*. 2014;63:240-8.
235. Lipshultz SE, Lipsitz SR, Mone SM, Goorin AM, Sallan SE, Sanders SP, Orav EJ, Gelber RD and Colan SD. Female sex and drug dose as risk factors for late cardiotoxic effects of doxorubicin therapy for childhood cancer. *The New England journal of medicine*. 1995;332:1738-43.
236. Liao P, Wang SQ, Wang S, Zheng M, Zheng M, Zhang SJ, Cheng H, Wang Y and Xiao RP. p38 Mitogen-activated protein kinase mediates a negative inotropic effect in cardiac myocytes. *Circ Res*. 2002;90:190-6.
237. Igea A and Nebreda AR. The Stress Kinase p38alpha as a Target for Cancer Therapy. *Cancer Res*. 2015;75:3997-4002.
238. Gharbi SI, Zvelebil MJ, Shuttleworth SJ, Hancox T, Saghir N, Timms JF and Waterfield MD. Exploring the specificity of the PI3K family inhibitor LY294002. *Biochem J*. 2007;404:15-21.
239. Herron TJ, Lee P and Jalife J. Optical imaging of voltage and calcium in cardiac cells & tissues. *Circ Res*. 2012;110:609-23.

240. Elrod JW, Wong R, Mishra S, Vagnozzi RJ, Sakthivel B, Goonasekera SA, Karch J, Gabel S, Farber J, Force T, Brown JH, Murphy E and Molkentin JD. Cyclophilin D controls mitochondrial pore-dependent Ca(2+) exchange, metabolic flexibility, and propensity for heart failure in mice. *J Clin Invest*. 2010;120:3680-7.
241. Schonekess BO, Allard MF, Henning SL, Wambolt RB and Lopaschuk GD. Contribution of glycogen and exogenous glucose to glucose metabolism during ischemia in the hypertrophied rat heart. *Circ Res*. 1997;81:540-9.
242. LeBrasseur NK, Schelhorn TM, Bernardo BL, Cosgrove PG, Loria PM and Brown TA. Myostatin inhibition enhances the effects of exercise on performance and metabolic outcomes in aged mice. *J Gerontol A Biol Sci Med Sci*. 2009;64:940-8.
243. Heineke J, Auger-Messier M, Xu J, Sargent M, York A, Welle S and Molkentin JD. Genetic deletion of myostatin from the heart prevents skeletal muscle atrophy in heart failure. *Circulation*. 2010;121:419-25.
244. Romanick M, Thompson LV and Brown-Borg HM. Murine models of atrophy, cachexia, and sarcopenia in skeletal muscle. *Biochim Biophys Acta*. 2013;1832:1410-20.